Journal of the
OPTICAL SOCIETY
of AMERICA

VOLUME 39, NUMBER 4 APRIL, 1949

The Correction of Slit-Width Errors

ARTHUR C. HARDY AND F. MANSFIELD YOUNG
Massachusetts Institute of Technology, Cambridge, Massachusetts
(Received December 16, 1948)

The original purpose of this investigation was to explore the possibility of providing a spectrophotometer with automatic means for correcting the error that results when a continuous source is used with a monochromator having slits of finite width. In connection therewith, it was necessary to make what appears to be the first rigorous analysis of slit-width errors. The results of this analysis can be applied to the experimental determination of any functional relationship when the size of the "probe" is significant.

INTRODUCTION

LORD RAYLEIGH[1] published a paper in 1871 on "A Correction Sometimes Required in Curves Professing to Represent the Connexion between Two Physical Magnitudes." As an illustration, he chose the problem of determining the distribution of heat in the spectrum of the sun or other source of light; and he showed how to make partial correction for the fact that, when a linear thermopile of finite width is placed in a spectrum, it indicates the integral of the energy over a finite band of wave-lengths.

When the image of the entrance slit of the dispersing system has the same width as the thermopile, a curve showing the spectral transmittance of an idealized system is triangular in shape. This special case was investigated by Runge[2] and Paschen.[3] When the widths are different, the pass band becomes trapezoidal. This case was treated by Hyde,[4] who also introduced a correction for variations in the spectral sensitivity of the receptor. The case of a pass band of arbitrary shape does not appear to have been investigated.

MATHEMATICAL FORMULATION OF THE PROBLEM

When a receptor having a spectral sensitivity $S(\lambda)$ is exposed to the energy $E(\lambda)$ from a continuous source, the response of the receptor is proportional to

$$\int_0^\infty E(\lambda)S(\lambda)d\lambda.$$

If, now, an absorbing substance having a spectral transmittance $t(\lambda)$ is inserted between the source and receptor, the response of the latter becomes

$$\int_0^\infty E(\lambda)S(\lambda)t(\lambda)d\lambda.$$

The ratio T of the two responses is

$$T=\frac{\int_0^\infty E(\lambda)S(\lambda)t(\lambda)d\lambda}{\int_0^\infty E(\lambda)S(\lambda)d\lambda}. \qquad (1)$$

The art of spectrophotometry is concerned, not with the effect of an absorbing substance when it is inserted between a given source and receptor, but with the determination of $t(\lambda)$ at one or more wavelengths. This is ordinarily accomplished by introducing a monochromator or equivalent device into the optical system. High accuracy in the determination of $t(\lambda)$ requires that the pass band of the monochromator be narrow. On the other hand, narrowing the pass band reduces the response of the receptor; and the theory of servo mechanisms

[1] Lord Rayleigh, Phil. Mag. **42**, 441 (1871).
[2] C. Runge, Zeits. Math. **42**, 205 (1897).
[3] F. Paschen, Wied. Ann. **60**, 712 (1897).
[4] E. P. Hyde, Astrophys. J. **35**, 237 (1912).

shows that this will reduce either the speed or the precision with which the data can be obtained. At the present state of the art, the pass band must often be wider than would be desirable from the standpoint of accuracy; and the analysis developed in the next section indicates corrections that can usually be applied.

To define the problem unambiguously, assume that the wave-length adjustment of the monochromator is held constant at some nominal value y, read on the wave-length dial. The monochromator can then be regarded as having a spectral transmittance $M(\lambda)$. That is, under these conditions, the monochromator is the equivalent of a narrow band-pass filter having a spectral transmittance $M(\lambda)$. Since the spectral transmittance of the monochromator is a function of y (in addition to being a function of λ), we shall designate it by $M(y,\lambda)$. Then, for the case where a monochromator is inserted in the optical system, Eq. (1) becomes

$$T(y)=\frac{\int_0^\infty E(\lambda)S(\lambda)M(y,\lambda)t(\lambda)d\lambda}{\int_0^\infty E(\lambda)S(\lambda)M(y,\lambda)d\lambda}. \qquad (2)$$

The fundamental problem in spectrophotometry[5] is to determine $t(\lambda)$ from observed values of $T(y)$.

SOLUTION OF THE INTEGRAL EQUATION

A formal solution of Eq. (2) can be obtained in the following manner for the type of functions encountered in the ordinary practice of spectrophotometry. Because $E(\lambda)$, $S(\lambda)$, and $M(y,\lambda)$ always occur in the form of a product, it is convenient to replace them by a single function, $W(y,\lambda)=E(\lambda)\times S(\lambda)M(y,\lambda)$, which characterizes the entire optical system. It is also convenient to introduce a change of variables, $\lambda=y+x$, where $d\lambda=dx$. With these changes, Eq. 2 becomes

$$T(y)\int_{-\infty}^{\infty}W(y,\lambda)dx=\int_{-\infty}^{\infty}W(y,\lambda)t(y+x)dx. \qquad (3)$$

Considering only a small range of y, $(a\leqslant y\leqslant b)$, the dependence of $W(y,x)$ on y can be considered one of magnitude only; i.e., the shape of the pass band of the monochromator can be considered to be independent of y in this region. Hence, $W(y,x)=\phi(y)W(y_0,x)$, where $\phi(y_0)=1$ and $a\leqslant y_0\leqslant b$. Substituting this expression in Eq. (3) yields

$$AT(y)=\int_{-\infty}^{\infty}W(y_0,x)t(y+x)dx, \qquad (4)$$

where

$$A=\int_{-\infty}^{\infty}W(y_0,x)dx$$

is introduced to simplify notation. It must be remembered, of course, that A is a function of y_0.

Now, $W(y,x)$ may be written as the sum of an even part, $W_e=\frac{1}{2}[W(y_0,x)+W(y_0,-x)]$, and an odd part, $W_0=\frac{1}{2}[W(y_0,x)-W(y_0,-x)]$. Hence,

$$\begin{aligned}W(y_0,x)&=W_e(y_0,x)+W_0(y_0,x)\\&=W_e(y_0,-x)-W_0(y_0,-x).\end{aligned}$$

Substituting in Eq. (4), and replacing x by $-x$, Eq. (4) becomes

$$AT(y)=\int_{-\infty}^{\infty}W_e(y_0,x)t(y-x)dx-\int_{-\infty}^{\infty}W_0(y_0,x)t(y-x)dx. \qquad (5)$$

Each term on the right-hand side of Eq. (5) is a convolution, a form which has a particularly simple Fourier Transform.[6,7] Taking the Fourier Transforms of both sides of Eq. (5),

$$A\{T(y)\}=\{t(y)\}\{W_e-W_0\}(2\pi)^{\frac{1}{2}}$$

from which

$$\{t\}=\frac{A\{T\}}{(2\pi)^{\frac{1}{2}}[\{W_e\}-\{W_0\}]}. \qquad (6)$$

Expanding the kernel of the Fourier Transform of $W_e(y_0,x)$ in a Taylor series gives

$$\begin{aligned}\{W_e\}&=1/(2\pi)^{\frac{1}{2}}\int_{-\infty}^{\infty}e^{i\omega x}W(y_0,x)dx\\&=1/(2\pi)^{\frac{1}{2}}\int_{-\infty}^{\infty}[1+i\omega x+\cdots+(i\omega x)^n/n!+\cdots]W(y_0,x)dx\\&=A/(2\pi)^{\frac{1}{2}}\left[1+\sum_{n=1}^{\infty}e_n(i\omega)^n\right]\end{aligned}$$

where

$$e_n=(1/An!)\int_{-\infty}^{\infty}x^nW_e(y_0,x)dx.$$

Since W_e is an even function, the e's corresponding to odd n's will vanish. Similarly, in the

[5] It goes without saying that the theory developed here can be applied to measurements of spectral reflectance by replacing $t(\lambda)$ by $r(\lambda)$ and $T(y)$ by $R(y)$.

[6] R. H. Cameron, Nat. Math. Mag. 15, 331 (1941).

[7] According to the convention used here, the Fourier Transform, $\{\ \}$, of a function $f(y)$ is

$$\{f(y)\}=1/(2\pi)^{\frac{1}{2}}\int_{-\infty}^{\infty}e^{i\omega y}f(y)dy.$$

expression for the transform of W_0,

$$\{W_0\} = A/(2\pi)^{\frac{1}{2}} \sum_{n=1}^{\infty} o_n (i\omega)^n$$

where

$$o_n = 1/An! \int_{-\infty}^{\infty} x^n W_0(y_0,x)dx,$$

the o's corresponding to even n's will vanish. If we consider a new set of coefficients

$$\alpha_n \equiv \frac{1}{An!} \int_{-\infty}^{\infty} x^n \omega(y_0,x)dx, \tag{7}$$

it is seen that, when n is odd, $\alpha_n = o_n$; and when n is even, $\alpha_n = e_n$. In terms of these new coefficients,

$$\{W_e\} - \{W_0\} = A/(2\pi)^{\frac{1}{2}} \left[1 + \sum_{n=1}^{\infty} (-1)^n \alpha_n (i\omega)^n\right]. \tag{8}$$

Substituting Eq. (8) in Eq. (6) and applying the binomial theorem to the denominator gives

$$\{t\} = \frac{\{T\}}{1 + \sum_{n=1}^{\infty} (-1)^n \alpha_n (i\omega)^n}$$

$$= \left[1 - \sum_{n=1}^{\infty} (-1)^n \alpha_n (i\omega)^n + \left[\sum_{n=1}^{\infty} (-1)^n \alpha_n (i\omega)^n\right]^2 - \cdots\right]\{T\}.$$

If use is now made of the theorem that

$$\{dT(y)/dy\} = -i\omega\{T(y)\},$$

the final expression for $t(y)$ is

$$t(y) = T(y) - \sum_{n=1}^{\infty} \alpha_n \frac{d^n T(y)}{dy^n} + \left[\sum_{n=1}^{\infty} \alpha_n \frac{d^n}{dy^n}\right]^2 T(y) - \cdots. \tag{9}$$

This expression can be written somewhat more compactly in the following form

$$t(y) = T(y) - \sum_{n=1}^{\infty} a_n [d^n T(y)/dy^n], \tag{10}$$

where the a's are defined in terms of the α's by Eq. 9. The first few values of a can be seen to be

$$\begin{aligned} a_1 &= \alpha_1 \\ a_2 &= \alpha_2 - \alpha_1^2 \\ a_3 &= \alpha_3 - 2\alpha_1\alpha_2 - \alpha_1^3 \\ a_4 &= \alpha_4 - \alpha_2^2 - 2\alpha_1\alpha_3 + 3\alpha_1^2\alpha_2 - \alpha_1^4. \end{aligned} \tag{11}$$

We may now take y_0 to be the wave-length at which $t(y)$ is to be computed. In this case,

$$\alpha_n = 1/An! \int_{-\infty}^{\infty} x^n W(y,x)dx. \tag{12}$$

It should be kept in mind that the α's (and hence the a's) are functions of y.

THE WAVE-LENGTH CALIBRATION

The wave-length scale of a monochromator is customarily calibrated by closing down the slits and then setting on spectrum lines of known wave-length from a discontinuous source, such as a mercury arc. This procedure would be adequate in spectrophotometry, were it not for the effect of using wide slits with a continuous source. Because of non-uniformity in the spectral distribution of energy from such a source, selectivity in the response of the receptor, and a certain amount of selective absorption in the optical system, this method of calibration does not indicate the effective wave-length of the pass band when wide slits are used.

The resulting wave-length error has been discussed by Van den Akker,[8] who has recommended a modification of the usual procedure. Using a discontinuous source, one measures at some wave-length the true value of the spectral transmittance of a filter whose spectral transmittance varies linearly with wave-length in the region of this wave-length. The line source used for calibration is then removed and replaced by the continuous source used in regular operation, the slits being set at their normal widths. In general, the spectrophotometer will now indicate a somewhat different value for the spectral transmittance of the filter, but it may be made to indicate the same value by altering the wave-length adjustment. If the instrument has previously been calibrated with narrow slits, the necessary alteration of the wave-length adjustment is a measure of the wave-length error at this wave-length. The procedure is repeated at as many wave-lengths as may be necessary.

In spectrophotometers of the automatic type, a cam is commonly used to produce the desired correspondence between the wave-length of the pass band of the monochromator and the wave-length scale of the recording paper. From what has been seen above, the best correspondence occurs when this cam is so cut that the wave-length error, determined by Van den Akker's method, is zero at all wave-lengths. The difficulty is that, if the wave-length corrections are embodied in this cam, a change in the receptor, for example, may require that the cam be replaced.

The way out of this difficulty is to cut the wave-length cam of the instrument on the assumption

[8] J. A. Van den Akker, J. Opt. Soc. Am. **33**, 257 (1943).

that narrow slits will be used; and then to make the necessary corrections by means of a second cam, which need not be cut to a high degree of accuracy. This second cam might be inserted in the driving mechanism, like the cam that corrects the errors in the screw of a dividing engine, but it is preferable to introduce the correction optically. For example, a straight edge placed across the top of the entrance or exit slit of the monochromator can, if it has the proper slope, cause the effective wave-length of the pass band to correspond with the wave-length that would be transmitted if the bilateral slits were narrowed to the limit. The proper slope can be determined by a modification of Van den Akker's procedure in which, instead of evaluating the wave-length error by changing the wave-length adjustment, the error is eliminated by changing the slope of the straight edge. When the proper slope has been found as a function of wave-length, a cam can be cut that will automatically maintain the straight edge at the proper slope as the spectrum is traversed.

GENERAL DISCUSSION OF THE SLIT-WIDTH ERROR

It was shown by Eq. (10) that the slit-width error can be expressed as the algebraic sum of a series of terms, $a_1[dT(y)/dy]$, $a_2[d^2T(y)/dy^2]$, $a_3[d^3T(y)/dy^3]$, $\cdots$. The coefficients of these terms were defined by Eqs. (11) and (12). Reference to these equations will show that, if the function $W(y,x)$ is known, all the a's can be computed. Then, by taking the derivatives of the data furnished by the instrument, complete correction of the slit-width error can be made.[9]

In principle, the function $W(y,x)$ can be found by any experimental technique that satisfies the definition of the function. As an example, $E(\lambda)$, $S(\lambda)$, and $M(y,\lambda)$ might be determined from three separate experiments, in which case their product is the desired function. In practice, it is rarely necessary to consider more than the first two correction terms; and the coefficients of these terms, a_1 and a_2, can be determined rather simply without knowing $W(y,x)$. As a matter of convenience, we shall discuss the determination of the first two correction terms in separate sections.

THE FIRST-ORDER CORRECTION TERM

If a spectrophotometer is calibrated by use of a line source and narrow slits, the reading y of the wave-length scale can be assumed to correspond with the wave-length λ. Then, ignoring the terms of second and higher order, the spectral transmittance $t(\lambda)$ of the sample is

$$t(\lambda)=T(\lambda)-a_1[dT(\lambda)/d\lambda]. \qquad (13)$$

[9] This does not apply if any of the functions has a structure that is fine by comparison with the width of the slit. In that case, the above solution does not converge.

Suppose now that the sample is a filter from the set used by Van den Akker in his method of determining the wave-length error. Over the limited spectral range employed, the spectral transmittance of such a filter can be represented by

$$t(\lambda)=p+q\lambda,$$

where p and q are constants. In terms of the variables used previously, this becomes

$$t(y+x)=t_0+t_1x,$$

where t_0 and t_1 are constants for a given adjustment of the instrument. Reference to Eqs. (4) and (11) will show that, for filters with these characteristics

$$T(y)=t_0+t_1\frac{\int_{-\infty}^{\infty}W(y,x)x\,dx}{\int_{-\infty}^{\infty}W(y,x)\,dx}$$

$$=t_0+t_1a_1=t(y+a_1).$$

From the fact that $T(y)$ is seen to be equal to $t(y+a_1)$, it follows that a_1 is exactly the wave-length error that is found by Van den Akker's method of calibration. Hence, for any sample, multiplying the slope of the observed transmittance at any wave-length by the wave-length error at that wave-length accomplishes the first-order correction.

It is interesting to note that

$$a_1=\frac{\int_{-\infty}^{\infty}W(y,x)x\,dx}{\int_{-\infty}^{\infty}W(y,x)\,dx}$$

and that this expression is of the form that one would use in calculating where the center of mass of the pass band of the entire optical system lies with reference to an origin at y. It follows from this that the optical compensator discussed in an earlier section can be regarded as a device for adjusting the center of gravity of the pass band so as to make $a_1=0$. It does more than this, however, because, with the type of functions that are ordinarily encountered in spectrophotometry, it makes the function $W(y,x)$ nearly symmetrical about $x=0$ when $W(y,x)$ is regarded as being a function of x. Reference to the derivation of Eqs. (11) will show that, if $W(y,x)$ is symmetrical, all the odd coefficients, a_1, a_3, a_5, etc. are zero.

THE SECOND-ORDER TERM

As discussed in an earlier section, the general procedure in correcting slit-width errors is to regard every term in Eq. (10) as a photometric error, and

to employ as many terms as may be necessary in a given set of circumstances. If only the first and second terms are important, it is somewhat simpler to attribute the first correction term to an error in the wave-length calibration. If the first term is so regarded, it is easily shown that

$$t(y+a_1)=T(y)-[a_2+(a_1^2/2)][d^2T(y)/dy^2] \quad (14)$$

where a_1 is the wave-length error.

The new coefficient of the second-order correction term can be found from measurements made by the instrument itself, using samples whose transmission characteristics bear some known relationship, one to the other. For example, let two pieces of colored glass be cut from the same melt. Then, if proper compensation is made for reflection losses at the time of measurement, it is known from Bouguer's Law that, at any wave-length, the true transmittances of the glasses are related as follows.

$$t_2=t_1^n$$
$$(dt_2/d\lambda)=nt_1^{n-1}(dt_1/d\lambda)$$
$$(d^2t_2/d\lambda^2)=nt_1^{n-1}(d^2t_1/d\lambda^2)+n(n-1)t_1^{n-2}(dt_1/d\lambda)^2$$

where n is the ratio of their thicknesses. The spectrophotometer readings for the two glasses are

$$T_1=t_1+\alpha_1(dt_1/d\lambda)+\alpha_2(d^2t_1/d\lambda^2)$$
$$T_2=t_2+\alpha_1(dt_2/d\lambda)+\alpha_2(d^2t_2/d\lambda^2).$$

By substitution, T_2 can be expressed in terms of t_1 and its derivatives. Also, T_1 can be raised to the nth power by means of the binomial theorem. When this is done, it is found that, neglecting higher order terms

$$T_2-T_1^n=[\alpha_2-(\alpha_1^2/2)]n(n-1)t_1^{n-2}(dt_1/d\lambda)^2.$$

Then, to a close approximation, the coefficient of the second-order correction term is

$$[a_2+(a_1^2/2)]=[\alpha_2-(\alpha_1^2/2)]$$
$$=\frac{T_2-T_1^n}{n(n-1)T_1^{n-2}(dT_1/d\lambda)^2}. \quad (15)$$

Although this coefficient has a formidable appearance, it should be remembered that, in most cases, it varies so slowly with wave-length that only a few points are needed to plot the coefficient as a function of wave-length. Once this curve has been plotted, it is a simple matter to make the second-order correction for any sample, merely by determining the product of the coefficient and the second derivative of the observed curve of spectral transmittance. The method of second differences is a convenient procedure in the determination of the second derivative of the observed curve.

Having found in the preceding section that the coefficient of the first-order correction term is related to the center of gravity of the pass band of the optical system, it is natural to look for some geometrical interpretation for the coefficient of the second term. From the definitions of α_1 and α_2 given previously, it follows that

$$2\left(a_2+\frac{a_1^2}{2}\right)=\frac{\int_{-\infty}^{\infty}W(y,x)x^2dx}{\int_{-\infty}^{\infty}W(y,x)dx}-a_1^2. \quad (16)$$

The first term on the right-hand side of this equation may be regarded as the moment of inertia of the pass band of the optical system about an axis at y, assuming the mass to be unity. From the discussion in the preceding section, it is clear that the center of mass of the pass band is at a distance a_1 from an origin at y. Hence, from the parallel axis theorem in mechanics, the coefficient $[a_2+(a_1^2/2)]$ is just half the moment of inertia of the pass band about an axis through its center of mass.

AUTOMATIC CORRECTION

The original purpose of this investigation was to explore the possibility of providing a spectrophotometer with automatic means for correcting the slit-width error, with special reference to the type of spectrophotometer that has been described by one of us.[10] We had in mind originally that, if the second slit of the double monochromator were made to oscillate, either actually or effectively, the phototube would receive a signal that could be interpreted in terms of the derivatives of the spectral transmittance curve of the sample. The optical compensator described in the section entitled The Wave-Length Calibration eliminated the need for all the corrections involving the odd derivatives, leaving only the correction involving the second derivative, inasmuch as the other even derivatives ordinarily have negligible effects.

Oscillating the wave-length of the pass band of the instrument did not prove to be an eminently satisfactory method of introducing the second-order correction. If the oscillation takes place at the synchronous frequency, the amount of second-order correction that can be introduced exactly compensates for the effective increase in slit width due to its oscillation, with no correction for the actual width of the slit. If the oscillation is made to take place at a non-synchronous frequency, the signal thus generated can be separated from the carrier signal by filtering. This signal can then be amplified to the desired extent, and can be made to introduce the proper amount of correction through a differential gear in the recording mechanism or in some equivalent manner. The fact that the amount of correction varies with the gain of the amplifier is only one of the undesirable features of such an arrangement.

[10] Arthur C. Hardy, J. Opt. Soc. Am. 25, 305 (1935).

After investigating many possibilities, it seemed to us that the simplest device is a retardation plate inserted between the Wollaston prism and the rotating Rochon prism. When such a device is used, the phase of the signal received by the phototube is a function of wave-length; and, for any wave-length setting of the instrument, the retardation plate can have such a thickness that the out-of-phase signal automatically supplies the second-order correction. To provide for varying the thickness of the retardation plate as the spectrum is traversed, the plate can be in the form of wedges (like a Babinet compensator, except that the optic axes should be parallel). Such wedges can be adjusted by means of the proper cam operated by the wave-length-drive mechanism.

THE EFFECTIVE WIDTH OF THE SLIT

If the entrance slit of an idealized monochromator were infinitely narrow and diffraction effects could be ignored, the pass band of the instrument would be rectangular in shape, and the width of the pass band would be exactly the width of the exit slit, expressed in wave-length units. With an entrance slit of finite width, the pass band of the monochromator is generally trapezoidal in shape, becoming triangular when the image of the entrance slit has the same width as the exit slit. In practice, one does not use a monochromator that can be assumed to possess no selective absorption, lens aberrations, etc. Nor does he use the monochromator by itself, since it is invariably combined with a light source and receptor whose characteristics modify the shape of the pass band. In the search for some reasonable definition of slit width under these circumstances, it has seemed to us that, since the pass band can have a great variety of shapes, its width should be defined with reference to the error that it causes. It has been seen that the first-order error can be regarded as a wave-length error and that the errors of higher order than the second are usually negligible. It seems best, therefore, to use the second-order error as the measure of the effective width of the slit. There is naturally a need for some standard slit shape to use as a reference; and, since there is no ambiguity concerning the width of the slit when the pass band is rectangular in shape, we propose that the width of the equivalent rectangular pass band be used to specify the effective width of the pass band when it has any other shape. If one evaluates $(a_2+a_1^2/2)$, the coefficient of the second-order term, for a rectangular pass band of width w and equates it to the coefficient when the pass band is of arbitrary shape, it is found that

$$w=(24[a_2+(a_1^2/2)])^{\frac{1}{2}}. \tag{17}$$

In the preceding section, it was shown how the coefficient of the second-order term can be determined.

TWO MISCELLANEOUS COROLLARIES

The photometric scale of a spectrophotometer is frequently calibrated in terms of optical density rather than spectral transmittance. When this is done, Eq. (14) can be shown[11] to take the following form

$$d(y+a_1)=D(y)-\left[a_2+\frac{a_1^2}{2}\right]\times\left[\frac{d^2D(y)}{dy^2}-2.3\left(\frac{dD(y)}{dy}\right)^2\right] \tag{18}$$

where $d(y+a_1)$ is the true density at any wave-length and $D(y)$ is the indicated value of the density. It will be noted that, in Eq. (18), the second-order correction term involves the first derivative of the spectral density curve as well as the second derivative.

Another useful corollary can be derived for the special case where the spectral density curve of the absorbing substance has a maximum (or minimum) at the wave-length at which the density is being determined. This case occurs frequently in the measurement of the concentration of an absorbing substance in solution, it being the usual practice to make the measurement at an absorption band. Since a similar measurement is always made for another solution of the same substance at a known concentration, it is of interest to evaluate the effect of the two slit-width errors on the determination of the concentration of the unknown. It has been shown elsewhere[11] that the ratio n of the concentrations is

$$n=m+2.3m(m-1)\left(3\alpha_4-\frac{\alpha_2^2}{2}\right)\frac{1}{D_1}\left(\frac{d^2D_1(u)}{dy^2}\right)^2, \tag{19}$$

where m is the observed value of the ratio and D_1 is the density of the standard solution. It will be noted that, although two slit-width errors are involved, they tend to compensate one another, the correction term being of a higher order than in the determination of the individual densities. This justifies the practice of making measurements of this sort at an absorption band, if justification is necessary.

ACKNOWLEDGMENT

We take this opportunity to thank Professor Francis B. Hildebrand of the Department of Mathematics at the Massachusetts Institute of Technology for much advice and assistance in the solution of the integral equation.

[11] For details, see Bachelor's Thesis of F. Mansfield Young, M.I.T., May, 1948.

A Preliminary Investigation of the Spectra of Uranium Isotopes*

J. RAND MCNALLY, JR.
Carbide and Carbon Chemicals Corporation, Oak Ridge, Tennessee
(Received December 15, 1948)

The isotope displacement effect is discussed with relation to other spectro-isotopic effects. The results of a preliminary investigation of this effect in uranium isotopes are presented. Spectrum shifts as large as a wave number between the U^{235} and U^{238} spectra are not uncommon, the shifts usually being toward the violet for the light isotope.

These wave-length differences have been correlated to the spectroscopic energy systems of U I and U II and are found to be of two types: (1) a simple isotopic displacement arising from configuration-nucleus interaction, and (2) a complex isotopic displacement arising from perturbations between close-lying levels. The magnitude of shift in U I is generally of the order 0.3 cm^{-1}, but ranges from -0.7 cm^{-1} to 1.5 cm^{-1} in U II. Configurations involving the s^2 electron group show the largest isotope shifts indicating an additive type of interaction for the s electrons and the nucleus.

INTRODUCTION

THE structure observed in line spectra is usually classified as fine structure or hyperfine structure. Fine structure arises from the electronic properties of spin, angular momentum, and magnetic moment associated with the electronic configurations. Hyperfine structure involves the properties of the nucleus as well. Nuclear spin and nuclear magnetic moment give rise to what is commonly called true hyperfine structure, while the nuclear mass is responsible for several types of isotope structure.[1] This paper is concerned primarily with isotope structure in line spectra, with particular emphasis on uranium.

The simplest kind of isotope structure is that due to the reduced mass variation in the Rydberg constant, and is frequently referred to as the normal effect. This normal effect has actually been observed in only a relatively few cases because of its rapid decrease with increasing atomic weight. For the lightest elements, hydrogen and deuterium, the normal effect is of the order of several wave numbers, while for uranium, the normal effect is negligibly small. Hughes and Eckart[2] showed that the effect in non-hydrogen-like atoms is considerably more complicated than a simple reduced mass correction. This added complexity is referred to as the specific effect, and has been observed in the lighter elements such as lithium,[2] helium,[3] neon,[4] and magnesium.[5]

The isotope displacement effect in the heavy elements was first observed by Schuler and Keyston[6] in the spectrum of thallium. In a number of spectrum lines they observed that the center of gravity of the h.f.s. components of the 203 isotope did not coincide with that of the 205 h.f.s. components. From this they concluded that one or both of the energy levels of one isotope was shifted with respect to the energy levels of the other isotope. Other isotopic shifts were soon recognized in the heavy elements mercury,[7] samarium,[8] lead,[9] tungsten,[10] and platinum.[11,12] The theory of isotope displacement in the heavy elements is not completely developed. It was suggested by Breit[13] that the addition of neutrons to the nucleus results in a dimensional change, such that the penetrating electrons experience slightly different binding forces. Breit's calculations for mercury, thallium, and lead indicate fair agreement with the experimental data, but it is probable that other influences should also be considered.

ISOTOPE DISPLACEMENTS IN THE HEAVY ELEMENTS

Perhaps the most comprehensive data on isotope displacements in the heavy elements have been given for platinum.[11] The important isotopes of platinum are 194, 195, 196, and 198. The isotope structure of one of the spectrum lines is shown in Fig. 1. The heavy black lines correspond to the even isotope lines, and the dotted line to the position of the center of gravity of the odd mass components. The separation of successive even mass isotopes is approximately constant and about 22 milli-wave numbers per mass unit. The centroid of the 195 h.f.s. pattern does not show the regularity of shift of the even masses but indicates greater shift to the ultraviolet.

Isotope displacements in the complex mercury

* Based on work performed under contract for the AEC by Carbide and Carbon Chemicals Corporation at Oak Ridge, Tennessee.

[1] S. Tolansky, *Hyperfine Structure in Line Spectra and Nuclear Spin* (Methuen & Company, Ltd., London, 1946).
[2] D. S. Hughes and C. Eckart, Phys. Rev. **36**, 694 (1930).
[3] A. Andrew and W. W. Carter, Phys. Rev. **74**, 838 (1948).
[4] J. H. Bartlett, Jr. and J. J. Gibbons, Jr., Phys. Rev. **44**, 538 (1933).
[5] J. P. Vinti, Phys. Rev. **56**, 1120 (1939).
[6] H. Schuler and J. E. Keyston, Zeits. f. Physik **70**, 1 (1931).
[7] H. Schuler and E. G. Jones, Zeits f. Physik **79**, 631 (1932).
[8] H. Schuler and T. Schmidt, Zeits. f. Physik **92**, 148 (1934).
[9] H. Kopfermann, Zeits f. Physik **75**, 363 (1932).
[10] N. S. Grace and H. E. White, Phys. Rev. **43**, 1039 (1933).
[11] S. Tolansky and E. Lee, Proc. Roy. Soc. **158A**, 110 (1937).
[12] B. Jaeckel, Zeits. f. Physik **100**, 513 (1936).
[13] G. Breit, Phys. Rev. **42**, 348 (1932).

TABLE I. Basic electronic states (U I).

Group A	$5f^36d7s^2$ $5f^36d^27s$ $5f^36d^3$	$5f^36d7s7p$ $5f^36d^27p$ $5f^37s^27p$
Group B	$5f^47s^2$ $5f^46d7s$ $5f^46d^2$	$5f^47s7p$ $5f^46d7p$

TABLE II. Basic electronic states (U II).

Group A	$5f^37s^2$ $5f^36d7s$ $5f^36d^2$	$5f^37s7p$ $5f^36d7p$
Group B	$5f^47s$ $5f^46d$	$5f^47p$

group also have received considerable attention. Mercury has six prominent isotopes: 198, 199, 200, 201, 202, and 204. The general appearance of its energy levels showing the isotope shift on a magnified scale is shown in Fig. 2. Characteristic of the displacement effect in all the heavy elements, the binding energy is greatest for the isotope of smallest mass, and increases in a regular way for the even isotopes. The odd mass isotopes show slightly greater binding energy than this regularity would indicate.

There are, then, at least two distinct phenomena to be found in the isotope displacement effect: First, there is a regular decrease in binding energy with increase of nuclear mass; and, second, there is an additional shift toward greater binding energy occurring in the case of the odd masses. In addition to these two primary effects, one might expect irregularities in the regular, even mass, isotope displacement because of possible discrete modes of

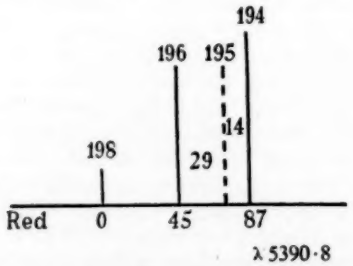

FIG. 1. Isotope structure in platinum line 5390A (after Tolansky and Lee).

binding additional neutrons in groups of twos. This has in fact been observed in the case of samarium,[8] where the addition of the second neutron pair gives an isotope shift which is only half as large as that due to the first added pair of neutrons. To further complicate the picture of the displacement effect, perturbations between close-lying levels of similar quantum nature should be expected also, just as in the case of fine structure perturbations.

The fact that there are no transitions between the energy levels of one isotope and those of another prevents one from measuring how much one energy system has been shifted relative to the other unless the absolute binding energy of the individual energy systems is obtained. Thus, these displacements measure only the relative shifts of two energy states. In most instances, however, the shift is considerably larger for the low energy states because of the greater penetration of electrons in these ground state configurations. Tolansky[1] pointed out that the terms which show the largest displacements do arise from configurations involving the strongly penetrating electrons. For example, the levels arising from the $5d^86s^2$ configuration in platinum show isotope shifts almost exactly twice that of configurations involving only one $6s$ electron. The displacement was found to be practically independent of the quantum character of the energy states (e.g., $^3F_2$, $^3F_3$) but markedly dependent on the degree of penetration of the optical electrons.

ISOTOPE DISPLACEMENTS IN URANIUM

The heavy elements in which the displacement effect has so far been studied have relatively simple spectra involving simple electron configurations. For this reason, a more thorough interpretation of the effect would be had through comparisons of the isotopic binding energies of many different type electrons (such as s, p, d, and f), as well as through investigations of large numbers of energy states involving complex electron configurations. The prospect of obtaining such information in the complex spectra of uranium was not recognized by ear-

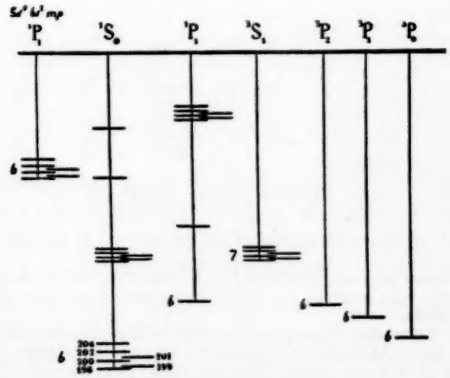

Isotope displacements in terms of the HgI spectrum. The displacements in all the terms are in the same order as those numbered in 6^1S_0.

FIG. 2. Isotope structure of energy levels in neutral mercury (after Tolansky).

lier investigators because of the approximate monoisotopicity of natural uranium. However, the availability of several isotopes of uranium now makes possible a study of truly complex isotopic spectra.

The spectra of uranium have been recorded by numerous investigators,[14] probably the most complete tabulation of wave-length data being found in the M.I.T. catalog. Attempts to analyze the complex atom, however, proved fruitless until very recently when the Zeeman effect was applied to the problem. The neutral atom, characterized by six valence electrons, succumbed to classification by Kiess, Humphreys, and Laun[15] at the National Bureau of Standards, and independently by Schuurmans, van den Bosch and Dijkwel[16] at Amsterdam. The spectrum of the singly-ionized atom was broken into by the group at Amsterdam and also independently by McNally and Harrison[17] at M.I.T. Analogous to thorium, it was found that uranium is a member of the second rare earth series of elements. Eleven important electron configurations of the neutral atom are shown in Table I. It is interesting to note that there are 386 energy levels associated with the f^3ds^2 electron configuration, but over 3000 levels in the f^3d^2s configuration and correspondingly many in the other configurations. Table II shows comparable complexity for the uranium ion—there being at least eight important configurations.

The first measurements of an isotope shift in uranium were reported by Long and Smith[18] at Oak Ridge, and the effect has already been satisfactorily applied by Burkhart, Stukenbroeker and Adams[19] at Oak Ridge to the determination of the isotopic constituency of mixtures of U^{235} and U^{238}. The magnitude of the effect is unusually large and ranges from a red shift of about 0.7 wave number for certain lighter isotope lines, to a violet shift of about 1.5 wave numbers. Wave-length separations as large as 0.7A have been observed.

A typical shift of lines in U^{235} and U^{238} spectra is shown in Fig. 3. Here, wave-length 4241A indicates a very slight red shift of U^{235}, while the violet shift of U^{235} is quite pronounced for the uranium line at wave-length 4244A. The violet shift here is approximately 1.4 wave numbers or about one-fourth of an angstrom. This corresponds roughly to a shift of 0.5 wave number per mass unit.

TABLE III. Average line shifts (U I)

Configuration	Shift ($\sigma_{235}-\sigma_{238}$)
f^3ds^2	0.3 cm^{-1}
f^3d^2s	0.1 cm^{-1}

A preliminary investigation of these line displacements in uranium has given a correlation of the effect with the energy systems of neutral and singly-ionized uranium. The shift is larger in the ion, although several of the sensitive lines of the neutral atom do show large shifts. As in the spectra of platinum and mercury, the configurations which involve the s^2 group show the largest shifts, substantiating the theory that isotope shifts are primarily of an additive nature.

The magnitude of the displacement and its dependence on two of the low electron configurations in neutral uranium are shown in Table III. The s^2 type configuration does show a larger average shift than the configuration involving only a single s electron. Table IV shows the average line shift in the case of singly-ionized uranium. Here, the penetrating s electrons give large violet shifts of the U^{235} lines while the relatively non-penetrating d or f electrons give a red shift in the U^{235} spectrum. If one assumes that the isotopic shifts in the excited configurations average to zero, these numbers then represent the individual energy level shifts.

Perturbations of close-lying levels, similar to those observed in mercury by Schuler and Jones,[6] are also found in uranium isotopic spectra. These further complicate the determination of meaningful average line shifts because of the sometimes large irregular shifts superimposed on the simple isotope

FIG. 3. Isotope shifts in uranium. The top spectrum of natural uranium shows three lines: 4241.669A (U II—40,50), 4244.372A (U II—25,25), and 4246.261A (U I—30,2). The middle spectrum is of a mixture of U^{235} and U^{238}, and the bottom spectrum of U^{235}. Isotope shifts measure 0.38 cm^{-1} (red shift), 1.38 cm^{-1} (violet), and 0.28 cm^{-1} (violet), respectively, and involve the low energy states f^3d^2, f^3s^2, and f^3ds^2, respectively.

[14] H. Kayser, *Handbuch der Spectroscopie*, (S. Hirzel, Leipzig, 1912) p. 734; K. W. Meissner, Ann. d. Physik **50**, 713 (1916); C. C. Kiess and W. F. Meggers, BS Sci. Pap. 16, 51 (1920) S372; G. R. Harrison, M.I.T. *Wave-length Tables* (John Wiley & Sons, Inc., New York, 1939); M.I.T. Card Catalog, M.I.T. Spectroscopy Lab., Cambridge, Massachusetts.

[15] C. C. Kiess, C. J. Humphreys, and D. D. Laun, J. Nat. Bur. Stand. of Research, RP 1729, **37**, 1 (1946).

[16] P. Schuurmans, J. C. van den Bosch and N. Dijkwel, Physica **XIII**, 117 (1947).

[17] J. R. McNally, Jr. and G. R. Harrison, unpublished material, M.I.T. Spectroscopy Lab., Cambridge, Massachusetts.

[18] D. R. Long and D. D. Smith, unpublished material, Carbide and Carbon Chemicals Corporation, Oak Ridge, Tennessee.

[19] L. E. Burkhart, G. Stukenbroeker, and S. Adams, Document Y-54, Stable Isotope Group, Carbide and Carbon Chemicals Corporation, Oak Ridge, Tennessee.

TABLE IV. Average line shifts (U II).

Configuration	Shift ($\sigma_{138}-\sigma_{144}$)
f^3s^2	0.9 cm^{-1}
f^3ds	0.2 cm^{-1}
f^3d^2	−0.2 cm^{-1}
f^4s	0.3 cm^{-1}
f^4d	−0.4 cm^{-1}

displacement. Table V illustrates such a case involving two perturbing energy levels in singly-ionized uranium. The levels are 23241 and 23554, both of which have a J value of 11/2. Note that despite large variations in the individual line shifts, the total average over a large number of lines involving each low level is in excellent agreement with the local average of the line pairs.

The marked dependence of the magnitude of isotope shift on the particular electron configurations may be used to advantage in extending the classification of the uranium spectra. Already we have applied this method to discover new energy states in uranium. There are still well over a hundred unclassified lines which show isotope shifts of magnitude one wave number or more. It is suspected that many of these lines belong to the sensitive configuration f^3s^2 of singly-ionized uranium, from which only two levels from this important configuration have been discovered.

CONCLUSION

This work on the isotope shift in uranium and on the classification of its spectra is continuing. It is believed that higher accuracy of measurement and more extensive data will be necessary to formulate more conclusive results than have been presented in this preliminary paper.

The investigation of other isotopes in the last row of the periodic table, such as those of thorium and plutonium, should aid considerably in the development of the theory of isotopic displacements. The wide splittings observed in uranium isotopic spectra indicate a probable similar wide structure in these other elements.

TABLE V. Isotopic perturbations in singly-ionized uranium.

Energy level	Isotope Shift (cm^{-1}) $^4I_{\frac{11}{2}}$	$^6K_{\frac{11}{2}}$	$^6L_{\frac{11}{2}}$	$^6K_{\frac{13}{2}}$
23241	0.38	−0.45	−0.46	−0.53
23554	1.38	0.62	0.57	0.58
Local av.	0.88	0.09	0.06	0.03
Total av.	0.90	0.10	0.10	0.10

ACKNOWLEDGMENTS

This work has been carried out as a special project of the Stable Isotopes Group under the supervision of Dr. C. P. Keim, whose interest and encouragement are gratefully acknowledged. The assistance of L. E. Burkhart on technical matters and the enthusiastic cooperation of D. D. Smith, who supplied the wave-length data on the isotopic shifts, are also gratefully acknowledged.

Note added in proof:—The author regrets overlooking a recent letter to the editor in The Physical Review (A. J. Dempster, Phys. Rev. **73**, 1125, 1948) concerning isotope 152 of samarium. The resolved, even-mass isotope shift in the samarium spectrum line λ5321A has been reported to be:[8]

$\sigma_{144}-\sigma_{148}=0.112$ cm^{-1} (overlapped by Sm^{149})
$\sigma_{144}-\sigma_{150}=0.180$ cm^{-1}
$\sigma_{144}-\sigma_{152}=0.283$ cm^{-1}
$\sigma_{144}-\sigma_{154}=0.333$ cm^{-1}

These $\Delta\sigma$'s, with the exception of that involving mass 152, can be fitted to an empirical equation in terms of the ΔM's as follows:

$$\Delta\sigma=0.0206\Delta M+0.002\langle\Delta M\rangle^2_{Av}-0.000073\langle\Delta M\rangle^3_{Av}$$

M	ΔM	$\Delta\sigma$(cm^{-1})	dev(cm^{-1})
144	0	0.000	0.000
148	4	0.110	0.002
150	6	0.180	0.000
152	8	0.255	0.028
154	10	0.333	0.000

It is pointed out in the present article that discrete modes of binding additional neutrons in groups of twos might introduce anomalies in the usually regular even-mass shift. Dempster presents evidence that the α-active isotope of samarium is not mass 148 as had been previously listed in the literature, but is mass 152. The anomalous spectrum shift of 0.028 cm^{-1} (or 3.5 microvolts) in the Sm^{152} component is therefore probably closely related to this α-activity and it is suggested that it may arise from new polarization effects or a marked discontinuity in the building up of the samarium nucleus. Samarium is unique in that it is the only element recognized as having stable isotopes and an α-active isotope.

JOURNAL OF THE OPTICAL SOCIETY OF AMERICA VOLUME 39, NUMBER 4 APRIL, 1949

The Determination of Flame Temperatures by Infra-Red Radiation

SHIRLEIGH SILVERMAN*
Applied Physics Laboratory, The Johns Hopkins University, Silver Spring, Maryland
(Received December 28, 1948)

The determination of flame temperatures by infra-red radiation has been reinvestigated based on the experiments of Schmidt, Henning, and Tingwaldt. Criteria for such a brightness thermometer are described, and means for minimizing some of the errors are discussed. It is concluded that (a) infra-red emission for the CO_2 band at 4.4 microns can be used at least for non-luminous flames which contain CO_2 as one of the products of combustion, (b) temperatures are obtained that are consistent to within less than 5 percent, and (c) observed temperatures tend to be lower than theoretical temperatures.

INTRODUCTION

THE subject of flame temperatures has always been of especial interest to investigators of combustion phenomena seeking to improve fuel performance and to understand better reaction processes. For the measurement of high temperatures (above 2000°K), particularly for turbulent flames of high mass flow, spectrographic methods have held much promise. In general three types of spectrographic techniques have been employed, all of which must assume thermal equilibrium in the flames studied. They are (i) the classical sodium line reversal technique, recently brought to a new peak of accuracy and usefulness,[1] (ii) the infra-red brightness thermometer,[2-4] which requires the infra-red analog of optical pyrometry, and (iii) the temperature dependence of the intensity distribution of the vibration-rotation lines of a thoroughly understood radical such as OH (for an excellent monograph on this subject there exists a report by Dieke and Crosswhite[5]). The work presented here deals with some results obtained by infra-red brightness thermometry of some laboratory flames.

The infra-red brightness thermometer is valid depending on the following conditions: (a) that the radiating gases be in thermal equilibrium, (b) that Kirchoff's law be valid for the radiating gases, and (c) that a comparison continuum from a blackbody or other standard emitter be available. Early work[2,3] has shown that flame gases such as ordinary laboratory flames in the regions outside the reaction zones are nearly in thermal equilibrium, since temperatures determined from brightness measurements in different spectral regions are in fairly good agreement. Kirchoff's law may be checked to substantiate condition (a) and the absence of chemiluminescence, and a standard continuum is readily available in the form of a heated metal strip or globar burner.

EXPERIMENTAL

To determine the temperature of a flame, its radiation is passed through a spectrometer set at a given wave-length, where there is pronounced emission. The energy recorded by the radiometric system is compared to that received from a continuous source whose temperature and emissivity are known. The calculations then follow from the laws of Kirchoff and Planck, namely,

$$D_G \sim \alpha_G (C_1/\lambda^5)(\exp(C_2/\lambda T_G)-1)^{-1} d\lambda, \quad (1)$$

$$D_F \sim \alpha_F (C_1/\lambda^5)(\exp(C_2/\lambda T_F)-1)^{-1} d\lambda, \quad (2)$$

$$D_T = (1-\alpha_F) D_G, \quad (3)$$

where D_G is the radiometer deflection for a gray-body of emissivity α_G at a temperature T_G, at wave-length λ for a spectral band of width $d\lambda$; D_F is the deflection at the same spectrometer setting for a flame at temperature T_F and emissivity α_F, while D_T, the flame transmission, is defined by Eq. (3). Substituting for α_F from Eq. (3) and dividing

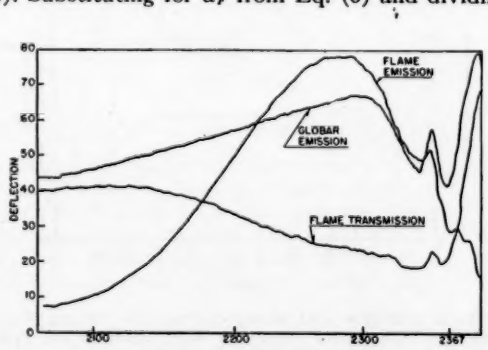

FIG. 1. These represent unretouched working curves of CO+oxygen flame emission and transmission, and globar emission (globar temperature: 1410°K).

* The work described in this paper was supported by the Bureau of Ordnance, U. S. Navy, under Contract NOrd-7386.

[1] H. M. Strong and F. P. Bundy, Phys. Rev. **74**, 1221 (1948).
[2] H. Schmidt, Ann. d. Physik **29**, 1027 (1909).
[3] F. Henning and C. Tingwaldt, Zeits. f. Physik **48**, 805 (1928).
[4] B. Lewis and G. von Elbe, *Combustion Flames and Explosions of Gases* (Cambridge University Press, London, 1938), Chap. XIX.
[5] G. H. Dieke and H. M. Crosswhite, Report CF-790 (The Johns Hopkins University, 1948).

Eq. (2) by Eq. (1) we obtain:

$$T_F=\frac{C_2}{\lambda \ln[1-(D_G-D_T/\alpha_G D_F)(\exp(C_2/\lambda T_G)-1)]}. \quad (4)$$

The experimental set-up consisted of a Perkin-Elmer 12-C spectrometer with automatic wave-length drive and recorder. The spectrometer was flushed continuously with dry nitrogen to reduce atmospheric absorption. An a.c. (Baird Associates) bolometer was used as the radiation receiver with a 10-cycle tuned amplifier and synchronized light chopper in the radiation beam. The flames were burned in a water-cooled flue with open ports placed directly in front of the globar housing. Radiation from either the flame or the globar, which was the standard continuum, filled the collimating mirror of the spectrometer.

Since we are concerned essentially with CO_2 radiation in these experiments, a LiF prism was used throughout for optimum resolution. A mechanical rectifier of the usual vibrating breaker type was used on the output of the tuned amplifier to effect linearity between energy incident upon the bolometer and amplifier output. The D_G *vs.* λ-curve was obtained with a globar, and the flame turned off. The D_F *vs.* λ-curve was obtained with continuum blanked out and flame burning. The D_T *vs.* λ-curve was obtained with the light chopper operating between continuum and flame.[6] This permits the flame to act as an absorption cell only, for its own radiation sends a d.c. signal to the bolometer and this is rejected by the tuned amplifier. The emissivity of the globar was determined[7] to be 0.84 in the spectral region 4–5 microns, and its temperature was determined by means of a Leeds & Northrup No. 8622 optical pyrometer. For optimum accuracy it is best to work with a band of high emissivity (generally, therefore, a fundamental and its wings) which lies in a region of the spectrum not too remote from the peak of the blackbody emission at the corresponding temperature. For hot CO_2, the very intense 4.4-mu band is found most suitable, although the 2.8-mu band can also be used. For the former band which consists of ν_3 and other bands for which $\Delta V_3=1$, analysis of repeated temperature measurements of a given wave-length setting indicates an experimental error of about 2.5 percent. Recorder noise caused by flame variations alone was less than one percent of the signal. Unretouched working curves are shown in Figs. 1 and 2. These curves supply the data for D_g, D_T, and D_F which are required for the calculation of T_F in Eq. (4).

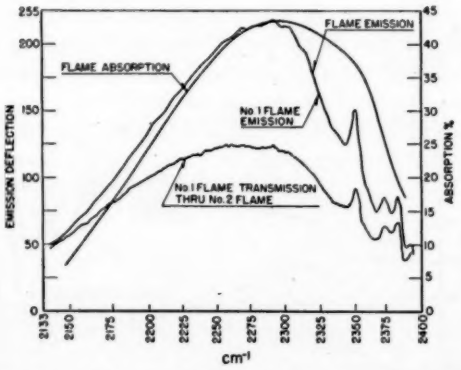

FIG. 2. Emission and absorption of CO—oxygen flame. These are unretouched curves for flame emission and flame transmission used for calculating flame absorption.

DISCUSSION

There are three principal sources of error in infra-red temperature measurements of this sort: (1) one obtains an average flame temperature since one observes radiation from the entire flame thickness; (2) self-absorption by the cooler outer layers of the flame tends to reduce the observed emission, and hence lowers the observed brightness temperature; (3) flame absorption as measured above will be a function of the effective slit-width of the spectrometer. However, these errors may be minimized. For example, errors of type 3 require that the absorptivity α_F at any wave-length λ be determined as a function of slit width. It is found that a constant value of α_F is attained for a slit width which is several times the fine structure separation of the vibration-rotation lines in the emission band. For CO_2 at 4.4 mu, this slit width is approximately 8 cm^{-1}. This was further verified by determining α_F using one flame as emitter and a second similar flame as absorber. Here α_F should be independent of the slit width since both emitter and absorber are affected identically by slit width corrections. Such curves are shown in Fig. 2. (1) and (2) may be minimized if one plots temperature *vs.* wave-length throughout an emission band, basing one's calculations on the emission and absorption data as obtained in the manner described above. The calculated temperature may be expected to rise with diminishing frequency for the following reason. The low frequency wing of the 4.4-mu CO_2 emission band is unusually pronounced both in extent and in intensity. In part this is caused by temperature broadening of individual rotation lines of high J-values from the transition 0 0 1→000.[8] Moreover, assuming the usual Boltzmann energy dis-

[6] S. Silverman, R. C. Herman, and G. A. Hornbeck, J. Chem. Phys. 16, 155 (1948).
[7] S. Silverman, J. Opt. Soc. Am. 38, 898 (1948).
[8] G. B. B. M. Sutherland, paper presented at 3rd International Combustion Symposium, University of Wisconsin, September, 1948.

tribution for temperatures around 2500°K, it is seen that a considerable portion of the wing arises from higher levels in the transitions involving the quantum number V_3. The higher levels are excited principally in the hottest part of the flame, *viz.*, the center; therefore, self-absorption by the cooler outer flame of the wing will be much less than self-absorption of the peak of the band. A rough estimate of the expected band shape leads one to expect that the bulk of the radiation at frequencies less than about 2200 cm^{-1} should come from the upper vibrational levels and, therefore, from the hottest parts of the flame. Consequently, if temperature be plotted *vs.* frequency, one should expect a rise in calculated temperature with decreasing frequency to about 2200 cm^{-1}, and a relatively uniform temperature from that point on. Such a plot is shown in Fig. 3 which represents data for a typical CO−oxygen flame.

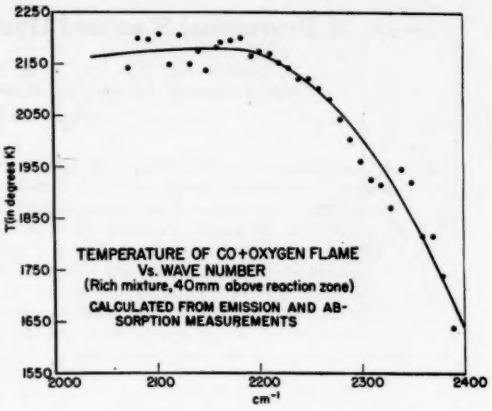

FIG. 3. This figure shows the plot of calculated temperature *vs.* frequency.

Experiments were also performed with CO−oxygen, oxy-methane, and oxy-acetylene flames. For all these flames, the emission of the 4.4-mu band of CO_2 was used. For the oxy-methane flame, temperatures ranged from 2100° to 2500°K, depending on the air-fuel ratio used, while for the oxy-acetylene flame values ranged from 2400° to 3000°K.

CONCLUDING REMARKS

The infra-red brightness technique may be applied to flame temperature measurements provided certain precautions are taken, particularly with respect to the phenomenon of self-absorption. Temperatures obtained are lower than the theoretically calculated values,[9] but this may be accounted for in part by the fact that the averaging technique employed included flame sections well above the zone of maximum temperature and in part by the fact that our flames were generally on the lean side. However, it is clear from the preceding section that temperatures measured at the lower frequencies will give values weighted toward the core temperatures, whereas temperatures measured at frequencies closer to the fundamental will give values weighted toward the cooler portions of the flame. In this latter frequency range for a very opaque gas the temperature will, in fact, be representative of the outer zones only. It is particularly worth noting that the experiments described herein indicate that the region of 2100 cm^{-1} is very suitable for temperature determinations of the usual hydrocarbon fuels. Since this region lies near the center of the well-known atmospheric transmission "window" around 4.7 mu, this technique should be applicable to temperature measurements of fairly distant sources (up to several hundred feet, at least) without excessive attenuation of the radiation.

The author wishes to express his thanks to Dr. R. C. Herman of this laboratory for several fruitful discussions in the course of these investigations.

[9] B. Lewis and G. von Elbe, reference 4, p. 399.

Physics Abstracts

For many years the dues of the American Physical Society have included a subscription to Physics Abstracts, published by the Institute of Electrical Engineers of London. There has been, however, no convenient method by which persons not members of the A.P.S. could receive this publication. The Optical Society of America has now instituted an arrangement under which any O.S.A. member can receive Physics Abstracts at an annual subscription price of $4.50. All correspondence in this connection should be addressed to the American Institute of Physics, 57 East 55th Street, New York 22, New York.

A Provisional Standard Observer for Low Level Photometry*

K. S. WEAVER
Kodak Research Laboratories, Eastman Kodak Company, Rochester, New York
(Received December 2, 1948)

A provisional observer for low level photometry is given by means of tables which show the relative spectral luminosity at luminance levels from the scotopic to the photopic regions. Derived tables show the spectral distribution of light from several Planckian or near Planckian sources, a Planckian radiator at 2360°K being used to define the illuminance scale.

Data are shown which indicate that a restricted additivity law, as herein defined, may be used at low luminance levels in evaluating stimuli of mixed spectral composition.

The I.C.I. standard photopic luminosity curve has been used as the terminal or photopic data in the formulation of this observer. However, data which have been accumulated in the 24 years since this luminosity function was adopted indicate that the blue-violet spectral region should be revised. The technique of low level photometry is discussed briefly.

INTRODUCTION

UNDER the date of June 15, 1942, there was issued a *Summary of American Opinion on BS/ARP18, British Standard Specification for Fluorescent and Phosphorescent Paint*, prepared by Dr. L. A. Jones of these Laboratories, at the request of the American Standards Association. With the approval of a majority of the authorities who contributed to the *Summary*, there was included a set of luminosity data which had been previously compiled for use in a general study of low brightness photometry.

These tables were based on observational data taken at the photopic and scotopic levels, together with interpolations for intermediate levels carried out by a method which was admittedly arbitrary but was considered reasonable as a first approximation.

Although the adoption of these luminosity data was considered merely tentative, mainly because of the inadequate experimental basis for the interpolation, the frequent requests received for copies of the tables indicate a continued interest which would seem to warrant their publication. It is highly desirable that the problem of low level photometry receive further discussion and experimental study, and a set of tables be accepted as a standard by the International Commission on Illumination.

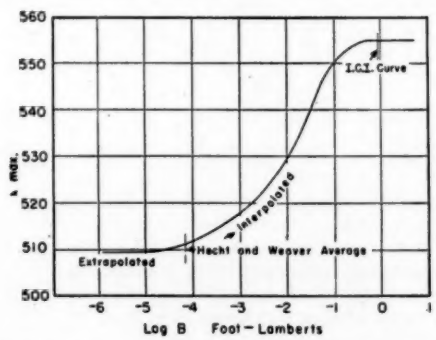

FIG. 1. $\lambda_{max.}$ *vs.* log$B$ as used for interpolation of luminosity curves.

METHOD USED IN THE INTERPOLATION

The I.C.I. luminosity curve was taken for the photopic region, that is, for luminance levels of about 0.55 foot-lambert or higher. The data of Hecht and Williams,[1] and of Weaver[2] were averaged to represent the luminosity function at 6.5×10^{-5} foot-lambert. Although Hecht and Williams used an intensity (specified as 2.7 times the dark-adapted threshold) which was probably lower than that used by Weaver, the curves are so nearly alike that the use of the average for the present purpose is justified.

The interpolation was carried out by a horizontal division of the wave-length intervals between these two curves into the same fractional intervals that are shown in Fig. 1, which represents the shift of the wave-length of maximum luminosity with luminance, Luminosity data for $\log^{-1}-4.5$ and $\log^{-1}-5.0$ foot-lambert were obtained by extrapolation, as indicated in Fig. 1. Figure 1 is based upon data previously published by the author,[2] for the lower luminance range combined with later unpublished data for the upper luminance range, and the data were adjusted to conform to the maximum of the I.C.I. curve of 555 millimicrons at a $\log^{-1}$ luminance of -0.25 foot-lambert.

The luminosity data derived by this procedure are listed in Table I for wave-length intervals of ten millimicrons and for the values of luminance shown as logarithms at the head of each column.

*Communication No. 1235 from the Kodak Research Laboratories.

[1] S. Hecht and R. E. Williams, "Visibility of monochromatic radiation and the absorption spectrum of the visual purple," J. Gen. Physiol. **5**, 1 (1922–23).

[2] K. S. Weaver, "The visibility of radiation at low intensities," J. Opt. Soc. Am. **27**, 36 (1937).

The maximum ordinate at each luminance level is unity.

CHOICE OF A STANDARD SOURCE FOR LOW LEVEL PHOTOMETRY

Because of the shift of the luminosity function with luminance, it is necessary to choose arbitrarily a light source of specified spectral composition as a standard for the specification of the luminance scale through the mesopic and scotopic regions. The illuminance or luminance obtained from sources of different spectral composition may be evaluated by comparison with the standard source, by means of a suitable photometer, or by computation, using a set of tables such as are described here.

At about the time the British Standard, BS/ARP 18, was received for comment, several photometricians in this country, including the writer, had been using a tungsten lamp at a color temperature of 2360°K for this purpose. This choice seemed logical in that it was easily obtainable and readily calibrated, of good stability because of the low temperature, and of relatively low candlepower, a convenience in low level photometry. The fact that British investigators were using the same standard made it even more desirable where test data were to be interchanged. For these reasons, the 2360°K source was used tentatively, as a standard, and all the tables which follow depend upon the photometric scale so defined.

TABLES DERIVED FROM TABLE I BASED ON A STANDARD SOURCE AT 2360°K

The I.C.I. luminosity data listed in Table II are the same as those in Table I. The data for lower luminance regions were obtained by multiplying each column of Table I by a factor chosen to yield a constant total luminous flux at all luminance levels for the standard source. This table gives the values of the relative spectral distribution of light for the equal-energy spectrum based on a standard source having a 2360°K blackbody distribution.

Table III is identical with Table II, except that all values were multiplied by 625 lumens per watt, the maximum efficiency of radiant energy at photopic levels for a value of c_2 of 14,320-micron degrees Kelvin, the value upon which the present international temperature scale is based. This table may be described as the absolute luminosity function when the photometric scale is based on a standard source at 2360°K.

In Tables IV to XI are given values of the spectral distributions of light for sources of color temperatures 2000°, 2360°, 2660°, 2850°, 3500°, and 5500°K, and for sunlight and daylight. In each table the total is adjusted to 100 percent for the I.C.I. data. The totals of the other columns show the relative effectiveness of the same amounts of energy at the lower levels.

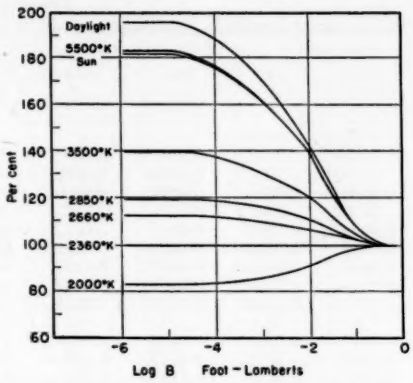

FIG. 2. Relative luminosity of several radiant sources as a function of luminance level.

The totals are plotted in Fig. 2. Here, the curve for 2360°K is horizontal at 100 percent, because a source at this temperature was used in defining the photometric scale. The curve for the equal-energy spectrum is very close to the curves for the 5500°K and sunlight sources throughout the whole luminance range. The effect of the choice of a different source for defining the photometric scale can readily be visualized by supposing that the curve for that source were moved to coincide with the 100 percent line, the ordinates of the other curves being kept at the same relative values.

METHODS IN LOW LEVEL PHOTOMETRY

Walsch,[3] in his résumé of low level photometry, recommends the use of a standard source at 2360°K, without employing compensating filters to reduce the color difference when it is encountered. Such a procedure may be expected to lead to results which depend upon the luminosity characteristic of the individual observer and therefore to difficulty in comparing data obtained in different laboratories.

It is now common practice to use compensating filters in photopic heterochromatic photometry, the visual characteristics of the observer becoming less and less a factor as a perfect energy match is approached. In some cases, such as in measurements on fluorescent or phosphorescent materials, which have a very low luminance, it may be difficult to determine the energy distribution and hence the kind of compensating filter required. In many cases, however, the spectral transmittance of the required compensating filter can be determined readily and the advantages of its use realized. One function of the luminosity tables is their use in the calculation

[3] J. W. T. Walsch, "The measurement or gauging of low values of illumination and brightness," Trans. I. E. S. (London) 6-7, 117 (1941–42).

TABLE I. Relative luminosity data.

λ	Log luminance (foot-lamberts) −0.25 I.C.I.	−0.5	−1.0	−1.5	−2.0	−2.5	−3.0	−3.5	−4.0	−4.5	−5.0
350									0.0002	0.0003	0.0003
6							0.0003	0.0004	0.0007	0.0008	0.0008
7					0.0002	0.0005	0.0009	0.0013	0.0018	0.0020	0.0022
8			0.0001	0.0002	0.0008	0.0015	0.0025	0.0034	0.0045	0.0051	0.0055
9	0.0001	0.0001	0.0002	0.0008	0.0022	0.0040	0.0063	0.0083	0.0104	0.0119	0.0127
400	0.0004	0.0004	0.0008	0.0022	0.0059	0.0098	0.0147	0.0185	0.0228	0.0253	0.0270
1	0.0012	0.0014	0.0023	0.0062	0.0140	0.0227	0.0305	0.0370	0.0452	0.0500	0.0530
2	0.0040	0.0044	0.0069	0.0152	0.0280	0.0427	0.0580	0.0690	0.0820	0.0900	0.0950
3	0.0116	0.0121	0.0165	0.0292	0.0505	0.0755	0.101	0.118	0.138	0.149	0.157
4	0.023	0.0240	0.0300	0.0496	0.0850	0.123	0.160	0.183	0.216	0.230	0.239
450	0.038	0.0395	0.0490	0.0810	0.136	0.187	0.237	0.268	0.310	0.326	0.339
6	0.060	0.0627	0.0775	0.127	0.202	0.277	0.339	0.376	0.423	0.441	0.455
7	0.091	0.0960	0.118	0.191	0.301	0.394	0.467	0.510	0.551	0.568	0.576
8	0.139	0.146	0.180	0.288	0.432	0.540	0.604	0.649	0.685	0.702	0.714
9	0.208	0.220	0.274	0.426	0.592	0.687	0.734	0.782	0.814	0.830	0.842
500	0.323	0.340	0.416	0.603	0.744	0.826	0.864	0.902	0.930	0.941	0.948
1	0.503	0.524	0.617	0.766	0.876	0.935	0.962	0.977	0.992	0.997	0.999
2	0.710	0.726	0.792	0.894	0.965	0.992	0.999	0.988	0.974	0.960	0.953
3	0.862	0.872	0.910	0.972	1.000	0.982	0.951	0.924	0.883	0.862	0.848
4	0.954	0.959	0.979	1.000	0.969	0.909	0.842	0.796	0.744	0.715	0.697
550	0.995	0.997	1.000	0.971	0.886	0.785	0.698	0.642	0.583	0.552	0.531
6	0.995	0.992	0.973	0.898	0.760	0.640	0.543	0.478	0.419	0.388	0.365
7	0.952	0.944	0.907	0.782	0.617	0.485	0.384	0.330	0.281	0.260	0.243
8	0.870	0.860	0.802	0.648	0.468	0.340	0.259	0.218	0.182	0.164	0.155
9	0.757	0.742	0.673	0.509	0.333	0.227	0.166	0.137	0.112	0.101	0.0945
600	0.631	0.616	0.544	0.374	0.224	0.145	0.101	0.0830	0.0670	0.0600	0.0560
1	0.503	0.490	0.416	0.257	0.142	0.0870	0.0600	0.0488	0.0388	0.0348	0.0324
2	0.381	0.366	0.296	0.168	0.0845	0.0504	0.0344	0.0280	0.0225	0.0202	0.0188
3	0.265	0.250	0.197	0.102	0.0480	0.0282	0.0194	0.0156	0.0127	0.0114	0.0105
4	0.175	0.162	0.122	0.0590	0.0270	0.0146	0.0107	0.0085	0.0070	0.0062	0.0058
650	0.107	0.0990	0.0710	0.0327	0.0147	0.0084	0.0058	0.0046	0.0037	0.0034	0.0032
6	0.061	0.0560	0.0390	0.0174	0.0078	0.0045	0.0031	0.0025	0.0020	0.0018	0.0017
7	0.032	0.0303	0.0206	0.0090	0.0041	0.0024	0.0017	0.0013	0.0011	0.0010	0.0009
8	0.017	0.0153	0.0103	0.0046	0.0022	0.0014	0.0009	0.0007	0.0006	0.0005	0.0005
9	0.0082	0.0076	0.0052	0.0024	0.0011	0.0007	0.0004	0.0003	0.0003	0.0002	0.0002
700	0.0041	0.0038	0.0026	0.0012	0.0006	0.0003	0.0002	0.0002	0.0001	0.0001	0.0001
1	0.0021	0.0019	0.0014	0.0006	0.0003	0.0002	0.0001				
2	0.0011	0.0010	0.0007	0.0003	0.0001						
3	0.0005	0.0005	0.0003	0.0001							
4	0.0003	0.0002	0.0002								
750	0.0001	0.0001									
6	0.0001										
7	0.0000										

of the luminous transmittance of filters employed for this purpose.

Except for the source designated as standard, the luminous transmittance of filters (either selective or neutral), the transmittances of sector disks, and the effect of varying the distance from the source will all depend upon the final luminance reached. Since the luminosity data are also a function of luminance, it may be necessary to make a trial calculation based on an estimated luminance before a final determination can be made. It may be more convenient at times to calculate the luminous transmittance of the filter for several values of luminance and select the proper point from a smooth curve relating the luminous transmittance to the luminance.

GENERAL ADDITIVITY LAW AS APPLIED TO LOW LEVEL PHOTOMETRY

The usual operations involved in photopic photometry depend to a large extent upon the validity of the additivity law. We measure the candlepower of lamps of various colors and apply the inverse-square law in calculating the illuminance obtained in service, or we compute the luminous transmittances of filters, used in many different applications, by weighting the spectral energy transmitted according to the I.C.I. standard luminosity data.

TABLE II. Relative spectral distribution of light for the equal-energy spectrum, based on a standard source at 2360°K.

λ	Log luminance (foot-lamberts) −0.25 I.C.I.	−0.5	−1.0	−1.5	−2.0	−2.5	−3.0	−3.5	−4.0	−4.5	−5.0
350									0.0005	0.0005	0.0006
6							0.0006	0.0008	0.0013	0.0016	0.0017
7					0.0004	0.0009	0.0017	0.0024	0.0035	0.0041	0.0045
8			0.0001	0.0003	0.0011	0.0025	0.0045	0.0064	0.0088	0.0103	0.0113
9	0.0001	0.0001	0.0003	0.0009	0.0032	0.0066	0.0112	0.0155	0.0205	0.0240	0.0261
400	0.0004	0.0005	0.0008	0.0028	0.0086	0.0160	0.0262	0.0346	0.0448	0.0511	0.0555
1	0.0012	0.0014	0.0025	0.0077	0.0204	0.0371	0.0543	0.0692	0.0889	0.101	0.109
2	0.0040	0.0045	0.0075	0.0190	0.0408	0.0697	0.103	0.129	0.161	0.182	0.195
3	0.0116	0.0123	0.0178	0.0365	0.0736	0.123	0.180	0.221	0.271	0.301	0.323
4	0.023	0.0243	0.0324	0.0619	0.124	0.201	0.285	0.342	0.425	0.465	0.492
450	0.038	0.0400	0.0529	0.1011	0.198	0.305	0.422	0.501	0.610	0.659	0.697
6	0.060	0.0636	0.0836	0.159	0.294	0.452	0.604	0.703	0.832	0.891	0.936
7	0.091	0.0973	0.127	0.238	0.438	0.643	0.832	0.954	1.084	1.148	1.185
8	0.139	0.148	0.194	0.360	0.629	0.882	1.076	1.214	1.347	1.418	1.469
9	0.208	0.223	0.296	0.532	0.862	1.122	1.308	1.463	1.601	1.677	1.732
500	0.323	0.345	0.449	0.753	1.084	1.349	1.539	1.687	1.829	1.901	1.950
1	0.503	0.531	0.666	0.956	1.276	1.526	1.714	1.827	1.951	2.014	2.055
2	0.710	0.736	0.855	1.116	1.406	1.620	1.780	1.848	1.915	1.940	1.960
3	0.862	0.884	0.982	1.214	1.457	1.603	1.694	1.728	1.736	1.742	1.744
4	0.954	0.972	1.056	1.249	1.411	1.484	1.500	1.489	1.463	1.445	1.434
550	0.995	1.011	1.079	1.212	1.291	1.282	1.243	1.201	1.146	1.115	1.092
6	0.995	1.006	1.050	1.121	1.107	1.045	0.967	0.894	0.824	0.784	0.751
7	0.952	0.957	0.979	0.976	0.899	0.792	0.684	0.617	0.553	0.525	0.500
8	0.870	0.872	0.865	0.809	0.682	0.555	0.461	0.408	0.358	0.331	0.319
9	0.757	0.752	0.726	0.636	0.485	0.371	0.296	0.256	0.220	0.204	0.194
600	0.631	0.625	0.587	0.467	0.326	0.237	0.180	0.155	0.132	0.121	0.115
1	0.503	0.497	0.449	0.321	0.207	0.142	0.107	0.0913	0.0763	0.0703	0.0667
2	0.381	0.371	0.319	0.210	0.123	0.0823	0.0613	0.0524	0.0442	0.0408	0.0387
3	0.265	0.253	0.213	0.127	0.0699	0.0460	0.0346	0.0292	0.0250	0.0230	0.0216
4	0.175	0.164	0.132	0.0737	0.0393	0.0238	0.0191	0.0159	0.0137	0.0126	0.0118
650	0.107	0.100	0.0766	0.0408	0.0214	0.0138	0.0102	0.0087	0.0073	0.0068	0.0065
6	0.061	0.0568	0.0421	0.0217	0.0114	0.0074	0.0055	0.0047	0.0040	0.0037	0.0034
7	0.032	0.0307	0.0222	0.0112	0.0060	0.0039	0.0030	0.0025	0.0021	0.0020	0.0019
8	0.017	0.0155	0.0111	0.0057	0.0031	0.0023	0.0016	0.0013	0.0011	0.0010	0.0009
9	0.0082	0.0078	0.0056	0.0030	0.0016	0.0011	0.0008	0.0006	0.0005	0.0005	0.0005
700	0.0041	0.0039	0.0029	0.0016	0.0008	0.0005	0.0004	0.0003	0.0003	0.0002	0.0002
1	0.0021	0.0020	0.0015	0.0008	0.0004	0.0003	0.0002				
2	0.0011	0.0010	0.0007	0.0004	0.0002						
3	0.0005	0.0005	0.0004	0.0002							
4	0.0003	0.0002	0.0002								
750	0.0001	0.0001									
6	0.0001										
Relative Totals:	100.0	101.2	106.5	120.2	136.6	150.2	161.1	168.2	175.9	179.8	182.5

The work of Ives,[4] and of Crittenden and Taylor,[5] together with the work of many other investigators in the field of homochromatic and heterochromatic photometry, may be taken as ample demonstration that the additivity law holds very well at high luminance levels under ordinary visual conditions.

In the mesopic and scotopic regions, it becomes necessary to recognize two concepts of the additivity law. The first, the general additivity law, concerns the addition of two or more separately evaluated luminances in an observational field. These may be of the same or of different spectral composition; compliance with the law in this case requires that the luminance of the combination must be equal to the sum of the luminances of the components.

In the mesopic and scotopic regions, the validity of the general additivity law for any source adopted as standard is implied in its adoption. For sources of different spectral composition, the shift of the luminosity function with luminance precludes exact compliance with the general additivity law. The

[4] H. E. Ives, "The addition of luminosities of different colors," Phil. Mag. **24**, 845 (1912).

[5] E. C. Crittenden and A. H. Taylor, "An interlaboratory comparison of colored photometric filters," Trans. I. E. S. **24**, 153 (1929).

TABLE III. Absolute spectral distribution of light for the equal-energy spectrum, based on a standard source at 2360°K.

λ	Log luminance (foot-lamberts) −0.25 I.C.I.	−0.5	−1.0	−1.5	−2.0	−2.5	−3.0	−3.5	−4.0	−4.5	−5.0
350									0.30	0.34	0.39
6							0.37	0.53	0.81	0.98	1.07
7					0.23	0.55	1.04	1.49	2.18	2.55	2.82
8	0.03	0.03	0.05	0.20	0.68	1.55	2.82	3.98	5.49	6.44	7.06
9	0.08	0.08	0.16	0.59	2.00	4.13	7.00	9.69	12.8	15.0	16.3
400	0.25	0.28	0.51	1.76	5.37	10.0	16.4	21.6	28.0	31.9	34.7
1	0.75	0.89	1.59	4.84	12.8	23.2	33.9	43.3	55.6	63.1	68.1
2	2.50	2.79	4.66	11.9	25.5	43.6	64.4	80.6	101	114	122
3	7.25	7.69	11.1	22.8	46.0	76.9	113	138	169	188	202
4	14.4	15.2	20.3	38.7	77.5	126	178	214	266	291	308
450	23.8	25.0	33.1	63.2	124	191	264	313	381	412	436
6	37.5	39.8	52.3	99.4	184	283	378	439	520	557	585
7	56.9	60.8	79.4	149	274	402	520	596	678	718	741
8	86.9	92.5	121	225	393	551	673	759	842	886	918
9	130	139	185	333	539	701	818	914	1001	1048	1083
500	202	216	281	471	678	843	962	1054	1143	1188	1219
1	314	332	416	598	798	954	1071	1142	1219	1259	1284
2	444	460	534	698	879	1013	1113	1155	1197	1213	1225
3	539	553	614	759	911	1002	1059	1080	1085	1089	1090
4	596	608	660	781	882	928	938	931	914	903	896
550	622	632	674	758	807	801	777	751	716	697	683
6	622	629	656	701	692	653	604	559	515	490	469
7	595	598	612	610	562	495	428	386	346	328	313
8	544	545	541	506	426	347	288	255	224	207	199
9	473	470	454	398	303	232	185	160	138	128	121
600	394	391	367	292	204	148	113	96.9	82.5	75.6	71.9
1	314	311	281	201	129	88.8	66.9	57.1	47.7	43.9	41.7
2	238	232	199	131	76.9	51.4	38.3	32.8	27.6	25.5	24.2
3	166	158	133	79.4	43.7	28.8	21.6	18.3	15.6	14.4	13.5
4	109	103	82.5	46.1	24.6	14.9	11.9	9.94	8.56	7.88	7.38
650	66.9	62.5	47.9	25.5	13.4	8.63	6.38	5.41	4.55	4.23	4.05
6	38.1	35.5	26.3	13.6	7.13	4.59	3.45	2.91	2.47	2.29	2.13
7	20.0	19.2	13.9	7.00	3.73	2.46	1.86	1.57	1.34	1.23	1.16
8	10.6	9.69	6.94	3.59	1.96	1.42	0.98	0.82	0.69	0.63	0.59
9	5.13	4.85	3.51	1.86	1.01	0.68	0.49	0.40	0.34	0.31	0.29
700	2.56	2.43	1.79	0.97	0.52	0.33	0.24	0.20	0.17	0.15	0.14
1	1.31	1.23	0.91	0.48	0.26	0.16	0.12				
2	0.66	0.61	0.46	0.24	0.12						
3	0.33	0.30	0.22	0.11							
4	0.16	0.15	0.11								
750	0.08	0.07									
6	0.04										
7	0.02										

curves of Fig. 2 show the extent to which the general additivity law fails for several non-standard sources. For saturated sources in the blue and red spectral regions, general additivity-law failure of much greater extent will be found.

Failure of the general additivity law has been demonstrated experimentally by Taylor,[6] who used a tungsten lamp at 2360°K as a standard source. Curve "*c*" of Taylor's Fig. 5 is of interest, since it shows a nearly constant luminous efficiency for the sextant green filter over a wide range of luminance; here additivity failure is relatively small.

[6] A. H. Taylor, "Vision at low brightness levels," Trans. I. E. S. **38**, 89, see also 97 (1943).

THE ADDITIVITY LAW AT CONSTANT FIELD LUMINANCE

The second concept of the additivity law can be illustrated as follows: Let us suppose that there are a number of sources of different spectral composition set at such distances from the field of observation that they all produce the same luminance, "*A*," when used singly. Then, using the sources together, let the distances for all of them be increased so that the radiation falling on the observational field from each one is reduced by the factors *a*, *b*, *c*, *d* . . ., and let the resulting luminance be "*A*," the same as before.

Compliance with the restricted additivity law

TABLE IV. Relative spectral distribution of light from 2000°K source, based on a standard source at 2360°K.

λ	Log luminance (foot-lamberts) −0.25 I.C.I.	−0.5	−1.0	−1.5	−2.0	−2.5	−3.0	−3.5	−4.0	−4.5	−5.0
350											
6											
7											
8							0.001	0.001	0.001	0.001	0.002
9					0.001	0.001	0.002	0.003	0.004	0.005	0.005
400				0.001	0.002	0.004	0.007	0.009	0.012	0.014	0.015
1		0.001	0.001	0.003	0.008	0.014	0.020	0.026	0.033	0.038	0.040
2	0.002	0.002	0.004	0.009	0.020	0.035	0.051	0.064	0.080	0.091	0.097
3	0.008	0.008	0.012	0.024	0.048	0.081	0.118	0.145	0.178	0.198	0.213
4	0.020	0.021	0.028	0.053	0.106	0.172	0.244	0.293	0.364	0.398	0.422
450	0.042	0.044	0.058	0.111	0.218	0.336	0.464	0.551	0.671	0.725	0.767
6	0.084	0.089	0.116	0.221	0.410	0.630	0.841	0.979	1.16	1.24	1.30
7	0.159	0.169	0.221	0.415	0.763	1.12	1.45	1.66	1.89	2.00	2.06
8	0.300	0.319	0.418	0.776	1.36	1.90	2.32	2.62	2.90	3.06	3.17
9	0.548	0.588	0.781	1.40	2.27	2.96	3.45	3.86	4.22	4.42	4.57
500	1.03	1.10	1.43	2.40	3.46	4.31	4.91	5.39	5.84	6.07	6.23
1	1.93	2.03	2.55	3.66	4.89	5.84	6.56	7.00	7.47	7.71	7.87
2	3.23	3.35	3.89	5.08	6.40	7.38	8.11	8.42	8.72	8.83	8.93
3	4.63	4.75	5.27	6.52	7.82	8.61	9.10	9.28	9.32	9.35	9.36
4	5.99	6.11	6.63	7.85	8.86	9.32	9.42	9.35	9.19	9.08	9.01
550	7.26	7.37	7.87	8.84	9.42	9.35	9.07	8.76	8.36	8.13	7.97
6	8.37	8.46	8.83	9.43	9.31	8.79	8.13	7.52	6.93	6.59	6.32
7	9.17	9.22	9.43	9.41	8.66	7.63	6.59	5.95	5.33	5.06	4.82
8	9.55	9.57	9.49	8.88	7.48	6.09	5.06	4.48	3.93	3.63	3.50
9	9.40	9.34	9.02	7.90	6.02	4.61	3.68	3.18	2.73	2.53	2.41
600	8.82	8.74	8.21	6.53	4.56	3.31	2.52	2.17	1.85	1.69	1.61
1	7.87	7.78	7.03	5.02	3.24	2.22	1.67	1.43	1.19	1.10	1.04
2	6.65	6.47	5.56	3.66	2.15	1.44	1.07	0.914	0.771	0.712	0.675
3	5.13	4.89	4.12	2.46	1.35	0.890	0.669	0.565	0.484	0.445	0.418
4	3.74	3.50	2.82	1.57	0.839	0.508	0.408	0.340	0.293	0.269	0.252
650	2.51	2.35	1.80	0.958	0.502	0.324	0.239	0.203	0.171	0.159	0.152
6	1.57	1.46	1.08	0.558	0.293	0.189	0.142	0.120	0.102	0.094	0.088
7	0.897	0.861	0.622	0.314	0.167	0.110	0.083	0.070	0.060	0.055	0.052
8	0.518	0.472	0.338	0.175	0.095	0.069	0.048	0.040	0.034	0.030	0.029
9	0.271	0.256	0.185	0.098	0.053	0.036	0.026	0.021	0.018	0.016	0.015
700	0.146	0.138	0.102	0.055	0.030	0.019	0.014	0.011	0.009	0.008	0.008
1	0.080	0.075	0.056	0.030	0.016	0.010	0.007				
2	0.043	0.040	0.030	0.016	0.008						
3	0.023	0.021	0.016	0.008							
4	0.012	0.011	0.008								
750	0.006	0.006									
6	0.003										
7	0.002										
Σ	100.0	99.6	98.0	94.4	90.8	88.3	86.5	85.4	84.3	83.7	83.4

requires that the sum, $a+b+c+d \ldots$, be equal to unity. This procedure is essentially equivalent to the determination of the luminosity function at a constant luminance level and its subsequent use in evaluating the luminance obtained from a source of specified intensity and spectral composition, or in computing the transmittance of a filter. Since the usefulness of a family of luminosity tables depends upon the validity of the restricted additivity law, it is important to consider the conditions under which the scotopic and photopic luminosity curves used here were obtained.

In many of the investigations upon which the I.C.I. luminosity curve is based, there was some variation in luminance in different spectral regions. In most cases, however, due attention was given to this factor, and it was concluded that the luminance of the comparison field was high enough to avoid any considerable Purkinje shift. We may therefore assume that, except for the blue-violet region, the I.C.I. data represent very closely the average luminosity function at constant field luminance.

Constant field luminance was maintained by Hecht and Williams, as well as by the present author, in their determinations of the scotopic luminosity function. The remaining question is

TABLE V. Relative spectral distribution of light from the standard 2360°K source.

λ	Log luminance (foot-lamberts) −0.25 I.C.I.	−0.5	−1.0	−1.5	−2.0	−2.5	−3.0	−3.5	−4.0	−4.5	−5.0
370								0.001	0.001	0.001	0.001
8						0.001	0.002	0.002	0.003	0.004	0.004
9					0.002	0.003	0.005	0.007	0.010	0.012	0.013
400			0.001	0.002	0.005	0.010	0.016	0.022	0.028	0.032	0.035
1	0.001	0.001	0.002	0.006	0.016	0.030	0.044	0.056	0.071	0.081	0.088
2	0.004	0.005	0.007	0.019	0.041	0.071	0.104	0.131	0.163	0.184	0.197
3	0.015	0.015	0.022	0.046	0.093	0.155	0.227	0.278	0.341	0.379	0.407
4	0.036	0.038	0.050	0.096	0.192	0.311	0.441	0.529	0.658	0.720	0.762
450	0.071	0.075	0.099	0.190	0.372	0.573	0.793	0.942	1.15	1.24	1.31
6	0.135	0.144	0.189	0.359	0.664	1.02	1.36	1.59	1.88	2.01	2.11
7	0.244	0.261	0.344	0.639	1.18	1.73	2.23	2.56	2.91	3.08	3.18
8	0.440	0.468	0.614	1.14	1.99	2.79	3.40	3.84	4.26	4.49	4.65
9	0.769	0.824	1.09	1.97	3.19	4.15	4.83	5.41	5.92	6.20	6.40
500	1.38	1.48	1.92	3.22	4.64	5.77	6.59	7.22	7.83	8.14	8.34
1	2.47	2.61	3.28	4.70	6.27	7.50	8.43	8.98	9.59	9.90	10.10
2	3.98	4.13	4.80	6.26	7.89	9.09	9.99	10.37	10.74	10.88	11.00
3	5.48	5.62	6.24	7.71	9.26	10.19	10.77	10.99	11.04	11.08	11.09
4	6.83	6.96	7.56	8.94	10.10	10.62	10.74	10.66	10.47	10.34	10.27
550	7.97	8.10	8.65	9.71	10.34	10.27	9.96	9.62	9.18	8.93	8.75
6	8.87	8.97	9.36	10.00	9.87	9.32	8.62	7.97	7.35	6.99	6.70
7	9.40	9.45	9.67	9.64	8.88	7.82	6.75	6.09	5.46	5.18	4.94
8	9.46	9.48	9.41	8.80	7.42	6.04	5.01	4.44	3.89	3.60	3.47
9	9.03	8.97	8.66	7.58	5.78	4.42	3.53	3.05	2.62	2.43	2.31
600	8.21	8.13	7.64	6.08	4.24	3.09	2.34	2.02	1.72	1.58	1.50
1	7.11	7.03	6.35	4.54	2.93	2.01	1.51	1.29	1.08	0.994	0.943
2	5.83	5.68	4.88	3.22	1.88	1.26	0.938	0.802	0.677	0.625	0.592
3	4.38	4.18	3.52	2.10	1.15	0.759	0.571	0.482	0.413	0.380	0.357
4	3.10	2.91	2.34	1.31	0.697	0.422	0.339	0.282	0.243	0.223	0.209
650	2.03	1.90	1.46	0.775	0.406	0.262	0.194	0.164	0.138	0.129	0.123
6	1.24	1.15	0.854	0.440	0.231	0.149	0.112	0.094	0.080	0.074	0.069
7	0.690	0.662	0.479	0.242	0.129	0.085	0.064	0.054	0.046	0.042	0.040
8	0.389	0.355	0.254	0.131	0.072	0.052	0.036	0.030	0.025	0.023	0.021
9	0.199	0.188	0.136	0.072	0.039	0.026	0.019	0.016	0.013	0.012	0.011
700	0.105	0.099	0.073	0.040	0.021	0.014	0.010	0.008	0.007	0.006	0.006
1	0.056	0.053	0.039	0.021	0.011	0.007	0.005				
2	0.030	0.028	0.021	0.011	0.006						
3	0.016	0.014	0.011	0.005							
4	0.008	0.007	0.005								
750	0.004	0.004									
6	0.002										
7	0.001										
Σ	100.0	100.0	100.0	100.0	100.0	100.0	100.0	100.0	100.0	100.0	100.0

that of the validity of the restricted additivity law.

EXPERIMENTAL CHECK OF THE RESTRICTED ADDITIVITY LAW AT LOW LUMINANCE LEVELS

This check of the restricted additivity law was done prior to the construction of the luminosity tables described, since the value of such tables depends upon the discovery of some simple principle upon which the evaluation of mixed stimuli at low luminance levels could be based. A light source, which consisted of a small box enclosing a lamp and containing a window of opal glass covered by several small apertures, was mounted on the 3-meter bar photometer. Each aperture was covered with a Wratten filter of high saturation and was supplied with a shutter which could be opened or closed at will.

The comparison field was exactly the same as that used in the work on the scotopic luminosity function and in the later work done at high luminance levels, some of which will be mentioned later. The color field was 2.6° in diameter, and the surrounding comparison field was 14° in diameter. Observation was binocular, with natural pupils and fixation.

The distance required for each filter separately to match the comparison field was first determined

TABLE VI. Relative spectral distribution of light from 2660°K source, based on a standard source at 2360°K.

λ	Log luminance (foot-lamberts) −0.25 I.C.I.	−0.5	−1.0	−1.5	−2.0	−2.5	−3.0	−3.5	−4.0	−4.5	−5.0
350											
6									0.001	0.001	0.001
7							0.001	0.001	0.002	0.002	0.002
8					0.001	0.002	0.003	0.004	0.006	0.007	0.008
9				0.001	0.003	0.006	0.009	0.013	0.017	0.020	0.022
400			0.001	0.003	0.009	0.017	0.028	0.036	0.047	0.054	0.058
1	0.002	0.002	0.003	0.010	0.026	0.048	0.070	0.089	0.115	0.130	0.141
2	0.006	0.007	0.012	0.030	0.064	0.109	0.161	0.202	0.252	0.285	0.305
3	0.022	0.023	0.033	0.068	0.138	0.230	0.337	0.414	0.508	0.564	0.605
4	0.051	0.054	0.072	0.137	0.275	0.446	0.633	0.759	0.944	1.03	1.09
450	0.099	0.104	0.138	0.263	0.516	0.795	1.10	1.31	1.59	1.72	1.82
6	0.182	0.193	0.253	0.481	0.890	1.37	1.83	2.13	2.52	2.70	2.83
7	0.317	0.339	0.443	0.830	1.53	2.24	2.90	3.33	3.78	4.00	4.13
8	0.554	0.590	0.773	1.43	2.51	3.51	4.29	4.84	5.37	5.65	5.85
9	0.940	1.01	1.34	2.41	3.90	5.07	5.91	6.61	7.24	7.58	7.83
500	1.64	1.76	2.29	3.83	5.52	6.87	7.84	8.59	9.31	9.68	9.93
1	2.87	3.03	3.79	5.45	7.27	8.70	9.77	10.41	11.12	11.48	11.71
2	4.50	4.66	5.41	7.07	8.90	10.26	11.27	11.70	12.13	12.29	12.41
3	6.03	6.19	6.87	8.50	10.20	11.22	11.86	12.10	12.15	12.20	12.21
4	7.34	7.48	8.13	9.61	10.86	11.42	11.55	11.46	11.26	11.12	11.04
550	8.38	8.51	9.09	10.21	10.87	10.79	10.47	10.11	9.65	9.39	9.19
6	9.12	9.22	9.62	10.27	10.15	9.58	8.86	8.19	7.55	7.19	6.88
7	9.46	9.50	9.72	9.69	8.93	7.87	6.79	6.13	5.49	5.21	4.97
8	9.32	9.34	9.27	8.67	7.31	5.95	4.94	4.37	3.84	3.55	3.42
9	8.72	8.66	8.36	7.32	5.58	4.27	3.41	2.95	2.53	2.35	2.23
600	7.78	7.70	7.24	5.76	4.02	2.92	2.22	1.91	1.63	1.49	1.42
1	6.61	6.54	5.90	4.22	2.72	1.87	1.41	1.20	1.00	0.924	0.877
2	5.33	5.19	4.46	2.94	1.72	1.15	0.857	0.732	0.618	0.570	0.541
3	3.93	3.75	3.15	1.88	1.04	0.681	0.512	0.433	0.370	0.341	0.320
4	2.74	2.57	2.07	1.15	0.615	0.372	0.299	0.249	0.214	0.197	0.185
650	1.76	1.65	1.26	0.673	0.353	0.227	0.168	0.143	0.120	0.112	0.107
6	1.06	0.984	0.729	0.376	0.197	0.127	0.096	0.081	0.068	0.063	0.059
7	0.581	0.557	0.403	0.203	0.108	0.071	0.054	0.046	0.039	0.036	0.034
8	0.322	0.294	0.211	0.109	0.059	0.043	0.030	0.025	0.021	0.019	0.018
9	0.162	0.153	0.111	0.059	0.032	0.021	0.016	0.013	0.011	0.010	0.009
700	0.084	0.080	0.059	0.032	0.017	0.011	0.008	0.007	0.005	0.005	0.005
1	0.045	0.042	0.031	0.017	0.009	0.006	0.004				
2	0.023	0.022	0.016	0.008	0.004						
3	0.012	0.011	0.008	0.004							
4	0.006	0.006	0.004								
750	0.003	0.003									
6	0.002										
7	0.001										
Σ	100.0	100.2	101.3	103.7	106.3	108.3	109.7	110.6	111.5	112.0	112.3

by each observer. Two or more shutters were then opened together, and the distance for a match was again determined.

In the first test at a luminance of 0.01 foot-lambert, four different colored apertures were used in every possible combination. The average additivity sums were 93.4 and 99.5 percent for two observers.

In a second experiment at 0.001 foot-lambert, seven observers were used. The complete data are shown in Table XII.

In these tests, the four apertures were covered by Wratten filters Nos. 24A, 16, 61, and 43. Each recorded value is the result of ten photometric settings, except that for Observer No. 1 the average of three independent sets was used, and for Observer No. 2 the average of two independent sets was used.

In a third experiment, six apertures were provided, Wratten filters Nos. 86 and 44 being added to those listed in the preceding paragraph. At a constant field luminance of 0.001 foot-lambert, Observer No. 2 made settings for each of the 57 combinations. The additivity sum ranged from 94.2 percent to 106.0 percent, with an average value of 99.5 percent.

TABLE VII. Relative spectral distribution of light from 2850°K source, based on a standard source at 2360°K.

λ	Log luminance (foot-lamberts) −0.25 I.C.I.	−0.5	−1.0	−1.5	−2.0	−2.5	−3.0	−3.5	−4.0	−4.5	−5.0
350											
6									0.001	0.001	0.001
7						0.001	0.001	0.002	0.003	0.003	0.003
8					0.001	0.002	0.004	0.006	0.008	0.009	0.010
9				0.001	0.004	0.007	0.013	0.018	0.023	0.027	0.029
400	0.001	0.001	0.001	0.004	0.012	0.022	0.036	0.048	0.062	0.070	0.076
1	0.002	0.002	0.004	0.013	0.034	0.061	0.090	0.114	0.147	0.167	0.180
2	0.008	0.009	0.015	0.037	0.080	0.137	0.202	0.253	0.316	0.357	0.382
3	0.027	0.028	0.041	0.084	0.169	0.283	0.414	0.508	0.623	0.692	0.743
4	0.062	0.065	0.087	0.166	0.332	0.537	0.762	0.915	1.14	1.24	1.32
450	0.117	0.123	0.163	0.312	0.610	0.940	1.30	1.54	1.88	2.03	2.15
6	0.211	0.224	0.294	0.560	1.03	1.59	2.13	2.47	2.93	3.14	3.29
7	0.363	0.388	0.507	0.949	1.75	2.56	3.32	3.81	4.32	4.58	4.73
8	0.624	0.664	0.870	0.162	2.82	3.96	4.83	5.45	6.04	6.36	6.59
9	1.04	1.12	1.48	2.67	4.32	5.62	6.56	7.33	8.02	8.41	8.68
500	1.80	1.92	2.50	4.19	6.03	7.50	8.56	9.38	10.17	10.58	10.85
1	3.09	3.26	4.09	5.87	7.83	9.36	10.52	11.21	11.97	12.36	12.61
2	4.78	4.95	5.76	7.51	9.46	10.90	11.98	12.44	12.89	13.06	13.19
3	6.33	6.50	7.22	8.92	10.71	11.78	12.45	12.70	12.76	12.80	12.82
4	7.61	7.75	8.42	9.96	11.25	11.83	11.96	11.87	11.67	11.52	11.44
550	8.57	8.71	9.30	10.44	11.12	11.05	10.71	10.35	9.88	9.61	9.41
6	9.23	9.33	9.74	10.39	10.26	9.69	8.97	8.29	7.64	7.27	6.96
7	9.46	9.51	9.73	9.70	8.93	7.87	6.80	6.13	5.49	5.22	4.97
8	9.22	9.25	9.17	8.58	7.23	5.88	4.89	4.33	3.80	3.51	3.38
9	8.54	8.48	8.19	7.17	5.47	4.18	3.34	2.89	2.48	2.30	2.19
600	7.54	7.47	7.01	5.58	3.90	2.83	2.15	1.85	1.58	1.45	1.37
1	6.35	6.27	5.67	4.05	2.61	1.79	1.35	1.15	0.963	0.887	0.842
2	5.06	4.93	4.24	2.79	1.63	1.09	0.815	0.696	0.587	0.542	0.514
3	3.70	3.53	2.97	1.77	0.975	0.642	0.483	0.407	0.349	0.321	0.301
4	2.56	2.40	1.93	1.08	0.574	0.348	0.279	0.232	0.200	0.184	0.172
650	1.63	1.53	1.17	0.623	0.327	0.211	0.156	0.132	0.111	0.103	0.099
6	0.970	0.903	0.669	0.345	0.181	0.117	0.088	0.074	0.063	0.058	0.054
7	0.529	0.507	0.367	0.185	0.099	0.065	0.049	0.041	0.035	0.032	0.031
8	0.291	0.266	0.190	0.098	0.054	0.039	0.027	0.022	0.019	0.017	0.016
9	0.145	0.138	0.099	0.053	0.029	0.019	0.014	0.011	0.010	0.009	0.008
700	0.075	0.071	0.052	0.028	0.015	0.010	0.007	0.006	0.005	0.004	0.004
1	0.040	0.037	0.028	0.015	0.008	0.005	0.004				
2	0.020	0.019	0.014	0.007	0.004						
3	0.010	0.010	0.007	0.004							
4	0.005	0.005	0.004								
750	0.003	0.002									
6	0.001										
7	0.001										
Σ	100.0	100.4	102.0	105.8	109.9	112.9	115.3	116.7	118.2	118.9	119.4

These results indicate that the restricted additivity law holds quite closely under the conditions of these experiments. The small failure found may be ascribed to a tendency on the part of some observers to estimate saturated colors a little brighter than the less saturated colors of the mixtures.

The validity of the restricted additivity law, depending as it does upon photometric settings with large color differences, cannot be judged on the rigorous basis that can be applied in measurements of purely physical quantities. In addition to the visual characteristics of the observer, the results may be influenced to a considerable extent by his psychological and physiological condition at the time of observation, as well as by the consistency with which he judges a photometric match.

It is concluded that the available experimental evidence indicates that the use of color-compensating filters in low level photometry is compatible with the visual processes of the average eye.

In these experiments, the comparison field was illuminated by a tungsten lamp set at approximately 2500°K. It is possible that tests made with a different quality of illumination of the comparison field or at lower luminance levels might lead to different results.

TABLE VIII. Relative spectral distribution of light from a 3500°K source, based on a standard source at 2360°K.

λ	Log luminance (foot-lamberts) −0.25 I.C.I.	−0.5	−1.0	−1.5	−2.0	−2.5	−3.0	−3.5	−4.0	−4.5	−5.0
350									0.001	0.001	0.001
6							0.001	0.001	0.002	0.002	0.003
7					0.001	0.002	0.003	0.004	0.006	0.007	0.008
8				0.001	0.002	0.005	0.009	0.013	0.018	0.021	0.023
9			0.001	0.002	0.008	0.016	0.027	0.037	0.049	0.057	0.062
400	0.001	0.001	0.002	0.008	0.023	0.044	0.072	0.095	0.122	0.140	0.152
1	0.004	0.004	0.008	0.024	0.063	0.115	0.168	0.215	0.276	0.313	0.338
2	0.014	0.016	0.026	0.066	0.142	0.243	0.359	0.450	0.561	0.635	0.680
3	0.045	0.047	0.069	0.142	0.286	0.478	0.700	0.860	1.05	1.17	1.26
4	0.099	0.105	0.139	0.266	0.534	0.865	1.23	1.47	1.83	2.00	2.12
450	0.180	0.189	0.250	0.478	0.936	1.44	2.00	2.37	2.88	3.12	3.30
6	0.310	0.328	0.432	0.821	1.52	2.33	3.12	3.62	4.30	4.60	4.83
7	0.510	0.545	0.712	1.33	2.45	3.60	4.66	5.35	6.07	6.43	6.64
8	0.840	0.895	1.17	2.18	3.80	5.33	6.50	7.34	8.14	8.57	8.88
9	1.35	1.45	1.92	3.45	5.59	7.28	8.49	9.49	10.39	10.88	11.24
500	2.24	2.39	3.11	5.22	7.51	9.35	10.67	11.69	12.68	13.18	13.52
1	3.71	3.92	4.91	7.05	9.41	11.25	12.64	13.47	14.38	14.85	15.15
2	5.54	5.75	6.67	8.71	10.98	12.65	13.90	14.43	14.95	15.15	15.31
3	7.10	7.28	8.09	10.00	12.00	13.20	13.95	14.23	14.30	14.35	14.36
4	8.25	8.41	9.14	10.81	12.21	12.84	12.98	12.88	12.66	12.50	12.41
550	9.02	9.16	9.78	10.98	11.70	11.62	11.26	10.88	10.38	10.10	9.89
6	9.41	9.51	9.93	10.60	10.47	9.88	9.14	8.48	7.79	7.41	7.10
7	9.37	9.42	9.63	9.60	8.85	7.79	6.73	6.07	5.44	5.17	4.92
8	8.88	8.90	8.83	8.26	6.96	5.67	4.71	4.17	3.66	3.38	3.26
9	8.00	7.95	7.67	6.72	5.12	3.92	3.13	2.70	2.32	2.16	2.05
600	6.88	6.82	6.40	5.09	3.56	2.58	1.96	1.69	1.44	1.32	1.25
1	5.65	5.58	5.04	3.61	2.32	1.59	1.20	1.03	0.857	0.790	0.749
2	4.40	4.28	3.68	2.42	1.42	0.949	0.707	0.605	0.510	0.471	0.446
3	3.13	3.00	2.52	1.50	0.827	0.544	0.409	0.345	0.296	0.272	0.256
4	2.12	1.98	1.60	0.892	0.476	0.288	0.231	0.192	0.166	0.152	0.144
650	1.32	1.24	0.947	0.504	0.264	0.171	0.126	0.107	0.090	0.084	0.080
6	0.769	0.716	0.530	0.273	0.144	0.093	0.070	0.059	0.050	0.046	0.043
7	0.410	0.394	0.285	0.144	0.077	0.050	0.038	0.032	0.027	0.025	0.024
8	0.221	0.202	0.145	0.075	0.041	0.030	0.020	0.017	0.014	0.013	0.012
9	0.108	0.103	0.074	0.039	0.021	0.014	0.010	0.009	0.007	0.006	0.006
700	0.055	0.052	0.038	0.021	0.011	0.007	0.005	0.004	0.004	0.003	0.003
1	0.028	0.027	0.020	0.010	0.006	0.004	0.003				
2	0.014	0.013	0.010	0.005	0.003						
3	0.007	0.007	0.005	0.003							
4	0.003	0.003	0.002								
750	0.002	0.002									
6	0.001										
Σ	100.0	100.7	103.8	111.3	119.7	126.2	131.2	134.4	137.7	139.4	140.5

THE I.C.I. LUMINOSITY FUNCTIONS

A major problem in low level photometry is that of securing sufficient retinal illuminance for acceptable precision. For this reason, a fairly large field observed binocularly, with natural pupils, is generally used. Of the three essentially different methods employed in photopic photometry—the flicker method, the single-step equality of brightness method, and the cascade or step-by-step equality of brightness method—the first is ruled out because of the rapid decrease in the sensitivity of the eye to flicker as the luminance is reduced. The single-step rather than the step-by-step method of equality of brightness photometry is generally preferred as being simpler; the choice is justified particularly at the lower levels by the reduced perception of color differences.

Following the experiments on the scotopic luminosity function reported in 1937,[2] an apparatus was devised by means of which the luminosity curves of fifteen observers were measured at photopic or near photopic levels, with the same field and conditions of observation.

The work at high luminance levels was done in order to determine whether the photopic luminosity curve obtained under these conditions of observation would differ materially from the I.C.I. curve.

TABLE IX. Relative spectral distribution of light from 5500°K source, based on a standard source at 2360°K.

λ	Log luminance (foot-lamberts) −0.25 I.C.I.	−0.5	−1.0	−1.5	−2.0	−2.5	−3.0	−3.5	−4.0	−4.5	−5.0
350									0.003	0.003	0.004
6							0.004	0.005	0.008	0.010	0.011
7					0.002	0.006	0.011	0.016	0.024	0.028	0.031
8			0.001	0.002	0.008	0.018	0.033	0.046	0.063	0.074	0.081
9	0.001	0.001	0.002	0.007	0.024	0.050	0.085	0.117	0.155	0.181	0.197
400	0.003	0.004	0.006	0.022	0.068	0.126	0.206	0.272	0.352	0.402	0.437
1	0.010	0.012	0.021	0.063	0.166	0.302	0.443	0.564	0.725	0.823	0.888
2	0.034	0.037	0.063	0.160	0.343	0.586	0.866	1.08	1.35	1.53	1.64
3	0.100	0.106	0.154	0.315	0.635	1.06	1.55	1.91	2.34	2.60	2.79
4	0.203	0.215	0.286	0.547	1.10	1.78	2.52	3.02	3.76	4.11	4.35
450	0.342	0.360	0.477	0.911	1.78	2.75	3.80	4.51	5.50	5.94	6.28
6	0.549	0.582	0.766	1.46	2.69	4.14	5.53	6.44	7.62	8.16	8.57
7	0.845	0.903	1.18	2.21	4.07	5.97	7.72	8.85	10.06	10.65	11.00
8	1.30	1.39	1.82	3.38	5.90	8.27	10.09	11.39	12.64	13.30	13.78
9	1.97	2.11	2.80	5.03	8.15	10.61	12.37	13.83	15.14	15.86	16.38
500	3.07	3.28	4.27	7.16	10.31	12.83	14.64	16.05	17.40	18.08	18.55
1	4.80	5.07	6.36	9.13	12.18	14.57	16.36	17.44	18.63	19.23	19.62
2	6.79	7.04	8.18	10.67	13.45	15.49	17.02	17.67	18.31	18.55	18.74
3	8.24	8.45	9.39	11.61	13.93	15.33	16.20	16.52	16.60	16.66	16.68
4	9.11	9.28	10.08	11.92	13.47	14.16	14.32	14.21	13.96	13.79	13.69
550	9.47	9.62	10.26	11.53	12.28	12.20	11.82	11.43	10.90	10.61	10.39
6	9.42	9.52	9.94	10.61	10.48	9.89	9.16	8.46	7.80	7.42	7.11
7	8.96	9.01	9.21	9.18	8.46	7.45	6.44	5.81	5.20	4.94	4.71
8	8.13	8.15	8.08	7.56	6.37	5.18	4.31	3.81	3.34	3.09	2.98
9	7.01	6.97	6.72	5.89	4.49	3.44	2.74	2.37	2.04	1.89	1.80
600	5.79	5.73	5.39	4.28	2.99	2.17	1.65	1.42	1.21	1.11	1.06
1	4.57	4.51	4.08	2.91	1.88	1.29	0.971	0.829	0.693	0.638	0.606
2	3.42	3.33	2.86	1.88	1.10	0.739	0.550	0.470	0.397	0.366	0.347
3	2.35	2.24	1.89	1.13	0.620	0.408	0.307	0.259	0.222	0.204	0.191
4	1.53	1.44	1.16	0.645	0.344	0.208	0.167	0.139	0.120	0.110	0.103
650	0.923	0.863	0.661	0.352	0.185	0.119	0.088	0.075	0.063	0.058	0.056
6	0.519	0.483	0.358	0.185	0.097	0.063	0.047	0.040	0.034	0.031	0.029
7	0.268	0.257	0.186	0.094	0.050	0.033	0.025	0.021	0.018	0.016	0.016
8	0.140	0.128	0.092	0.047	0.026	0.019	0.013	0.011	0.009	0.008	0.008
9	0.067	0.063	0.046	0.024	0.013	0.009	0.006	0.005	0.004	0.004	0.004
700	0.033	0.031	0.023	0.012	0.007	0.004	0.003	0.003	0.002	0.002	0.002
1	0.016	0.015	0.011	0.006	0.003	0.002	0.001				
2	0.008	0.008	0.006	0.003	0.002						
3	0.004	0.004	0.003	0.001							
4	0.002	0.002	0.001								
750	0.001	0.001									
Σ	100.0	101.2	106.8	120.9	137.7	151.3	162.1	169.1	176.7	180.5	183.1

Since it is desirable that a set of luminosity data for low level work be adjusted to the I.C.I. data at the upper luminance level, the results of this work are pertinent to the present discussion.

Measurements on the fifteen observers were made at 0.1, 1.0, and 7.0 foot-lamberts. It was found that, under these test conditions, the luminosity function over this luminance range shows no change significantly greater than the probable error of the measurements, and, except for the spectral region, 400–500 millimicrons, is similar to the I.C.I. luminosity function.

In Fig. 3 are shown, for the blue-violet region, the I.C.I. curve with our curve for 1.0 foot-lambert. As a check on the high values found in the blue-violet region, a direct measurement of the transmittance of a Corning No. 5113 blue-glass filter was made by twenty observers, seven of whom had participated in the determination of the luminosity curve.

The values of transmittance varied from 0.25 percent to 0.76 percent, with an average value of 0.43 percent. The transmittance computed from the I.C.I. data is 0.19 percent, and that computed from our data is 0.39 percent. Although the precision of such measurements is low, the comparison of the blue color field being made directly against the illumination from a tungsten lamp at 2800°K, it seems significant that the average observed transmittance agreed within 10 percent with that computed from our luminosity data, while the lowest observed value was 30 percent higher than

TABLE X. Relative spectral distribution of sunlight, based on a standard source at 2360°K.

λ	Log luminance (foot-lamberts) −0.25 I.C.I.	−0.5	−1.0	−1.5	−2.0	−2.5	−3.0	−3.5	−4.0	−4.5	−5.0
350									0.001	0.001	0.001
6							0.001	0.001	0.002	0.002	0.003
7					0.001	0.002	0.003	0.005	0.007	0.008	0.009
8				0.001	0.003	0.006	0.011	0.015	0.021	0.025	0.027
9			0.001	0.003	0.009	0.019	0.032	0.044	0.059	0.069	0.075
400	0.002	0.002	0.004	0.012	0.037	0.069	0.113	0.149	0.193	0.220	0.239
1	0.007	0.008	0.014	0.042	0.112	0.203	0.297	0.378	0.486	0.552	0.596
2	0.025	0.028	0.047	0.119	0.256	0.438	0.647	0.810	1.01	1.14	1.22
3	0.077	0.081	0.117	0.241	0.486	0.811	1.19	1.46	1.79	1.99	2.13
4	0.170	0.180	0.240	0.459	0.919	1.49	2.11	2.54	3.15	3.45	3.65
450	0.315	0.331	0.438	0.837	1.64	2.53	3.49	4.15	5.05	5.46	5.77
6	0.528	0.559	0.735	1.40	2.59	3.97	5.31	6.18	7.32	7.84	8.23
7	0.841	0.899	1.17	2.20	4.05	5.94	7.69	8.82	10.02	10.61	10.95
8	1.31	1.40	1.83	3.40	5.94	8.33	10.16	11.46	12.72	13.39	13.87
9	1.99	2.14	2.84	5.10	8.26	10.76	12.54	14.03	15.35	16.08	16.61
500	3.13	3.35	4.36	7.31	10.52	13.09	14.93	16.37	17.74	18.44	18.92
1	4.85	5.12	6.42	9.22	12.30	14.71	16.53	17.62	18.81	19.42	19.81
2	6.85	7.10	8.25	10.77	13.56	15.63	17.17	17.83	18.47	18.72	18.91
3	8.30	8.52	9.46	11.69	14.04	15.44	16.32	16.65	16.72	16.78	16.80
4	9.18	9.35	10.16	12.01	13.57	14.27	14.43	14.32	14.07	13.90	13.79
550	9.65	9.80	10.46	11.75	12.52	12.43	12.05	11.65	11.11	10.81	10.59
6	9.49	9.59	10.01	10.69	10.55	9.96	9.22	8.52	7.86	7.47	7.16
7	8.93	8.97	9.18	9.15	8.43	7.43	6.41	5.79	5.19	4.92	4.69
8	8.06	8.08	8.01	7.49	6.32	5.14	4.27	3.78	3.32	3.07	2.96
9	6.90	6.86	6.62	5.80	4.42	3.38	2.70	2.33	2.01	1.86	1.77
600	5.72	5.67	5.33	4.24	2.96	2.15	1.63	1.41	1.20	1.10	1.04
1	4.52	4.47	4.03	2.88	1.86	1.28	0.962	0.820	0.686	0.632	0.599
2	3.38	3.29	2.83	1.87	1.09	0.731	0.544	0.465	0.393	0.362	0.344
3	2.33	2.22	1.87	1.12	0.614	0.404	0.304	0.257	0.220	0.202	0.190
4	1.52	1.42	1.15	0.639	0.341	0.206	0.166	0.138	0.119	0.109	0.102
650	0.915	0.855	0.655	0.349	0.183	0.118	0.087	0.074	0.062	0.058	0.055
6	0.515	0.479	0.355	0.183	0.096	0.062	0.047	0.039	0.033	0.031	0.029
7	0.263	0.253	0.183	0.092	0.049	0.032	0.024	0.021	0.018	0.016	0.015
8	0.137	0.125	0.090	0.046	0.025	0.018	0.013	0.011	0.009	0.008	0.008
9	0.065	0.061	0.044	0.023	0.013	0.009	0.006	0.005	0.004	0.004	0.004
700	0.031	0.030	0.022	0.012	0.006	0.004	0.003	0.002	0.002	0.002	0.002
1	0.016	0.015	0.011	0.006	0.003	0.002	0.001				
2	0.008	0.007	0.005	0.003	0.001						
3	0.004	0.003	0.003	0.001							
4	0.002	0.002	0.001								
750	0.001	0.001									
Σ	100.0	101.3	106.9	121.2	137.8	151.1	161.4	168.1	175.2	178.8	181.2

the transmittance computed from the I.C.I. data.

Similar indications that the blue luminosity is higher than that indicated by the I.C.I. luminosity curve are to be found in the literature dealing with the more usual types of photometric field.

The data reported by Crittenden and Taylor[5] on the dark-blue filter, DB_3, in their Table IV, show a similar result in a comparison of the transmittance determined on several equality-of-brightness photometers with that computed by the Colorimetric Section of the Bureau of Standards utilizing the I.C.I. luminosity data.*,[7,8]

Gibson and Tyndall[9,10] in fact, show in their Table III data of their own and several other determinations which are higher in the blue-violet region than that finally adopted by them. The present blue-violet data seem to have their origin and chief field of application in optical pyrometry through blue filters. It is estimated that the differences

* Smaller and less definite differences, because smaller color steps are involved, are indicated in the case of the international measurements on the blue-glass filters used to step up the tungsten intensity scale (see reference 7) and in the work of Wensel, Roeser, Barbrow, and Caldwell (see reference 8) on the derivation of tungsten filament standards.

[7] Comité d'Études sur la Photométrie Hétérochrome, Commission Internationale de L'Éclairage, 542 (1931).

[8] Wensel, Roeser, Barbrow, and Caldwell, "Derivation of photometric standards for tungsten-filament lamps," Bur. Stand. J. Research **13**, 161, see also 167 (1934).

[9] K. S. Gibson and E. P. T. Tyndall, "Visibility of radiant energy," J. Opt. Soc. Am. **9**, 403 (1924).

[10] G. Wald, "Human vision and the spectrum," Science **101**, 653 (1945).

TABLE XI. Relative spectral distribution of daylight, based on a standard source at 2360°K.

λ	Log luminance (foot-lamberts) −0.25 I.C.I.	−0.5	−1.0	−1.5	−2.0	−2.5	−3.0	−3.5	−4.0	−4.5	−5.0
350									0.002	0.003	0.003
6							0.003	0.004	0.007	0.008	0.009
7					0.002	0.005	0.009	0.014	0.020	0.023	0.026
8			0.001	0.002	0.007	0.015	0.027	0.038	0.053	0.062	0.068
9	0.001	0.001	0.002	0.006	0.020	0.041	0.069	0.096	0.126	0.148	0.161
400	0.003	0.003	0.006	0.020	0.060	0.112	0.183	0.242	0.314	0.358	0.389
1	0.010	0.012	0.021	0.064	0.168	0.305	0.447	0.570	0.732	0.831	0.897
2	0.036	0.040	0.067	0.171	0.367	0.626	0.925	1.16	1.45	1.63	1.75
3	0.106	0.112	0.162	0.332	0.670	1.12	1.64	2.01	2.47	2.74	2.94
4	0.222	0.234	0.312	0.597	1.20	1.94	2.75	3.30	4.10	4.48	4.74
450	0.393	0.414	0.548	1.05	2.05	3.16	4.37	5.19	6.32	6.82	7.22
6	0.637	0.675	0.888	1.69	3.12	4.80	6.41	7.47	8.84	9.46	9.94
7	0.976	1.04	1.36	2.55	4.70	6.90	8.92	10.23	11.63	12.31	12.71
8	1.48	1.58	2.07	3.84	6.71	9.41	11.48	12.96	14.38	15.13	15.68
9	2.20	2.36	3.13	5.62	9.11	11.86	13.82	15.46	16.92	17.72	18.30
500	3.36	3.59	4.68	7.84	11.29	14.05	16.03	17.57	19.05	19.80	20.31
1	5.16	5.45	6.84	9.81	13.10	15.67	17.60	18.76	20.03	20.68	21.10
2	7.18	7.45	8.65	11.29	14.22	16.39	18.01	18.69	19.37	19.63	19.83
3	8.59	8.81	9.79	12.10	14.52	15.97	16.88	17.22	17.30	17.36	17.38
4	9.35	9.53	10.36	12.25	13.84	14.55	14.71	14.60	14.35	14.17	14.06
550	9.61	9.76	10.42	11.70	12.46	12.38	12.00	11.60	11.06	10.77	10.54
6	9.40	9.51	9.92	10.60	10.46	9.88	9.14	8.45	7.79	7.41	7.10
7	8.81	8.86	9.06	9.03	8.32	7.33	6.33	5.71	5.12	4.86	4.63
8	7.88	7.90	7.83	7.32	6.17	5.02	4.17	3.69	3.24	3.00	2.89
9	6.70	6.66	6.43	5.63	4.29	3.28	2.62	2.27	1.95	1.81	1.72
600	5.46	5.40	5.08	4.04	2.82	2.05	1.56	1.34	1.14	1.05	0.994
1	4.24	4.19	3.78	2.70	1.74	1.20	0.902	0.769	0.643	0.592	0.562
2	3.12	3.03	2.61	1.72	1.01	0.673	0.501	0.429	0.361	0.334	0.316
3	2.10	2.01	1.69	1.01	0.555	0.365	0.275	0.232	0.198	0.183	0.171
4	1.34	1.26	1.01	0.566	0.302	0.183	0.147	0.122	0.105	0.097	0.091
650	0.794	0.743	0.569	0.303	0.159	0.102	0.076	0.064	0.054	0.050	0.048
6	0.438	0.408	0.303	0.156	0.082	0.053	0.040	0.033	0.028	0.026	0.025
7	0.222	0.213	0.154	0.078	0.041	0.027	0.021	0.017	0.015	0.014	0.013
8	0.114	0.104	0.074	0.039	0.021	0.015	0.011	0.009	0.007	0.007	0.006
9	0.053	0.050	0.036	0.019	0.010	0.007	0.005	0.004	0.003	0.003	0.003
700	0.026	0.024	0.018	0.010	0.005	0.003	0.002	0.002	0.002	0.001	0.001
1	0.013	0.012	0.009	0.005	0.002	0.002	0.001				
2	0.006	0.006	0.004	0.002	0.001						
3	0.003	0.003	0.002	0.001							
4	0.001	0.001	0.001								
750	0.001	0.001									
Σ	100.0	101.4	107.9	124.2	143.6	159.5	172.1	180.3	189.2	193.6	196.6

pointed out would result in a change of from 1 to 2 percent in establishing the candlepower scale for gas-filled tungsten lamps, starting with the original carbon international standards.

If we are to "evaluate lights according to their general usefulness,"[11] which is a reasonable criterion, allowance must be made for the low luminosity factor of the I.C.I. data, when the blue-violet region is involved.

There are indications in the field of colorimetry that the I.C.I. standard coordinate system, of which the I.C.I. luminosity function is an essential part, does not adequately account for the visual appearance of colors which differ mainly in their reflectance of violet light.[12]

Enough data have accumulated since the I.C.I. luminosity curve was adopted in 1924 to warrant some revision. It is realized that such revision would lead to considerable inconvenience, because of the large number of tables and data which have been based on the 1924 standard. As time goes on, this difficulty can only increase. It is for this reason that we suggest that the matter be considered by the International Commission on Illumination as soon as possible.

[11] K. S. Gibson, "Spectral luminosity factors," J. Opt. Soc. Am. **30**, 51, see also reply of E. C. Crittenden to German National Committee, p. 58 (1940).

[12] A. E. Jacobsen, "Non-adaptability of the I.C.I. system to some near-whites which show absorption in the far-blue region of the spectrum," J. Opt. Soc. Am. **38**, 442 (1948).

CONCLUSION

A significant distinction in relative importance may be made among several objectives which require special consideration in heterochromatic photometric technique. Of primary importance is the reproducibility of the work of a single observer using a fixed apparatus. It is also highly desirable that results obtained in different laboratories shall be comparable without the use of a number of selected or calibrated observers.

These objectives can be attained in most cases by means of color-compensating filters. The eye

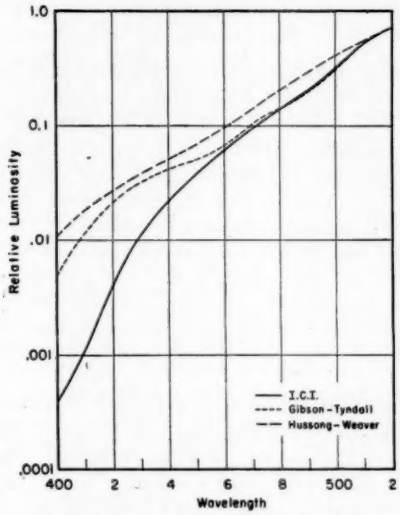

FIG. 3. A comparison of the I.C.I. luminosity function with other data in the blue-violet spectral region.

then becomes a null instrument, and the effect of the visual peculiarities of individual observers is small. The assignment of photometric values to the observations is then a matter of computing the transmittance of the filters by means of the tables. The general adoption of one set of tables should lead to results which are consistent from time to time and from one laboratory to another.

In the photometry of line sources, such as mercury lamps, color compensation is more difficult to attain, and exact energy match nearly impossible. In such cases, the use of filters which give a good subjective match, and care in the control of the conditions of observation, particularly of the field size, make it possible to obtain satisfactory results in the photopic region. Photometry of line sources at low luminance levels may be affected to a larger extent by differences in the spectral distribution of energy in the test and comparison fields. This point does not seem to have been studied experimentally to any great extent; it is of importance in the utilization of sodium and mercury illumination for street-lighting.

TABLE XII. A check of the restricted additivity law at 0.001 foot-lambert, employing seven observers.

Color	Observer 1*	2**	3	4	5	6	7	av.
RY	99.3	102.8	88.2	106.9	108.6	104.0	97.3	101.0
RG	85.0	95.4	96.5	91.9	113.5	89.8	97.3	95.6
RB	85.6	98.8	93.2	102.0	110.4	88.5	101.3	97.2
YG	96.2	97.1	100.3	96.9	92.0	90.5	97.5	95.8
YB	96.9	99.7	98.1	100.0	84.9	94.5	103.6	96.8
GB	101.2	104.3	104.1	90.1	98.9	103.6	106.6	101.3
RYG	91.6	96.9	94.8	93.5	99.1	95.2	98.4	95.6
RYB	91.4	96.4	92.1	96.2	102.6	86.5	101.3	95.2
RGB	89.8	99.2	95.9	99.2	108.3	89.7	97.3	97.0
YGB	96.6	101.8	97.4	98.6	93.9	84.5	100.2	96.2
RYGB	92.5	96.6	94.8	95.3	97.0	87.8	98.1	94.6
av.	93.3	99.0	95.9	97.4	100.8	92.2	99.9	96.9

* Obtained 93.4 at 0.01 foot-lambert.
** Obtained 99.5 at 0.01 foot-lambert.

A third objective, of less importance than those mentioned, is that our methods of photometry should evaluate lights in accordance with ordinary visual experience or in accordance with their general usefulness. It is in the attainment of this objective that proper evaluation of the relative luminosity of the spectrum and of the additive process of the eye is of most significance. Determination of these factors can only be approximated. Visual experience is affected to a considerable extent by the conditions under which it takes place, by the psychological and physiological condition of the observer at the time of observation, and by the spatial configuration of the visual field.

For this reason, a final choice of luminosity data will require careful selection of data obtained under different conditions.

The tables given in the preceding pages should facilitate the securing of consistent results in different laboratories. Their compatibility with ordinary visual experience is expected to be approximate only. It is desirable that additional data be obtained from which a more representative set of tables can be prepared.

The final selection of a standard source upon which to base the luminance scale should be made with due consideration of the methods that are likely to be used in low level photometry.

When color-correcting filters are employed, the required computation of luminance can be made about as conveniently with one standard source as with another. On the other hand, when color-correcting filters are not employed, unless the standard source is defined in such terms that it can be realized by the use of an unfiltered tungsten lamp, the required comparison lamp filter as well as the computations needed for the reduction of the test data are likely to be omitted. Work done in this way will be based on a tungsten luminance scale, regardless of what may be standard.

This is one of the reasons why a tungsten lamp at 2360°K is considered a good choice.

The author wishes to acknowledge the cooperation of H. E. Hussong, who participated in all the experimental work which has been described.

A Rapid Mobile Analyzer for Minute Amounts of Lead in Air

HENRY AUGHEY
*E. I. du Pont de Nemours & Company, Wilmington, Delaware**
(Received November 18, 1948)

Atmospheric contamination by lead presents acute problems in analysis and control to the chemical industry. A mobile instrument of extreme sensitivity has been developed which furnishes a rapid indication and an approximate assay of localized relatively high concentrations of lead, combined or elemental. Samples are drawn through a condensed spark discharge adjusted to minimize air lines and to excite the lead spectrum which is photographed with a small quartz instrument. Visual examination of a series of exposures provides data on lead concentration as a function of time and location. A sensitivity of better than one part in 20 million can be maintained in routine operation. Instantaneous response has been realized by substitution of the photoelectric Geiger counter for the photographic plate, as described in detail in the following paper.

CONTAMINATION of the atmosphere by lead presents to the chemical industry acute problems in analysis and control. In order to avoid toxic conditions, the concentration of lead must be kept at extremely low levels. In fact, many states and municipalities have defined "maximum permissible" limits by statute. This limit averages 0.15 mg per cubic meter and is only one part in seven million on a weight basis. Obviously it is essential to maintain much lower average concentrations if the limit is significant. A mobile lead analyzer of extreme sensitivity has been developed for this purpose which furnishes an instantaneous indication and an approximate assay of localized high concentrations of lead. This material may be in the form of elemental lead or it may be an inorganic or organic compound of lead.

When this problem was first attacked, the requirements were recognized as sensitivity, speed, and specificity for lead. Spectroscopy appeared to offer the most promising techniques and various approaches were considered. Calculations indicated that x-ray mass absorption was not nearly sensitive enough. There appeared to be no way in which the specificity associated with x-ray emission methods could be realized. Ultraviolet absorption offered no general solution because of the varying nature of the samples, which might include organic and inorganic lead compounds and lead dust. Interference in manufacturing areas from transient traces of organic compounds possessing strong ultraviolet absorption eliminated this approach. The need for a rapid method did not permit concentrating the samples before analysis. Because of specificity and sensitivity, emission spectroscopy was selected for investigation as the most likely prospect.

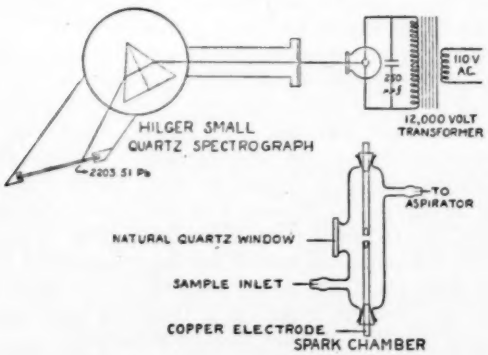

FIG. 1. Photographic lead detector.

The most sensitive arc line for lead is wave-length 4057.8A; the corresponding spark line is 2203.5A. Spark excitation of airborne material appeared more feasible than arc excitation since the high wattages and attendant heat from the arc seemed undesirable in a mobile device. The relatively high dispersion and resolution of the small quartz spectrograph (Hilger) in the far ultraviolet (16A/mm at 2200A) proved adequate. As a matter of fact, at the extremely low concentrations of lead involved in the program, no line other than 2203.5A has been observed which could be assigned to the lead spectrum.

Figure 1 shows a diagram of the original photographic instrument. Air was drawn through an electrode chamber in which a high voltage condensed spark continuously played between copper electrodes, exciting the lead spark spectrum from the traces of lead in air. The source presented an uncommon problem, that of exciting traces of material flowing between the electrodes. The proper conditions of excitation were found to be very critical and could be determined only by careful experiments. A 12,000-volt transformer supplied the power. Lead-free copper electrodes $\frac{1}{4}$" in diameter were satisfactory. Optimum sensitivity was realized when a condenser across the electrodes was adjusted to the minimum capacity (250 micromicrofarads) which still prevented appearance of

* Contribution No. 257 from Chemical Department, Experimental Station.

air lines. Larger capacity increased the intensity of the electrode spectrum at the expense of the lead line. A fixed gap of $\frac{1}{4}''$ and a fixed rate of air flow (1 cu.ft./min.) through the spark chamber were required for reproducible results. Resulting spectra were recorded on lantern slide plates.

Intensity variations of the lead line compared visually with adjacent lines from the copper electrode spectrum as an intensity reference provided the basis for quantitative data. Calibration was carried out by measurement of air containing minute amounts of tetraethyl lead. Chemical analyses by the dithizone method[1] were compared with photographic plates secured on the instrument, samples being obtained from a common stream at identical times. Figure 2 shows one of these calibrations calculated in optical density of the lead line.

For convenience and mobility the entire assembly was mounted on wheels so it could be moved about over a large area. The only external requirement was a source of 110-volt a.c. Samples were introduced through a length of Saran tubing which restricted the test to any suspected point.

Spectra were originally compared visually to disclose trends in lead concentration as a function of time and place. Normal operation involved a number of successive samplings followed by plate development, and the cycle required one to three hours before any resulting data could be utilized. Operation for about a year in this fashion demonstrated the inherent soundness and utility of the method. This experience justified further improvement directed mainly toward obtaining results much more rapidly.

A direct reading device using a fast detector of energy was indicated. There was no difficulty in detecting lead in about one part in fifty million using photographic exposures of one minute. This is rather feeble energy for photocells, but the photoelectric Geiger counter[2] appeared to have possibilities, especially in the far ultraviolet. No photoelectric Geiger tubes with quartz windows were on the market at the time. By arrangement, the research laboratory of the North American Philips Company undertook the construction and installation of a photoelectric Geiger tube with associated power supplies, scaling, and integrating circuits. These were assembled with the previously described spectrograph and source unit as an experimental model to test the soundness of the entire proposal. This experimental model has performed well in the exploratory program.

[1] Wilkins, Willoughby, Kraemer, and Smith, Ind. Eng. Chem. Anal. Ed. **7**, 33–36 (1935).

[2] O. S. Duffendack and W. E. Morris, J. Opt. Soc. Am. **32**, 3–24 (1942).

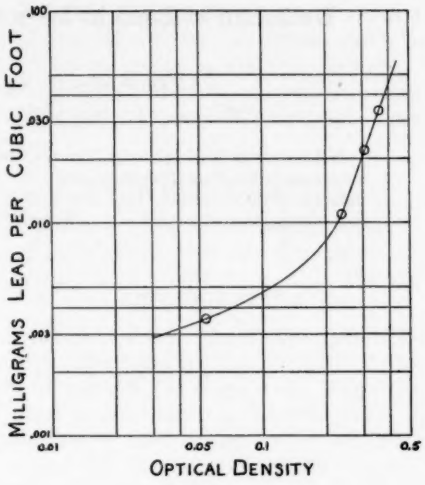

FIG. 2.

The technique has not been developed to a point where continuous quantitative measurements are available over periods involving many hours or days. Electrode disintegration and mechanical and electrical instability are always present. The photographic method has afforded to date the highest realized sensitivity. Although the Geiger tube is extremely sensitive to feeble light, statistical effects when counting at a rate of less than a hundred pulses a minute, combined with the above instabilities, obscure small changes and do not permit the realization of the full instrumental sensitivity on counts made over practical periods.

The device has been tried only for lead. Similar sensitivity and specificity for mercury is to be expected. The high energy of the spark source permits excitation of materials present both in elemental and in combined forms and offers in addition a rapid analysis in cases where such extreme sensitivity is not needed. Dusts involving elements such as arsenic, barium, and beryllium are suggested examples.

The following paper by Dr. O. G. Koppius discusses the application of the photoelectric Geiger counter to our instrument and is a more detailed exposition of the currently used device.

ACKNOWLEDGMENTS

It is a pleasure to acknowledge the skillful assistance of Mr. Fred Baum in all the laboratory phases of this work. In addition, I should like to express my appreciation for their technical assistance to the representatives of the Organic Chemicals Department at whose instance this work was undertaken. The assistance of Engineering Department personnel is also acknowledged.

Detection of Lead in Air with the Aid of a Geiger-Müller Counter

O. G. KOPPIUS
Philips Laboratories, Inc., Irvington-on-Hudson, New York
(Received December 14, 1948)

A detector of lead in air will be described. It utilizes a spark source for the excitation of the lead spectrum, a small quartz spectrometer for the dispersion, and a quartz Geiger-Müller counter for the detector of the radiation. The lower limit of detection is of the order of 20 micrograms of lead per cubic foot of air. The instrument is mobile and ideally suited to locate areas of high lead concentration in air.

I. INTRODUCTION

THE detection of traces of an element by means of its characteristic spectral lines emitted in an arc or spark spectrum is well known. In the last decade many industrial applications have been made, such as the routine analysis of iron and steel for calcium, silicon, manganese, chromium, etc. With modern equipment, the method is capable of high speed and precision. In a majority of the applications the photographic plate has been used as a detector of the radiation.

A number of investigators have studied the properties of Geiger-Müller counters for the detection of ultraviolet radiation.[1–8] They have found them to be very sensitive and reasonably reliable in the ultraviolet region of the spectrum. Only recently the application of Geiger-Müller counters to spectrochemical analysis has been reported.[9]

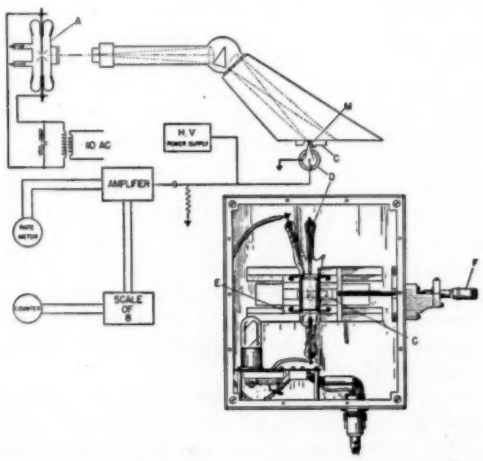

FIG. 1. Schematic drawing of the instrument for the detection of lead in air with the aid of a Geiger-Müller counter and an illustrated drawing of the Geiger counter housing: (A) copper spark source, (B) Hilger *E*-3 spectrograph, (C) exit slit with mirror, *M*, and (D) quartz Geiger-Müller counter.

The object of the present investigations was the detection of lead in air, or any other gas in concentrations of the order of a few parts per ten million by weight of air under standard conditions (20 micrograms per cubic foot of air, S.T.P.), without the aid of a photographic plate. As was shown in the preceding paper on the photographic method of analysis, the spectrum of lead can be excited by passing the gas contaminated with lead through a condensed spark discharge between pure copper electrodes. Because photographic methods of detection were too slow and time consuming, it was advantageous to construct an instrument which almost instantly would locate areas of high lead concentration.

When the problem was first undertaken in 1944, photo-multiplier tubes, sensitive to the 2203A lead line, were not readily available. For this reason, and in view of the favorable results of other investigators, a quartz Geiger-Müller counter was chosen as the detector. The counters have been sufficiently reliable during their lifetime so that during the past three years the instrument has been kept in almost continuous operation.

II. APPARATUS

A schematic drawing of the instrument together with the front view of the G-M counter and slit mechanism is shown in Fig. 1. The radiation from the spark source, *A*, is dispersed by means of a small Hilger, *E*-3, quartz spectrograph, *B*. The slit system, *C*, which replaces the photographic plate, is mounted in the focal plane of the instrument. The width of the slit is adjusted to pass only the 2203A lead line. The quartz G-M counter, *D*, is placed behind the slit in such a way as to intercept all the radiation passing through the slit. The front view shows the G-M counter, the slit translating mechanism, and the preamplifier mounted in a shielded, light-tight metal housing which replaces the photographic plate holder and the plate rack of the spectrograph. The electronic components for

[1] B. Rajewsky, Physik. Zeits **32**, 121 (1931).
[2] G. Locher, Phys. Rev. **42**, 525 (1932).
[3] Angelo Drigo, Alti ist venato sci. Pt. **2**, 97, 1 (1937–38).
[4] Alexandre Dauvillier, Comptes Rendus **209**, 394 (1939).
[5] M. N. Dyachenko, J. Phys. U.S.S.R. **3**, 479 (1940).
[6] Alexandre Dauvillier, J. de phys. et rad. **8**, 3, 29 (1942).
[7] O. S. Duffendack and W. E. Morris, J. Opt. Soc. Am. **32**, 8 (1942).
[8] Charles Racz, J. Chem. Phys. **39**, 175 (1942).
[9] R. Hanau and R. W. Wolfe, J. Opt. Soc. Am. **38**, 377 (1948).

the G-M counter have been described elsewhere.[10] The spark source, A, and power supply have been discussed in the previous paper.

Figure 2 is an isometric drawing of the housing containing the G-M counter, the slit translating mechanism and the preamplifier. In the Hilger spectrograph, the rays at 2203A converge onto their focus in the focal plane in a beam subtending in an angle of about 20°, while the spectral plane itself is situated obliquely to this beam (cf. Fig. 1). As a consequence, the configuration of the 2203A radiation beam passing through the slit is rather unfavorable to be caught in the counter tube. Therefore, a mirror of stainless steel was mounted on the body of the slit, in the manner shown in Figs. 1 and 2, permitting all the radiation passing through the slit to be reflected directly into the counter. Without the use of a mirror, any G-M tube of conventional design would have failed to include all of the radiation within the available solid angle defined by the counter tube aperture system.

The carriage, E, holding the slit and G-M counter can be moved along ways parallel to the focal plane of the instrument by means of the micrometer, F. The angle of the mirror, M, on the slit, C, was adjusted to the optimum value required by the beam geometry to reflect all of the 2203A lead line radiation into the counter. Since it is advantageous to be able to scan a portion of the spectrum on either side of the lead line, the rectangular hole in the counter cathode was made large enough to include all the radiation which would pass through the slit within the desired scanning region.

The source, as well as the spectrograph and electronic controls, is mounted in an airtight box in which an inert atmosphere such as nitrogen can be maintained. In this way the possible fire hazard presented by an open spark was eliminated.

Figure 3 is a photograph of the quartz G-M counter. The cathode of the counter was pure (O.F.H.C.) copper, $\frac{15}{16}''$ O.D., with a .015″ wall, and $1\frac{1}{2}''$ long. A rectangular slot $\frac{5}{8}''$ by $\frac{1}{4}''$ is cut lengthwise in the side wall to receive the radiation. The anode is a tungsten wire 3 mils in diameter. The envelope of the counter is clear fused quartz, and the electrodes are introduced through graded seals. The cylinder has rings turned to provide a snug slip fit inside the quartz tubing. In addition, it is necessary to use a somewhat flexible cathode lead connecting wire to prevent vibrations of the cathode from breaking the graded seal.

The counter was thoroughly pumped and outgassed. The electrodes were heated in the presence of pure hydrogen until the surfaces were bright. The tube was finally repumped, filled, and sealed with 6 mm of alcohol vapor and 20 cm of argon. The counter has a threshold voltage of about 1400 volts, a plateau about 200 volts wide, and a background count of about twenty per minute. The photoelectric threshold of the counter is below the transmission limit of a one-millimeter thickness of pyrex glass.

[10] H. Lifshutz and J. Lawson, Rev. Sci. Inst. 9, 83 (1938).

III. EXPERIMENTAL RESULTS

The air which is suspected of being contaminated with lead is pumped through the spark source chamber. The lead atoms as well as the copper atoms of the electrodes are excited in the spark discharge. The radiation from the spark is dispersed by the spectrograph so that only the radiation from the 2203A lead line falls on the photoelectron counter as explained above. The rate of arrival of the quanta at the counter tube, i.e., the radiation intensity of wave-length 2203A, is proportional to the amount of lead present and is measured by counting the total number of discharges per unit time or by averaging the number of counts on a rate meter.

Since the lead detector is used primarily to locate areas of high lead concentration, it is not necessary to use the method of "internal control" to obtain a high precision in the analysis. For this reason, only one counter is employed to monitor the variation in intensity of the 2203A lead line.

The Hilger E-3 spectrograph was found to have adequate resolution. In order to test this condition, a photograph of the copper spark spectrum was taken with the spectrograph. The photographic plate was then replaced with the G-M counter and

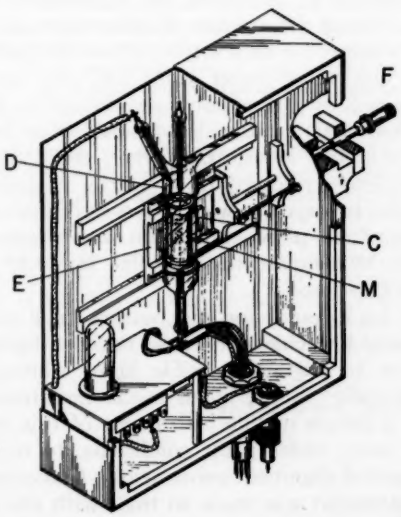

FIG. 2. Isometric drawing of the Geiger counter housing and the translating mechanism: (C) exit slit with mirror, M, (D) quartz Geiger-Müller counter, (E) movable carriage, and (F) micrometer screw.

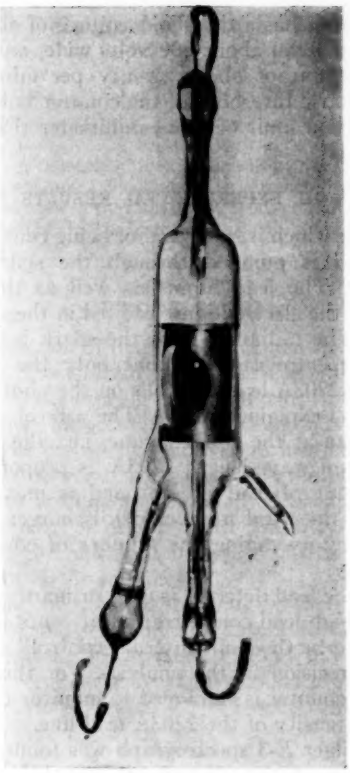

FIG. 3. Photograph of the quartz Geiger counter.

the spectrum, within the vicinity of the lead line, was scanned by adjusting the micrometer screw, *F*, and noting the number of counts per second on the rate meter for each setting of the micrometer.

The microphotometer trace and the spectrum determined by the counter are shown in Fig. 4. As can be seen readily, the resolution in the two cases is almost identical. Further, the 2203A line is completely resolved from nearby copper lines. Since the two spectra were taken on different days and since no plate calibration was made, it is difficult to compare the true line intensity ratios for the two cases.

The background for the counter tube trace is extremely low chiefly because the counter is not sensitive to scattered visible light, whereas the photographic plate responds to this radiation.

For a simple mobile instrument of this type it is not easy, under plant conditions, to maintain good optical alignment permanently. Consequently, the instrument was made so that, with the aid of the micrometer screw, *F*, the wave-length region on either side of the lead line can be readily scanned. This adjustment enables the operator to set the instrument quickly on the lead line position after locating the adjacent copper lines. Further, the over-all stability and sensitivity of the detector can be checked by measuring the relative intensities of the 2200A and 2195.8A copper lines. These values remain approximately constant.

The calibration curve for the amount of lead in air as a function of the number of counts recorded per unit time was most difficult to establish. The most suitable method found was the use of known amounts of tetraethyl lead in air. The presence of other vapors has little or no effect on the accuracy of the analysis. The calibration curve which was established is shown in Fig. 5.

The lower limit of detectability was found to be of the order of 20 micrograms of lead per cubic foot of air at standard conditions. The accuracy of the analytical curve leaves much to be desired. However, since the principal function of the instrument is to locate areas of high lead concentration, the absolute accuracy of the results is of secondary importance. Since the calibration curve is to a first approximation linear, the areas of high lead concentration can at least be compared qualitatively. The lower limit of detectability is determined chiefly by the erratic behavior of the spark discharge, which emits a continuously changing background radiation. Upon this background is superimposed the radiation that is to be detected from the excited lead atoms.

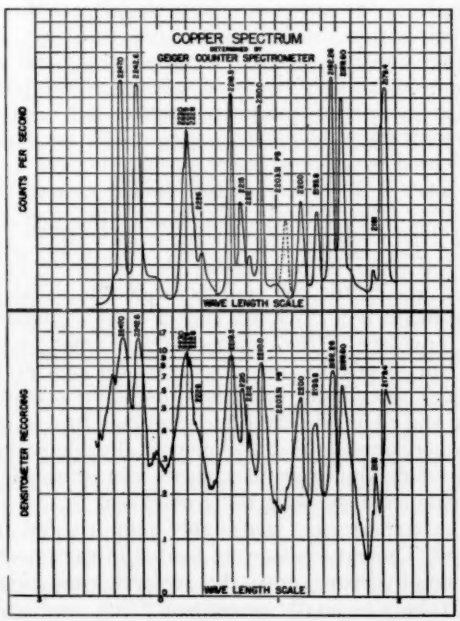

FIG. 4. Comparison of the densitometer recording and the spectrum determined by means of a Geiger counter.

IV. RECOMMENDATIONS AND SUMMARY

The accuracy and the lower limit of detectability for the determination of lead in air for an instrument of this type could certainly be improved by using the method of "internal control." In this manner the ratio of the number of counts of a suitable copper line to that of the lead line, particularly if they were a homologous pair, would average out most of the erratic behavior of the spark discharge.

According to the investigation of Dauvillier,[4-6] the spectral sensitivity of the counters can be markedly changed and can be made much greater for radiations in this wave-length region than was feasible in the course of this investigation.

The use of Geiger-Müller counters for spectrographic analysis seems practicable and convenient. It has been found possible to use a quartz G-M counter as a detector of ultraviolet radiation in a direct reading semi-quantitative instrument. The present limitations on the accuracy of the results, and the lower limit of detectability, are fixed by the erratic behavior of the source.

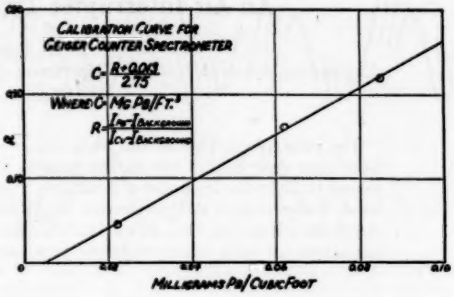

FIG. 5. Calibration curve.

Book Review

Physical Aspects of Color

P. J. BOUMA. Pp. 312, Figs. 113. Elsevier Publishing Company, Inc., New York, 1948. Price $5.50.

Notwithstanding the difficulty and expense of colored illustration in by-gone days, it has generally been felt imperative by writers on color to insert some colored diagrams. Even Young in 1803 illustrated his color theory by a hand-tinted color triangle in the otherwise black and white Royal Society publication. Here, however, we find a book which attempts the tour de force of describing aspects of color without (except for a pastel-shaded formalized rainbow on the jacket) a single colored illustration. Dr. Bouma has written an interesting and informative volume; but without some color charts, and colored illustrations of the elementary phenomena of color mixture, it is doubtful whether any author could really get the subject across. In consequence some problems of great importance, such as subtractive color mixture, which could be easily clarified by appropriate examples, are dimly treated. "The process of subtractive color mixture is governed by much less simple laws than that of additive mixture" is practically all we are offered as against several chapters on additive mixture calculations. A clear discussion of the perennial "yellow plus blue makes green" misunderstanding, which is a "must" in any discussion of color, is not to be found.

The author has obviously devoted most attention to the things that interested him most, which is apt to be the case with books written by practicing engineers rather than teachers, who are disciplined to present a subject in a well-balanced way, and who are aware from experience of the hurdles most significant to the student. There is, as indicated above, an extremely full discussion of additive color mixture, of the geometrical treatment used in the C. I. E. coordinate system, of illuminating engineering, light sources, photometry, and colorimetry. There is nothing of value on color photography, a great deal on theories of color vision and color blindness, an overfull and overcharitable exposition of the work of Goethe and Ostwald. It is stated that the physical basis of the latter's system is defective and contradictory; why it is might well have been explained and further discussion omitted.

The history of color science in its early stages is very attractively written, but the more recent history is not presented in good perspective. This is undoubtedly due in part to the hiatus in European libraries in the American optical literature of the first World War period. Such subjects as artificial daylight (not "very imperfect" as Bouma states) and the trichromatic analysis and specification of color now generally used, were extensively discussed here before 1920. It will be rather surprising to the fairly numerous living charter members of the O.S.A. to read that "the O.S.A. for sixty years has functioned as the official system in America."

It must not be gathered from these comments that the book is not to be recommended to the serious student of the subject. It is a very solid production with a wealth of information and sound exposition. Preferably its study should be preceded by something more elementary,—with colored plates!

HERBERT E. IVES
Upper Montclair, New Jersey

An Air Interrupter Type Spectrographic Light Source

J. H. ENNS AND R. A. WOLFE
Engineering Research Institute, Department of Physics, University of Michigan, Ann Arbor, Michigan
(Received January 18, 1949)

The principle feature of this source is an air interrupter, some of whose operating characteristics have been described in two earlier papers. This paper presents a general technical description of the source to illustrate its unusual flexibility. A procedure followed in selecting source parameters is outlined. Experimental data presented are those obtained by the usual photographic method and from direct recording type time of wait curves. Several examples are given to show the most suitable source conditions for some widely different type samples.

I. INTRODUCTION

THE introduction of an air jet interrupter to the control circuit of a spectrographic spark source was first described by Fowler and Wolfe.[1] At about the same time in 1944 a study of sources was started at the University of Michigan, supported by the Leeds and Northrup Company of Philadelphia, Pennsylvania. One of the developments in this program was an air interrupter illustrated in Fig. 1, whose turbulent free air stream is able to control the breakdown voltage between its two electrodes to within several percent.[2] This is as good a control as achieved with the well-known synchronous interrupter and has certain advantages such as wider flexibility in the number of discharges possible per unit of time and independence of breakdown voltage from line voltage fluctuations. A sufficiently large line voltage variation could change the number of sparks per half-cycle, but this is always detected in the oscilloscope pattern.

II. SPARK SOURCE

The basic electrical principles of a spark source have been sufficiently described by Kaiser[3] and the authors.[2] A certain amount of repetition is now introduced, using the usual simplified spark source diagram of Fig. 2. The leakage resistance R_4 (one-megohm, 25-watt) in parallel with the analytical gap G_2 minimizes the effect that this gap might have upon the breakdown voltage E.

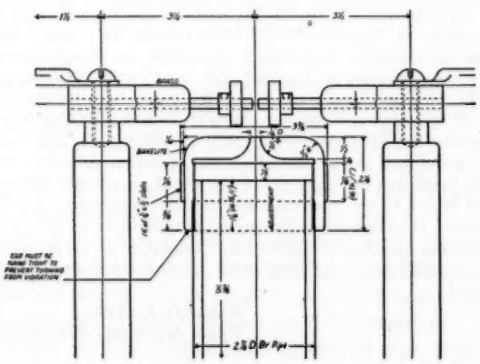

FIG. 1. Air interrupter.

Figure 3 is a moving picture of oscilloscope patterns showing the charging cycle voltage across the condenser C. The patterns are for a one-, two-, three-, and four-spark per half-cycle operation.

To the operator, important circuit elements are C, R_3, and L. In addition, it is only essential to operate at a fixed number of breaks per half-cycle shown by the oscilloscope and a fixed transient current I in the discharge circuit as measured by a thermocouple type radiofrequency meter. The final adjustment of I is made by turning a front panel dial coupled mechanically to vary the interrupter electrode spacing.

The breakdown voltage E can be read on the calibrated oscilloscope, but is even more closely automatically re-established with the adjustment of gap spacing G_1 to give the desired current I. The peak current $J_0=E(C/L)^{\frac{1}{2}}$ is now fixed, which is to say that the shape of the transient discharge has been reproduced.

The combined wattage W dissipated in the two gaps G_1 and G_2 can be computed to a fair degree of accuracy from

$$W=(nCE^2/2)-I^2R_3, \qquad (1)$$

where n is the number of transients per second. In selecting source conditions to give uniform sampling of the analytical electrodes, W comes out to be of the same order of magnitude. Along with E and J_0 (transient shape), W is reproduced in the adjustment of I for any particular set of source conditions.

The intensity of spectrum lines is an increasing function with W simply because of the increased rate in evaporation. The intensity ratio of two lines is a function of W because of differential evaporation and of J_0 because of the usual differences in excitation potentials. Higher peak current transients favor the excitation of the higher energy

[1] R. G. Fowler and R. A. Wolfe, J. Opt. Soc. Am. **35**, 170 (1945).
[2] J. H. Enns and R. A. Wolfe, A.S.T.M. Tech. Publ. No. 76, (1948).
[3] H. Kaiser and A. Wallraff, Ann. d. Physik **34**, 297 (1939).

lines. Only line pairs having a common energy level origin are identically affected by fluctuating excitation conditions if self-reversal is not a factor.[4]

III. SPARK-INITIATED A.C. AND PULSATING D.C. ARC SOURCES

Another development to come out of this study of sources is an arc source whose basic circuit is shown in Fig. 4. When comparing this circuit with that of Fig. 2, it is apparent that a minimum of equipment is involved and a simple operation converts one source into the other. The electrical energy loss in the ballast resistance is roughly only about one-tenth of what it is in the standard high voltage a.c. arc. Operation as an alternating current arc source is illustrated by the upper film strip in Fig. 5. This is a two-gun oscilloscope record showing cyclic current flow through the analytical gap and the resulting instantaneous intensity of the iron arc line Fe-3067 from an iron sample. It shows that while current flow is very uniform, the line intensity varies considerably. This is in agreement with similar records obtained from spark source excitation.[2]

In operation at the outset of each half-cycle in the 60-c.p.s. wave the spark source initiates current flow through the analytical gap. Following this breakdown, the 60-c.p.s., 220-volt line supply is able to maintain current flow through the low reactance bypass circuit R_5 and L_2. Current flow continues for the remainder of the half-cycle as in any conventional a.c. arc source. This circuit is readily adaptable to rectified operation when a high voltage rectifier tube is placed in the charging circuit at point a in Fig. 4. The source is now a d.c. pulsating arc, as illustrated by current and spectrum line traces of Fig. 5, center film strip. The bottom film compares for a.c. arc source operation the instantaneous intensity of the line Fe-3067 against the over-all light (filtered to exclude all radiation above 4000A). In this case it is interesting to note the close agreement between instantaneous fluctuations for these two signals.

In either type of arc source operation the air interrupter serves as a controlling device, always starting current flow through the analytical gap at the same position in the a.c. wave. As in the spark source already described, after resetting of all the stepped circuit elements, fine adjustment of current flow is made by turning the front panel dial which varies the interrupter electrode spacing.

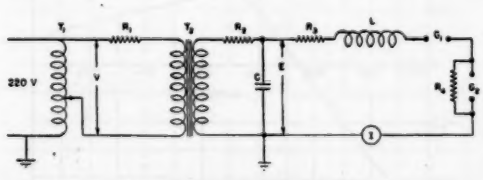

FIG. 2. Spark source circuit.

FIG. 3. Moving pictures of the charging cycle condenser voltage for a 1, 2, 3, and 4 sparks per half-cycle operation.

IV. SOME EFFECTS OF SPARK SOURCE EXCITATION CONDITIONS UPON INTENSITY RATIOS

This section outlines a procedure that has been carried through to demonstrate the flexibility of the air interrupter type spark source. Results show the correlation obtained between source parameters and intensity ratios. In addition to the tabulated data obtained by the usual photographic plate method, direct recording graphs are included to show line intensity *versus* time and intensity ratio *versus* time curves.

A. Sources of Constant Gap Energy and Variable Peak Currents

Table I lists four widely different source conditions that were selected on the basis of desirable energy input into the analytical gap. During preliminary trials the sample pins were examined visually with a magnifying glass following a 30-second run. This was sufficiently close to the total required time for each photographic process of 15-second pre- and 12-second exposure time. The general spectrum intensity, as well as the computed total gap energy W, is about the same in each of the four sources. However, the peak current J_0 is varied by a factor of more than two. In what follows J_0 will be considered as the independent variable and its effect upon the intensity ratio is to be investigated.

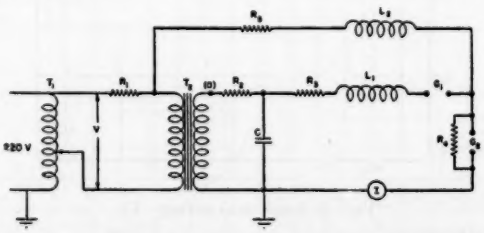

FIG. 4. Spark-initiated arc source circuit.

[4] G. H. Dieke and H. M. Crosswhite, J. Opt. Soc. Am. **33**, 425 (1943).

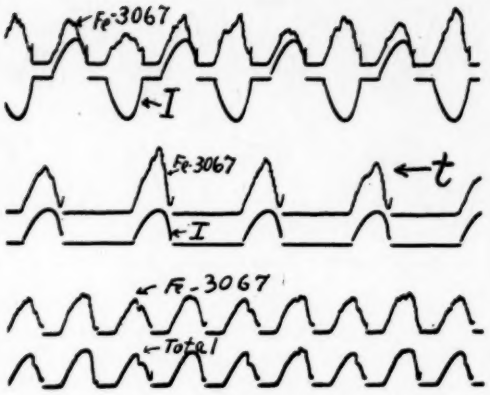

FIG. 5. Cyclic current flow and light output from a.c. and d.c. pulsating arc source.

B. Analytical Samples and Line Selection

The analysis was made for Cr and Mn from steel samples listed in Table II. Line pairs for the photographic method were selected from a paper by P. R. Irish[5] and are given in Table III along with their excitation potentials. The two Fe lines in this table marked with an asterisk go with the Cr and Mn lines in the direct recording technique, since the given line pairs were too close to each other for multiplier tube pick-up.

The sample pins, $\frac{7}{32}$ inch in diameter, were re-ground prior to each exposure to a dome shape of approximately $\frac{1}{2}$-inch radius of curvature. It was always felt that grinding reproducibility as here employed was not too good. For this reason, as well as to reduce the usual photographic effects, each photographic value listed below is the average value obtained from three repeat exposures on the same plate.

C. Analytical Curves

(1) *Photographic Data*

In Figs. 6 and 7 it is shown that while the slope of the analytical curves is essentially constant, the curves themselves are displaced with some degree

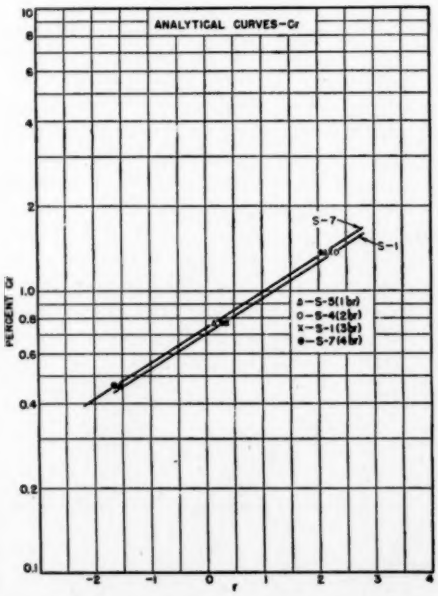

FIG. 6. Analytical curves—Cr.

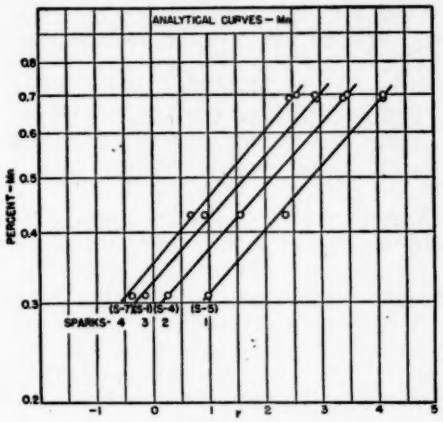

FIG. 7. Analytical curves—Mn.

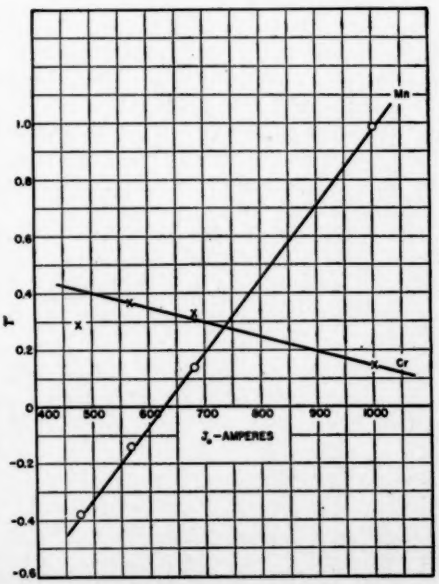

FIG. 8. Log intensity ratio r *versus* peak current J_0.

[5] P. R. Irish, "Spectrographic analysis of alloy," Steel (August 9, 1943).

TABLE I. Spark source parameters.

Source	Sparks per h.c.	R_1	R_3*	L**	C	I	E	J_0	W
S-5	1	7	0.6	10	0.016	24	25,000	1000	255
S-4	2	9	1.1	10	0.008	17	24,000	680	235
S-1	3	9	1.1	10	0.008	17	20,000	566	258
S-7	4	8	1.1	10	0.01	17	15,000	475	222

* R_3—0.1-ohm residual resistance is included.
** L—microhenries.

TABLE II. Samples.

Sample	Cr	Mn
1	1.36	0.43
5	2.22	0.31
6	0.77	0.70
12	0.46	0.69

TABLE III.

Element	Line	Excitation potential	Boiling C°
Cr	2862.57 II	12.58	2482
Fe	2876.80 II	16.02	3000
*Fe	2621.67 II	12.65	
Mn	2933.06 II	12.77	2151
Fe	2936.90 I	4.20	3000
*Fe	3067.24 I	4.93	

of order parallel to each other. This displacement is also illustrated in Fig. 8, where the log intensity ratio r for the particular sample of r near zero is plotted against J_0. For Cr (sample 6, Table II) r decreases with increasing J_0, while for Mn (sample 5) the inverse is true. Also the change in r per unit change in peak current J_0 is appreciably larger for Mn than for Cr.

This observed relationship between r and J_0 is in part explained by the excitation potential ratios of the two line pairs listed in Table III. In the photographic method for Cr/Fe, the values are 12.58 over 16.02 volts, while for Mn/Fe 12.77 over 4.20 volts. Increasing peak currents, according to

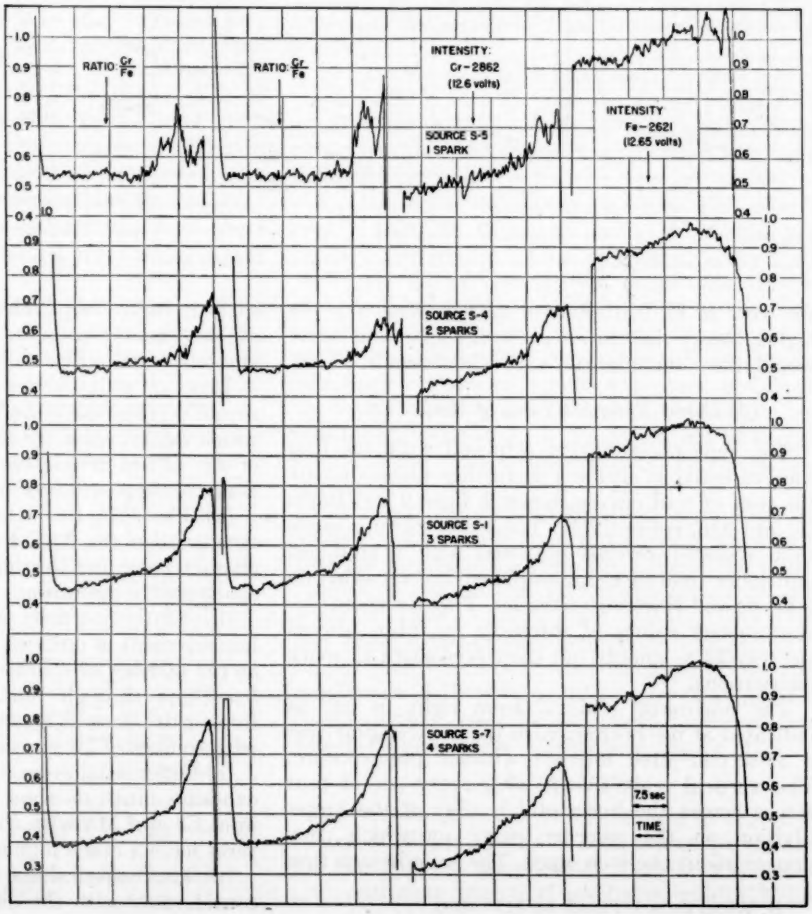

FIG. 9. Recorder time of wait curves for Cr with Table I source parameters.

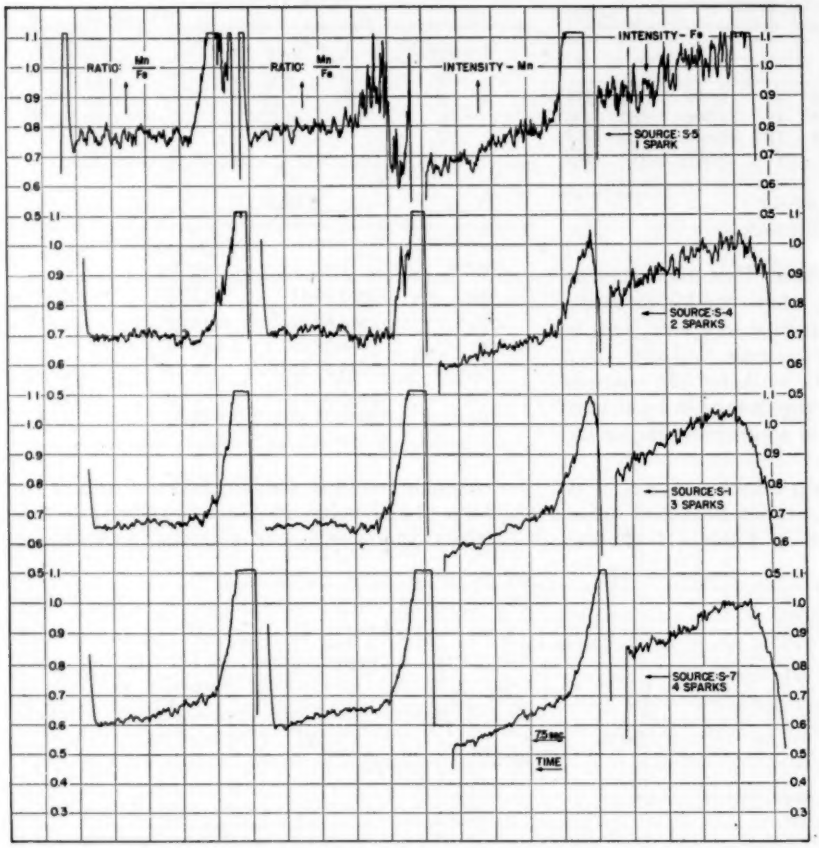

FIG. 10. Recorder time of wait curves for Mn with Table I source parameters.

the work of H. Witte,[6] favor field excitation of the higher energy lines in the cathode region and hence would affect the intensity ratios as shown in Fig. 8.

(2) *Direct Recorded Time of Wait Curves*

The type of excitation achieved with the four sources listed in Table I is further illustrated by the time of wait curves shown in Figs. 9 and 10 for Cr and Mn, respectively. These are tracings made from recorder records obtained with a standard multiplier tube pick-up, amplified and recorded on a Leeds and Northrup recorder. They represent instantaneous values of intensity or ratio, filtered electrically to smooth out the larger spark to spark fluctuations.

The horizontal scale is from right to left as indicated at the bottom, each curve extending over a 35-second time interval without pre-exposure. The vertical scale shown with every set of four traces across the horizontal is that of the larger division on the recorder paper on which they appear about one inch apart. The scale is such that each division is equivalent to a 20 percent change of the amount present, or 2 percent change per one-tenth inch, the smallest recorder scale division.

Time of wait curves obtained in this manner reveal certain source and excitation characteristics which do not show up so well in the photographic or any of the cumulative direct recording methods. Some of these will now be considered.

(a) The 2621 Fe II line is of more uniform intensity than the 3067 Fe I line. This is a general characteristic for the higher energy level lines in spark source excitation.

(b) All the intensity and ratio curves reveal an improvement in uniformity of excitation conditions as the number of sparks per half-cycle is increased from one through four. With steel samples no further decrease in fluctuations was observed even with sources of 20 sparks.

(c) Differential evaporation and the required pre-exposure intervals show up clearly. Compared to iron, Cr and Mn with their lower boiling temperatures have a much higher initial line intensity.

(d) The over-all shape of the ratio curves changes considerably with the different sources. Generally,

[6] H. Witte, Zeits. f. Physik **88**, 415 (1934).

TABLE IV. Photographic log-intensity ratio r, averaged from three exposures.

				Cr $-r$				Mn $-r$		
I	E	J_0	W	189*	192*	195*	190*	191*	193*	194*
19	22,000	622	301	+0.21	+0.24	+0.19	−0.003	+0.05	−0.14	−0.10
17	20,000	566	258	+0.28	+0.30	+0.33	−0.17	−0.12	−0.18	−0.17
15	18,000	510	219	+0.43	+0.37	+0.49	−0.09	−0.17	−0.30	−0.28
13	16,000	453	183	+0.76	+0.46	+0.55	−0.22	−0.21	−0.38	−0.31

* Refers to photographic plate number, Cr-sample 6, Mn-sample 5.

an exposure is taken during that time interval while the slope of the ratio curve is zero or a minimum. Of the four sources here shown, the four-spark source appears least desirable from this standpoint. Fortunately, other source parameters for a four-spark operation can be selected to give a fixed ratio in as little as ten seconds for these same elements and lines.

D. Accuracy of Resetting a Source

In practice it is possible that the breakdown voltage changes from time to time. This may or may not affect the number of discharger per unit of time, depending on the type of interrupter employed. To illustrate this point, as well as to show the accuracy with which a given excitation condition could be re-established, the S-1 source of Table I was only varied in changing the breakdown voltage to give the four r.m.s. currents listed in Table IV. (See Figs. 11 and 12.) The affected electrical quantities and the resulting photographic log-intensity ratios are also tabulated. Each of the r values is the average obtained from three repeat exposures.

In Fig. 9 the log ratio values have been plotted against J_0. The direction of the slope is here the same as in Fig. 6, but much less in magnitude for

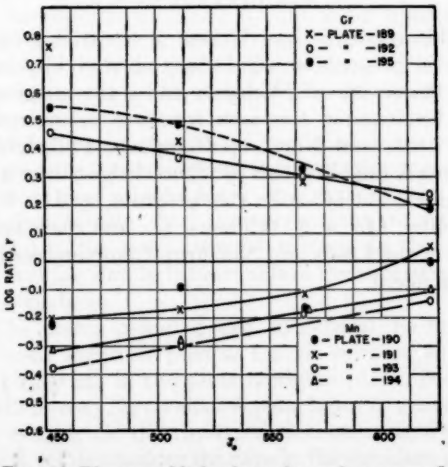

FIG. 11. Photographic log-intensity ratio r *versus* J_0 from Table IV.

TABLE V. Spark source parameters now in use in industrial laboratories.

Alloy	No. sparks	C	L*	R_3	E	I
Ferrous	3	0.008	10	1	20,000	17
Copper	4	0.0045	100	5	17,000	8
Lead	10	0.0015	100	5	17,000	5
Al	2	0.012	350	0	20,000	12
Ni-Cr	4	0.0045	300	0	17,000	5

* L in microhenries.

Mn. From a study of the time of wait curves for Mn shown in Fig. 10, a fifteen-second pre-exposure appears not enough for the 15- and 13-ampere sources. The log ratio in these two cases is somewhat too large.

The 19-ampere source (purposely boosted to 19.2 amperes for taking the recorder curves) shows the effect of overheating. A rise in ratio sets in at the time when the discharge settles to a point and forms a single large crater.

By the scattering of the points in Fig. 9, it is certain that the 17-ampere source yields the best reproducible results. This is so for both Cr and Mn as shown by the results from seven separate test plates. These plates were taken over an extended time interval of about one month during which period source parameters were changed many times. The optimum source condition was more difficult to detect when the results from individual exposures were plotted, in that then pin shape reproducibility and photographic errors became important.

Although little has so far been done with the recorder records in a quantitative way, when plotting the steady value ratio for each of the source conditions (except the S-5 source) against J_0, the result is again a straight line. Working back from this slope, a 100-ampere change in J_0 came out to be equivalent to 0.063 percent change in Mn content for a 0.70 percent Mn concentration. The corresponding result for the photographic method was 0.065 percent per 100-ampere change in J_0.

V. CONCLUSION

To summarize what has been said in regard to source flexibility, Table V lists source parameters for five different alloys which have been found to give optimum analytical results in routine indus-

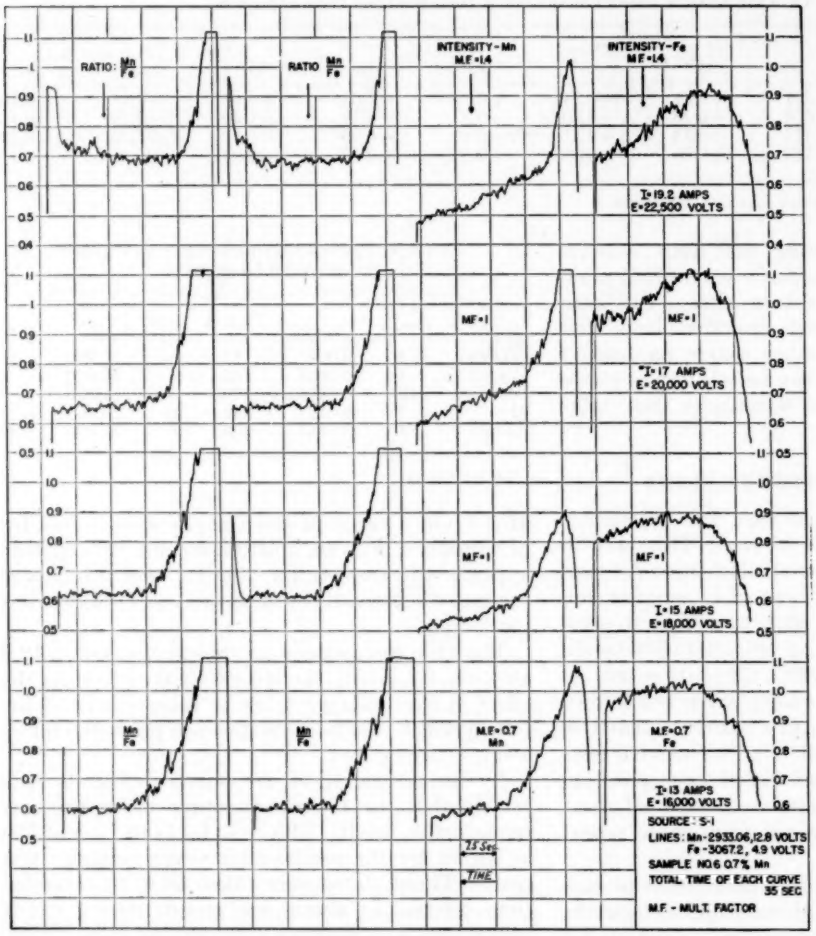
RATIO: Mn/Fe
RATIO Mn/Fe
INTENSITY - Mn M.F = 1.4
INTENSITY - Fe M.F = 1.4
I = 19.2 AMPS E = 22,500 VOLTS
M.F = 1
M.F = 1
I = 17 AMPS E = 20,000 VOLTS
M.F = 1
M.F = 1
I = 15 AMPS E = 18,000 VOLTS
Mn/Fe
Mn/Fe
M.F = 0.7 Mn
M.F = 0.7 Fe
I = 13 AMPS E = 16,000 VOLTS
.25 Sec.
TIME
SOURCE : S-1
LINES : Mn - 2933.06, 12.8 VOLTS
Fe - 3067.2, 4.9 VOLTS
SAMPLE NO.6 0.7% Mn
TOTAL TIME OF EACH CURVE 35 SEC
M.F. - MULT. FACTOR

FIG. 12. Recorder time of wait curves for source conditions listed in Table IV.

trial applications.[7] A future plan is to study excitation conditions for these and a variety of other type samples from direct recording records. Whatever the method of taking data may be, the source needs to have flexibility in transient shape and the number of discharges per unit of time. It should also be possible to reset readily to a given condition with a maximum in accuracy. The work with the air interrupter source has shown that it possesses all of these characteristics.

[7] R. A. Wolfe and E. J. Jemal, Bull. A.S.T.M., No. 129, 45–52 (August, 1944).

VI. ACKNOWLEDGMENTS

This report is based upon a research program now in progress in the Department of Physics at the University of Michigan under the auspices of the Engineering Research Institute, sponsored by the Leeds and Northrup Company, Philadelphia, Pennsylvania. We wish to acknowledge the valuable technical aid given to this program by Dr. R. C. Machler, Mr. A. J. Williams, Jr., and their associates of the Leeds and Northrup Company research department.

JOURNAL OF THE OPTICAL SOCIETY OF AMERICA VOLUME 39, NUMBER 4 APRIL, 1949

The General Theory of Isoplanatism for Finite Aperture and Field

MARIO DI JORIO
Associazione Ottica Italiana, Publication and Bibliographical Research Office, Firenze, Italy
(Received September 4, 1947)

In the introduction we have generalized the definition of isoplanatism and established the corresponding representation for centered systems. In Part I we explain the theory for the meridional bundles, applying the general differential law for two independent wave surfaces. The angle of field may have any finite magnitude. After having found Eq. (35), we transform it conveniently, so that there appear in it only the intrinsic variables which are introduced for the bundles under consideration and the total aberration of aperture, obtaining the condition (42) in invariant form. This is a necessary and sufficient condition.

The explained theory is valid for optical systems more general than centered systems, *viz.*, for those which have only a single plane of symmetry, in which the isoplanatic, linear element can have any direction.

Though we defer the general discussion of the conditions to a later paper in which the theory will be extended to extra-meridional bundles, we make a first analysis of formula (42) deducing from it (Sections II.9–17) some characteristic laws. The extension of the validity of the form of some conditions, for instance those of HERSCHEL and LIHOTZKY-STAEBLE, for general values of fields, shows the principal ray is an axis of bundle even more important than the optical axis in the centered systems.

In the Appendix we shall present some comments on main aspects of the theory.

I. INTRODUCTION

1.

LET us consider an optical system which can be supposed to be centered around an axis which may be called the x axis in the object-space and the x' axis in the image-space. We denote the outside refractive indices by n and n', respectively. Let us consider two object points S and $\bar{S}$, with the infinitesimal separation dl, measured from S to $\bar{S}$. These two points determine a vector the length of which (always >0) is dl.

The two bundles of rays and their wave surfaces emerging from these two points are called isoplanatic when:

(1) there exists a wave surface corresponding to $\bar{S}$ which can be superimposed to a wave surface corresponding to S except for rigid translation and rotation;

(2) the other wave surfaces of the two bundles can be superimposed one by one if we coordinate the wave surfaces which have the same path difference from the surface S considered in (1).

In such a case the element dl is said to be isoplanatic.

We note that the second condition is automatically fulfilled with the first, because when two wave surfaces are superimposed the rays of the two bundles coincide, since the rays are the trajectories normal to the common wave surface. In this case, the rays are simply the normals of the superimposed wave-surfaces.

The points S and $\bar{S}$ can, in general, lie in two different meridian planes. Let us suppose at first that they are in the same meridian plane, because it will be easy, as we shall explain later, to generalize the results. Of the ray-bundles emanating from S and $\bar{S}$, let us consider the rays in the meridian plane forming two meridian bundles. In general the latter are no longer stigmatic in the image-space but still lie in the meridian plane. Since this plane is a plane of symmetry for the image bundles, the condition of isoplanatism requires that the bundle of meridian rays corresponding to $\bar{S}$ be congruent to that corresponding to S. So we can conclude that the rigid rotation of the above mentioned wave surface corresponding to $\bar{S}$ must be around an axis normal to the meridian plane itself.

This paper consists of two parts. In the first we try to find the condition of isoplanatism for meridian bundles. In the second we look for the analogous condition for the skew rays of the bundles.

Let us follow such a method for the reader's convenience, because the considerations relative to the meridian bundles are useful for the extra-meridian ones.

In Fig. 1, P represents the center of the entrance-pupil and p and $\bar{p}$ represent the principal rays relative to S and $\bar{S}$. The angles of field of the two object points are Ω and $\Omega+d\Omega$, respectively. To establish the direction of dl, we specify the angle γ

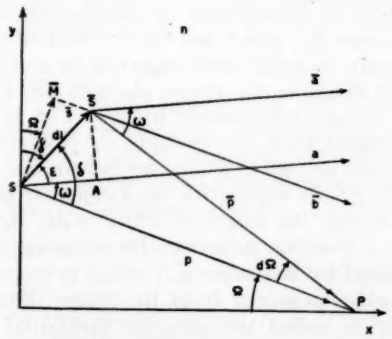

FIG. 1. Fundamental representation in the object-space in tangential isoplanatism.

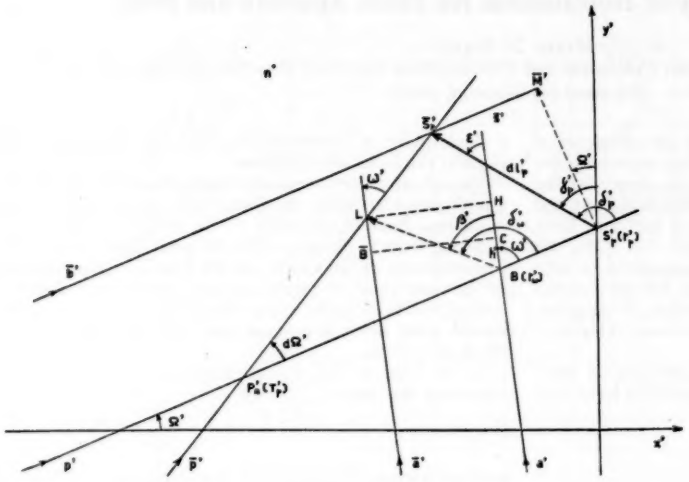

FIG. 2. Fundamental representation in the image-space in tangential isoplanatism.

which the y axis makes with the line element, measured from y.

In the image-space (Fig. 2), the principal rays are transformed into p' and $\bar{p}'$ forming the angles of field Ω' and $\Omega'+d\Omega'$. Their intersection point is P_Ω' which is, in general, not to be found on the x' axis because of the spherical aberration of the principal rays. The point P_Ω' is none other than the tangential (or meridional) image point of P on the ray p. The point S has a tangential (or meridional) image point $S'p$ on the ray p. In this symbol we use the subscript p for the first letter of the word "paraxial," since such an image is formed by the neighboring (although meridional) rays with regard to the principal ray p, which is the axis of the bundle emanating from S. By means of this definition we enlarge the common meaning of the word "paraxial" which is usually applied to the rays around the x axis of the system. Now it indicates, in a wider meaning, the rays around the axis of a general bundle.

Analogously the object point $\bar{S}$ gives rise, along the ray $\bar{p}$, to a tangential (or meridional) paraxial image point $\bar{S}_p'$, which lies on $\bar{p}'$. The line element $S_p'\bar{S}_p'$ may be called the tangential (or meridional) paraxial image of the object element $S\bar{S}$. For this reason it may be denoted by dl_p'. Let us orient this segment from S_p' towards $\bar{S}_p'$, following the same criterion with which we orient the object segment $S\bar{S}$. It represents the tangential paraxial image vector, the length of which is dl_p', which is always a positive quantity. Its direction can be determined by the angle γ_p', which it makes with the y'-axis, measured from the latter. The angle γ_p' may be called the paraxial tangential image of γ.

Isoplanatism can be imposed so that a given pair of rays, forming between themselves an infinitesimal angle, correspond to each other, one emerging from $\bar{S}$, the other from S. Since principal rays p and $\bar{p}$ represent the axes of the bundles with respect to the two given object points and the entrance pupil, it is logical to demand that p and $\bar{p}$ correspond to each other.

This condition is, after all, no restriction, since the entrance pupil may be anywhere.

Once we have stated this, we can say that isoplanatism, if it exists, must also exist if we stop down the entrance pupil so that only the principal rays and their immediate neighborhoods pass through. Then the condition of congruence asks that $\bar{S}'$ correspond to S_p'. We can obtain this result in different ways, for instance, thus. Let us rotate the image bundle corresponding to $\bar{S}$ around an axis through P_Ω' normal to the meridian plane of an angle $-d\Omega'$, so that $\bar{p}'$ coincides with p'. In this way, $\bar{S}_p'$ falls on p', but at a point different from S_p'. Then let us transfer $\bar{p}'$ along p', so that $\bar{S}_p'$ coincides with S_p'. When we have obtained this, no other movement is possible. Another way to obtain the superposition is the following: Let us rotate the image bundle relative to $\bar{S}$ around an axis normal to the meridian plane passing through $\bar{S}_p'$, until $\bar{p}'$ has the same direction as p'. Having done this, if there is isoplanatism, the rays of the image congruences corresponding to $\bar{S}$ and S must be parallel to each other ray by ray. Hence to obtain the correspondence, it is sufficient to add the translation $\bar{S}_p'S_p'$.

We have now found a pair of wave surfaces which, in the case of isoplanatism, must be congruent to each other; they are those which pass through $\bar{S}_p'$ and S_p' and are normal to $\bar{p}'$ and p', respectively. Let us assume these wave surfaces as corresponding to each other. As we have already said, the other pairs of wave surfaces that are

congruent to each other, correspond to an equal difference of optical length from the ones above.

Therefore, to solve the problem, we must, first of all, calculate the difference of optical length for the above mentioned wave surfaces.

2.

Let us consider emanating from $\bar{S}$ a ray $\bar{b}$ parallel to p (Fig. 1). It makes with $\bar{p}$ an infinitesimal angle (the angular aperture of $\bar{b}$ with respect to the axis of the bundle, to which $\bar{b}$ belongs also), equal in absolute value to $|d\Omega|$. Now $\bar{b}$ belongs to the tangential, infinitesimal pencil having $\bar{p}$ as axis, and its conjugate $\bar{b}'$ (Fig. 2) goes through $\bar{S}_p'$. Let us draw the normal from S to $\bar{b}$, the foot point of which is $\bar{M}$, and the normal $S_p'\bar{M}'$ from S_p' to b'. The rays p and $\bar{b}$ being parallel to each other can be considered as belonging to the same normal congruence, of which $S\bar{M}$ represents the trace of an element of the wave surface passing through S. In the image space p' and $\bar{b}'$ still belong, therefore, to a normal congruence, and $S_p'\bar{M}'$, being by construction normal to $\bar{b}'$, represents the trace of the element of the wave surface through S_p'. Such a trace, p' and $\bar{b}'$ being infinitely near to each other, is therefore to be regarded as normal also to p', and thus makes with y' the angle Ω'.

We can therefore write for the optical length:

$$(SS_p')_p=(\bar{M}\bar{M}')_{\bar{b}}=(\bar{M}\bar{S})_{\bar{b}}+(\bar{S}\bar{S}_p')_b+(\bar{S}_p'\bar{M}')_{\bar{b}'}$$

and since $\bar{S}_p'$ is the meridional focus of the tangential, infinitesimal pencil, we have:

$$(\bar{S}\bar{S}_p')_{\bar{b}}=(\bar{S}\bar{S}_p')_{\bar{p}}.$$

Thus we obtain:

$$(\bar{S}\bar{S}_p')_{\bar{p}}-(SS_p')_p=-n\bar{s}-n'\bar{s}', \qquad (1)$$

where $n\bar{s}$ and $n'\bar{s}'$ are the optical lengths of $(\bar{M}\bar{S})_{\bar{b}}$ and $(\bar{S}_p'\bar{M}')_{\bar{b}'}$, respectively.

In the case of Figs. 1 and 2, $\bar{s}$ and $\bar{s}'$ are positive. Orientating $S\bar{M}$ from S towards $\bar{M}$ and assuming analogous conventions for the image space we obtain from Figs. 1 and 2 the following algebraic equations:

$$n\bar{s}=n\sin(\Omega-\gamma)dl, \qquad (2)$$

$$n'\bar{s}'=-n'\sin(\Omega'-\gamma_p')dl_p'. \qquad (3)$$

Substituting in expression (1) we have:

$$(\bar{S}\bar{S}_p')_{\bar{p}}-(SS_p')_p=n'\sin(\Omega'-\gamma_p')dl_p'-n\sin(\Omega-\gamma)dl, \qquad (4)$$

a relation which gives the optical distance between the two chosen wave surfaces.

II.

1.

We are now at the most important part of the problem, and are looking for the condition which the optical system must satisfy to make the meridional bundles isoplanatic.

We obtain the solution of the problem using the general condition, previously stated, characterizing the connection between two image waves belonging to different congruences infinitely near each other.[1]

In the *Appendix* we find some criticisms which will be useful to make evident both this general condition and its application to isoplanatism.

Let us consider a general ray, a, emanating from S at an angle ω with the principal ray. In the image space it becomes a ray a' with an angle ω' with the principal image ray. Let us consider now, a ray $\bar{a}$ starting from $\bar{S}$ parallel to a. Its angle with the principal ray (angular aperture) is nearly ω. In the image space it is transformed into a ray $\bar{a}'$ having an angular aperture still nearly equal to ω'. B and L are supposed to be the points in which these image rays meet the respective principal rays. In the case of isoplanatism the condition

$$L\bar{S}_p'=BS_p' \qquad (5)$$

must be fulfilled and also the difference of optical length (in the image congruence of S) between the wave surface through B normal to a' and that passing through S_p' normal to p' must be equal to the difference of optical length (in the image-congruence of $\bar{S}$) between the wave surface through L normal to $\bar{a}'$ and that passing through $\bar{S}_p'$ normal to $\bar{p}'$. Therefore the optical length $(\bar{S}L)_{\bar{a}}$, and $(SB)_a$ are not equal; but their difference is that given by expression (1) or (4).

Let us choose on $\bar{a}'$ a point $\bar{B}$ such that

$$(\bar{B}L)_{\bar{a}'}=-n\bar{s}-n'\bar{s}',$$

hence

$$BL=\frac{-n\bar{s}-n'\bar{s}'}{n'}. \qquad (6)$$

Then

$$(\bar{S}\bar{B})_{\bar{a}}=(SB)_a.$$

The points B and $\bar{B}$ are those demanded by the above quoted condition. Let us then project $\bar{B}$ on a' at C, finding that

$$h'=BC=BH-\bar{B}L.$$

Let us call β' the angle that the vector BL (oriented from B towards L, corresponding to dl_p') makes with the ray a' measured from the latter. Then the preceding formula becomes, if equations (6), (1) and (4) are substituted,

$$(h')=n'BL\cos\beta'+n\sin(\Omega-\gamma)dl-n'\sin(\Omega'-\gamma_p')dl_p', \qquad (7)$$

where BL denotes the length of a vector and is therefore a positive quantity.

Let us project $\bar{S}$ on a at A (Fig. 1).

[1] M. Di Jorio, Ottica 1, 3 (1947).

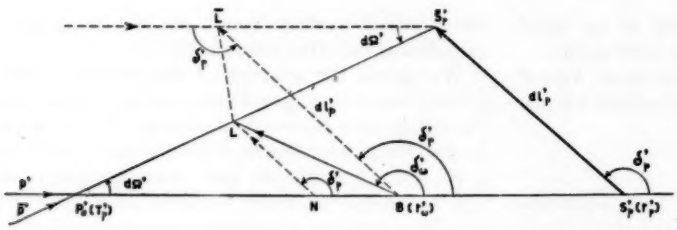

FIG. 3. Illustration of the calculation of BL/dl_p' and $\cos\beta'$.

The condition of isoplanatism is now found by applying to Eq. (7) the formula (3) of reference (1). Thus we obtain

$$(SA)_a=(h'). \tag{8}$$

Let us denote by ϵ the angle which dl makes with the ray a taking the latter as origin side. It may be seen from Fig. 1 that

$$\epsilon=90°-(\Omega-\gamma+\omega),$$

and then:

$$(SA)_a=n\sin(\Omega-\gamma+\omega)dl. \tag{9}$$

Formula (8) by the last relation and (7), gives the desired condition for isoplanatism, namely,

$$n[\sin(\Omega-\gamma)-\sin(\Omega-\gamma+\omega)]dl$$

$$=n'\left[\sin(\Omega'-\gamma_p')-\frac{BL}{dl_p'}\cos\beta'\right]dl_p'. \tag{10}$$

This formula is already remarkable as it undoubtedly represents the solution of the problem from the optical point of view. It would allow us to derive directly some important properties (see Section II.14). But we prefer to transform it by calculating BL/dl_p' and $\cos\beta'$. This investigation is of a completely geometrical nature.

Transforming the left side of expression (10) we can write it thus:

$$n[\sin(\Omega-\gamma)(1-\cos\omega)-\cos(\Omega-\gamma)\sin\omega]dl$$

$$=n'\left[\sin(\Omega'-\gamma_p')-\frac{BL}{dl_p'}\cos\beta'\right]dl_p'. \tag{11}$$

We emphasize that according to our conventions the quantities dl, dl_p', and BL are positive numbers representing the length of vectors.

In the following pages we shall calculate separately BL/dl_p' (see Eq. (17) of Section II.2): $\cos\beta'$ (see Eq. (24) of Section II.3) and finally their product [see Eq. (25) of Section II.4].

However, the product $(BL/dl_p')\cos\beta'$ can be obtained directly by another method, as we shall show in Section II.5.

2.

We pass on to the calculation of (BL/dl_p'). We must examine the two triangles $P_\Omega'LB$; $P_\Omega'\bar{S}_p'S_p'$, which have the following characteristics: the angle in P_Ω' is common to both and of infinitesimal size; $L\bar{S}_p'=BS_p'$. For the reader's convenience the two triangles are shown in Fig. 3. The segment BL may be called a tangential image of $S\bar{S}$ referred to the aperture ω. To the object-vector dl there correspond an infinite number of tangential images: one for each aperture. Hence the vectors dl_p' and BL are, respectively, the paraxial image and the image corresponding to the aperture ω.

The direction of these object-vectors can be conveniently referred to the principal ray p, which forms the angle Ω with the x axis. Let us indicate this direction-angle by δ, measured from p. So δ gives the direction of the object-vector dl (Fig. 1), and δ_p' and δ_ω' give the directions of the image-tangential vectors corresponding respectively to the paraxial angle and the angle representing the aperture ω (Figs. 2, 3).

We see from Fig. 1 that:

$$\delta=\omega+\epsilon, \tag{12}$$

and from Fig. 2:

$$\delta_p'=90°-(\Omega'-\gamma_p'), \tag{13}$$

$$\delta_\omega'=\omega'+\beta'. \tag{14}$$

From $\bar{S}_p'$ (Fig. 3) let us draw the parallel to p' and on it construct $\bar{L}$ such that:

$$\bar{L}\bar{S}_p'=L\bar{S}_p'=BS_p'.$$

The angle made by this parallel and $\bar{p}'$, measured from the parallel, has the value $d\Omega'$. The triangle $L\bar{L}\bar{S}_p'$ is isosceles. Let us connect B and $\bar{L}$. The vector $B\bar{L}$ is then by construction equal to dl_p' (the vectors are parallel, of equal direction, and of equal length).

On the principal ray p' we determine the position of the points S_p', B, and P_Ω', by their algebraic distances from an arbitrary origin on the same ray p'. For instance, we can establish the origin at the intersection point of p' with the last surface of the optical system.

We designate the above mentioned distances by the letter t, writing T for the points on the principal rays of the entrance-pupil. Therefore the points S_p', B and P_Ω' have the algebraic distances t_p', t_ω', and T_p', respectively. These lengths have been written in brackets beside the corresponding points in Figs. 2, 3.

From the triangle $L\bar{L}\bar{S}_p'$ (Fig. 3) we obtain:

$$L\bar{L}=\bar{L}\bar{S}_p'\cdot d\Omega'=(t_p'-t_\omega')d\Omega'. \tag{15}$$

This formula is algebraic and its value is positive if, going from L towards $\bar{L}$, we proceed in the positive sense of the straight line $L\bar{L}$. The orientation of this straight line is determined by the rule that p', $L\bar{L}$, and z' (the normal to the meridian plane) form a left handed coordinate system.

From triangle $BL\bar{L}$ we have:

$$(BL)^2=(dl_p')^2+(t_p'-t_\omega')^2(d\Omega')^2 -2(t_p'-t_\omega')\cos(L\bar{L},\,B\bar{L})dl_p'd\Omega',$$

where the bracket $(L\bar{L},\,B\bar{L})$ indicates the angle between the straight line $L\bar{L}$ and the vector $B\bar{L}$, measured from $L\bar{L}$. This angle is given by the equation

$$(L\bar{L},\,B\bar{L})=-[90°-(\delta_p'-\tfrac{1}{2}d\Omega')].$$

Substituting this in the preceding formula we have

$$(BL)^2=(dl_p')^2+(t_p'-t_\omega')^2(d\Omega')^2 -2(t_p'-t_\omega')\sin\delta_p'dl_p'd\Omega'. \tag{16}$$

This relation is algebraic: dl_p' is essentially positive, being the length of the vector $B\bar{L}$, and δ_p' is the algebraic angle that this vector makes with the ray p'.

From the triangle $S_p'\bar{S}_p'P_\Omega'$ we have:

$$dl_p'/d\Omega'=(t_p'-T_p')/\sin(\delta_p'-d\Omega'),$$

and hence:

$$d\Omega'=(\sin\delta_p'/t_p'-T_p')dl_p',$$

which is an algebraic formula with the same sign conventions as in formula (16).

Substituting this value in the preceding expression of $(BL)^2$ we obtain:

$$\frac{(BL)^2}{(dl_p')^2}=\frac{(t_p'-T_p')^2+(t_p'-t_\omega')^2\sin^2\delta_p'-2(t_p'-T_p')(t_p'-t_\omega')\sin^2\delta_p'}{(t_p'-T_p')^2}.$$

Taking out $\sin^2\delta_p'$ as common factor, we have:

$$\frac{(BL)^2}{(dl_p')^2}=\frac{(t_p'-T_p')^2+(t_\omega'^2-t_p'^2+2t_p'T_p'-2t_\omega'T_p')\sin^2\delta_p'}{(t_p'-T_p')^2}.$$

By adding and subtracting in the second parenthesis of the numerator the term $T_p'^2$, we obtain:

$$\frac{(BL)^2}{(dl_p')^2}=\frac{(t_p'-T_p')^2-(t_p'-T_p')^2\sin^2\delta_p'+(t_\omega'-T_p')^2\sin^2\delta_p'}{(t_p'-T_p')^2}.$$

Thus we obtain the formula:

$$\frac{BL}{dl_p'}=\frac{[(t_p'-T_p')^2\cos^2\delta_p'+(t_\omega'-T_p')^2\sin^2\delta_p']^{\frac{1}{2}}}{|t_p'-T_p'|}, \tag{17}$$

where in the denominator the lines indicate the absolute value, because BL and dl_p' are lengths of vectors.

We note that in this formula δ_p is to be regarded as known, as it gives the direction of the paraxial tangential image of the object $S\bar{S}$.

When $\delta_p'=90°$, formula (17) may be simplified as follows:

$$\frac{BL}{dl_p'}=\frac{|t_\omega'-T_p'|}{|t_p'-T_p'|}. \tag{18}$$

This formula shows that in this particular case, at least in regard to the calculation of the length of the vector BL, this vector and dl_p' can be considered as parallel. Figure 3 becomes Fig. 4, and the value of BL is derived immediately from the similar triangles $S_p'\bar{S}_p'P_\Omega'$, BLP_Ω'. This condition has been discussed in a preceding publication in which δ_p' was equal to 90°.[2]

But in general, if the paraxial tangential image is *not* normal to the principal ray, BL cannot be considered as parallel to dl_p' and formula (17) is needed.

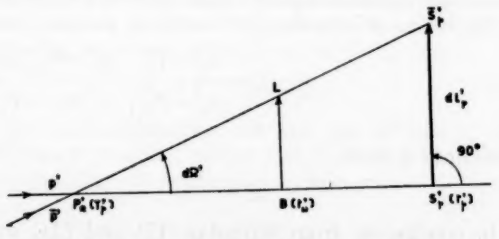

FIG. 4. Special case in which the tangential image S_p', $\bar{S}_p'$ is normal to the principal ray p'.

[2] M. Di Jorio, Ottica 1, 13 (1947).

We notice that, if BL and dl_p' indicate algebraic values, according to the convention expressed by formula (15), formula (18) can be written without absolute value sign as

$$BL/dl_p' = (t_\omega' - T_p')/(t_p' - T_p'). \tag{19}$$

Analogously, in formula (17) the absolute value sign can be omitted, if we define as negative the root of the numerator when $t_\omega' - T_p' < 0$. This may be seen by referring to formula (19), which is a particular case of formula (17).

As we have already noted at the end of Section II.1, the calculation of the separate expression (BL/dl_p') is not necessary in order to calculate the product $(BL/dl_p')\cos\beta'$ which appears in formulas (10) and (11). The expression (17) will however be employed in the theory of isoplanatism for *extra-meridian* bundles.

3.

Let us turn now to the calculation of $\cos\beta'$, appearing in the fundamental formulas (10) and (11).

From formula (14), we derive:

$$\cos\beta' = \cos\delta_\omega' \cos\omega' + \sin\delta_\omega' \sin\omega'. \tag{20}$$

This formula enables us to find $\cos\beta'$, if we know the angle δ_ω' which gives the direction (referred to the principal ray p') of the tangential image vector of aperture ω.

From the triangle $BL\bar{L}$ (Fig. 3) we have:

$$BL/dl_p' = \sin(B\bar{L}, L\bar{L})/\sin(BL, L\bar{L}),$$

where $(B\bar{L}, L\bar{L})$ and $(BL, L\bar{L})$ indicate the angles between the vectors $B\bar{L}$, BL and the orientated straight line $L\bar{L}$, taking, respectively, as origins $B\bar{L}$, BL. These angles are given by the relations:

$$(B\bar{L}, L\bar{L}) = 90° - (\delta_p' - \tfrac{1}{2}d\Omega'),$$
$$(BL, L\bar{L}) = 90° - (\delta_\omega' - \tfrac{1}{2}d\Omega').$$

Substituting in the preceding formula we obtain:

$$BL/dl_p' = \cos\delta_p'/\cos\delta_\omega'. \tag{21}$$

In this formula BL and dl_p' are lengths of vectors and hence are always positive.

From formula (21) and formula (17) we obtain:

$$\cos\delta_\omega' = \frac{|t_p' - T_p'| \cdot \cos\delta_p'}{[(t_p' - T_p')^2 \cos^2\delta_p' + (t_\omega' - T_p')^2 \sin^2\delta_p']^{\frac{1}{2}}}. \tag{22}$$

Formula (21) shows us that, since $\cos\delta_p'$ and $\cos\delta_\omega'$ must have the same signs, $|\delta_p'|$ and $|\delta_\omega'|$ are simultaneously greater or less than 90°. Particularly, if dl_p' is normal to p', BL must be normal to p' also and the vectors dl_p' and BL are parallel. This parallelism exists, therefore, not only as we have seen from formula (18) for the calculation of the length BL, but also for the calculation of β'. This condition has been assumed in the above-mentioned publication with respect to formula (18) and now we see it demonstrated.

In formula (20), besides $\cos\delta_\omega'$, there appears also $\sin\delta_\omega'$ which we obtain easily by means of the formula $\sin^2\delta_\omega' + \cos^2\delta_\omega' = 1$, and we find:

$$\sin\delta_\omega' = \frac{\pm(t_\omega' - T_p')\sin\delta_p'}{[(t_p' - T_p')^2 \cos^2\delta_p' + (t_\omega' - T_p')^2 \sin^2\delta_p']^{\frac{1}{2}}}.$$

In this formula we can avoid the double sign, by the simple artifice of multiplying its right side by the expression:

$$\frac{t_p' - T_p'}{|t_p' - T_p'|}$$

which in absolute value equals unity. Thus we obtain:

$$\sin\delta_\omega' = \frac{(t_p' - T_p')(t_\omega' - T_p')\sin\delta_p'}{|t_p' - T_p'| \cdot [(t_p' - T_p')^2 \cos^2\delta_p' + (t_\omega' - T_p')^2 \sin^2\delta_p']^{\frac{1}{2}}}. \tag{23}$$

In fact, analyzing Fig. 3 and all the possible cases in which Fig. 3 can appear, we see that δ_p' and δ_ω' have their equal or opposite signs according to either the positive or negative product $(t_p' - T_p') \cdot (t_\omega' - T_p')$.

By means of formulas (22) and (23), formula (20) becomes:

$$\cos\beta' = \frac{t_p' - T_p'}{|t_p' - T_p'|} \frac{(t_p' - T_p')\cos\delta_p' \cos\omega' + (t_\omega' - T_p')\sin\delta_p' \sin\omega'}{[(t_p' - T_p')^2 \cos^2\delta_p' + (t_\omega' - T_p')^2 \sin^2\delta_p']^{\frac{1}{2}}}, \tag{24}$$

thus finding $\cos\beta'$.

4.

In conclusion, from formulas (17) and (24) we calculate the expression

$$(BL/dl_p') \cdot \cos\beta',$$

which appears in the fundamental Eqs. (10) and (11):

$$\frac{BL}{dl_p'} \cdot \cos\beta' = \cos\delta_p' \cos\omega' + \frac{t_\omega' - T_p'}{t_p' - T_p'} \sin\delta_p' \sin\omega', \tag{25}$$

which is a very simple formula.

5.

As we have already stated at the end of Section II.1, the product $(BL/dl_p')\cdot\cos\beta'$ can be calculated quickly in this way.

From the triangle $BL\bar{L}$ (Fig. 3) we derive immediately

$$(BL/dl_p')=(\cos\delta_p'/\cos\delta_\omega') \tag{26}$$

which is formula (21).

From formula (14) we have:

$$\cos\beta'=\cos\delta_\omega'\cos\omega'+\sin\delta_\omega'\sin\omega' \tag{27}$$

which is formula (20).

Multiplying member by member of formulas (26) and (27), we have

$$(BL/dl_p')\cdot\cos\beta'=\cos\delta_p'\cos\omega'+\cos\delta_p'\tan\delta_\omega'\sin\omega'. \tag{28}$$

The value of $\tan\delta_\omega'$ may be calculated by finding separately $\sin\delta_\omega'$ and $\cos\delta_\omega'$. The latter is derived from formula (26):

$$\cos\delta_\omega'=(dl_p'/BL)\cos\delta_p'. \tag{29}$$

$\sin\delta_\omega'$ is derived immediately. In Fig. 3 let us draw the vector NL parallel to $S_p'\bar{S}_p'$. We have

$$\frac{NL}{dl_p'}=\frac{|t_\omega'-T_p'|}{|t_p'-T_p'|} \tag{30}$$

because NB, being infinitesimal, is negligible with respect to $P_\Omega'N$.

From the triangle NLB we have also:

$$\sin\delta_\omega'=(NL/BL)\cdot\sin\delta_p',$$

and by formula (30)

$$\sin\delta_\omega'=\frac{|t_\omega'-T_p'|}{|t_p'-T_p'|}\frac{dl_p'}{BL}\sin\delta_p'.$$

In this formula the absolute values need not be used because, as we have already seen with regard to formula (23), δ_p' and δ_ω' have either the same or opposite signs according to whether the $(t_\omega'-T_p')/(t_p'-T_p')$ is positive or negative. Thus:

$$\sin\delta_\omega'=\frac{t_\omega'-T_p'}{t_p'-T_p'}\frac{dl_p'}{BL}\sin\delta_p'. \tag{31}$$

Formula (31) together with formula (29) gives:

$$\tan\delta_\omega'=\frac{t_\omega'-T_p'}{t_p'-T_p'}\tan\delta_p'. \tag{32}$$

Substituting in formula (28) we have,

$$\frac{BL}{dl_p'}\cdot\cos\beta'=\cos\delta_p'\cos\omega'+\frac{t_\omega'-T_p'}{t_p'-T_p'}\cdot\sin\delta_p'\sin\omega' \tag{33}$$

which is formula (25). When $\delta_p'=90°$, this formula becomes:

$$\frac{BL}{dl_p'}\cos\beta'=\frac{t_\omega'-T_p'}{t_p'-T_p'}\sin\omega',$$

and we find again that the vectors BL and dl_p' can be considered parallel to each other. In fact, in this case formula (26) gives $\delta_\omega'=\pm90°$ and formula (14) gives correspondingly $\cos\beta'=\pm\sin\omega'$. So that by the comparison with formula (30) we show that BL is homologous to NL.

Formula (33) may be written in terms of the angles Ω' and γ_p' by making a substitution according to formula (13), thus:

$$\frac{BL}{dl_p'}\cdot\cos\beta'=\sin(\Omega'-\gamma_p')\cos\omega'+\frac{t_\omega'-T_p'}{t_p'-T_p'}\cos(\Omega'-\gamma_p')\sin\omega', \tag{34}$$

6.

By means of formula (34) the fundamental Eq. (11) becomes completely calculable:

$$n[\sin(\Omega-\gamma)(1-\cos\omega)-\cos(\Omega-\gamma)\sin\omega]dl=n'\left[\sin(\Omega'-\gamma_p')(1-\cos\omega')-\frac{t_\omega'-T_p'}{t_p'-T_p'}\times\cos(\Omega'-\gamma_p')\sin\omega'\right]dl_p'. \tag{35}$$

This equation represents the condition which the optical system must satisfy in order that the meridional bundles considered be isoplanatic.

As we have shown from a general point of view,[3] such a condition is not only necessary but also *sufficient*.

The simplicity of the structure of formula (35) is to be noted. The first member is composed of two terms. The first of those $n\sin(\Omega-\gamma)(1-\cos\omega)dl$ is an invariant of the optical transformation, while the second $-n\cos(\Omega-\gamma)\sin\omega dl$, passing from the object space to the image, leads to the corresponding expression multiplied by the factor:

$$(t_\omega'-T_p')/(t_p'-T_p').$$

The axial aberration (on the pseudo axis p' of the image bundle), which can be called the *total* tangential aperture aberration, is equal to

$$t_\omega'-t_p'.$$

The preceding ratio can be expressed as function

[3] M. Di Jorio, Ottica 1, 3 (1947).

of this total aperture aberration as follows:

$$\frac{t_\omega'-T_p'}{t_p'-T_p'}=1+\frac{t_\omega'-t_p'}{t_p'-T_p'},$$

and formula (35) may thus be written:

$$n[\sin(\Omega-\gamma)(1-\cos\omega)-\cos(\Omega-\gamma)\sin\omega]dl$$
$$=n'[\sin(\Omega'-\gamma_p')(1-\cos\omega')$$
$$-\cos(\Omega'-\gamma_p')\sin\omega']dl_p'$$
$$-n'\frac{t_\omega'-t_p'}{t_p'-T_p'}\cos(\Omega'-\gamma_p')\sin\omega' dl_p'. \quad (36)$$

The expression of the right side corresponds to the one on the left side except for the second term. This term depends on the total aperture aberration:

$$-n'\frac{t_\omega'-t_p'}{t_p'-T_p'}\cos(\Omega'-\gamma_p')\sin\omega' dl_p'.$$

The above expression (36) is therefore invariant if total aperture aberration is zero, i.e., if the meridional image bundle is stigmatic.

We have called the difference $t_\omega'-t_p'$ total aperture aberration, as it depends really upon the aperture ω of the bundle and vanishes when $\omega\to 0$. It is, therefore, an aberration referred to S_p'. We have introduced the adjective "total" to distinguish this aberration from that which is generally called, in the optical calculation, aperture aberration. These two aberrations coincide in special cases of correction of the image relative to S, and always when the field Ω is zero.

Introducing a symbol commonly used in optical calculations, formula (36) may be written thus:

$$\Delta n[\sin(\Omega-\gamma_p)(1-\cos\omega)-\cos(\Omega-\gamma_p)\sin\omega]dl_p$$
$$=n'\frac{t_\omega'-t_p'}{t_p'-T_p'}\cos(\Omega'-\gamma_p')\sin\omega' dl_p', \quad (37)$$

where the symbol Δ denotes the difference between the values that the expression under the symbol has respectively in the image space and in the object space.

From formula (37) we deduce that the condition for isoplanatism of a stigmatic meridional image-bundle is

$$\Delta=0. \quad (38)$$

This condition should be more exactly called the condition of *aplanatism*.

Since the second member of formula (37) is zero in the object-space, we can include it also in the symbol Δ:

$$\Delta n\Big[\sin(\Omega-\gamma_p)(1-\cos\omega)-\cos(\Omega-\gamma_p)\sin\omega$$
$$-\frac{t_\omega-t_p}{t_p-T_p}\cos(\Omega-\gamma_p)\sin\omega\Big]dl_p=0. \quad (39)$$

In formula (39) the condition of isoplanatism is written in invariant form. Formula (38) evidently is then correct for the new definition of Δ given by formula (39).

We want to emphasize the simple dependence of the condition of isoplanatism upon the orientations γ_p (or γ) and γ_p' of the corresponding linear elements.

7.

The equations found for the condition of isoplanatism can be easily made independent of explicit reference points and axes of the optical system, and expressed only by intrinsic quantities of the bundles in question, which we call *intrinsic variables*. In condition (35) and in the following equations, derived from it, all the quantities are already intrinsic, except Ω, γ, Ω' and γ_p', which refer to the coordinate axes (x, y) and (x', y'). Observing that in equation (35) there appear only the differences $\Omega-\gamma$, $\Omega'-\gamma_p'$, we can now introduce by means of equation (13) and the analogous form for the object-space, the intrinsic variables δ, δ_p'.

Equation (35) becomes

$$n[\cos\delta(1-\cos\omega)-\sin\delta\sin\omega]dl$$
$$=n'\Big[\cos\delta_p'(1-\cos\omega')$$
$$-\frac{t_\omega'-T_p'}{t_p'-T_p'}\sin\delta_p'\sin\omega'\Big]dl_p', \quad (40)$$

and formula (39) becomes:

$$\Delta n\Big[\cos\delta_p(1-\cos\omega)-\sin\delta_p\sin\omega$$
$$-\frac{t_\omega-t_p}{t_p-T_p}\sin\delta_p\sin\omega\Big]dl_p=0. \quad (41)$$

This equation can formally be simplified, introducing the intrinsic variables ϵ (Fig. 1), ϵ' (Fig. 2), related to ω and to δ by formula (12) and by the analogous relation for the image-space. In fact, in formula (41) we can make the following partial development:

$$\cos\delta_p(1-\cos\omega)-\sin\delta_p\sin\omega$$
$$=\cos\delta_p-\cos(\delta_p-\omega)=\cos\delta_p-\cos\epsilon$$

obtaining:

$$\Delta n\left(\cos\delta_p-\cos\epsilon-\frac{t_\omega-t_p}{t_p-T_p}\sin\delta_p\sin\omega\right)dl_p=0. \quad (42)$$

This is the general equation of tangential isoplanatism, in terms of the intrinsic variables, in a simple form and easy to remember. The intrinsic variables referring to tangential isoplanatism are then:

$$dl_p,\ \delta_p,\ \omega,\ \epsilon,\ t_\omega,\ t_p,\ T_p \quad (43)$$

in which: 1°) δ_p denotes the angle between the vector dl_p and the direction of the principal ray p; if $\mathbf{p}$ denotes a *unit* vector coinciding with the principal ray, we can say that δ_p is the angle between the vectors $\mathbf{p}$ and dl_p, with $\mathbf{p}$ as first side; 2°) ϵ denotes the angle between the general ray a and the vector dl_p, taking a as first side; 3°) t_ω, t_p, T_p are coordinates on the principal ray, measured from any one of its points; 4°) $t_\omega-t_p$ represents the total aperture aberration.

There result the following relations:

$$\left.\begin{array}{ll}\Omega-\gamma=90°-\delta; & \Omega'-\gamma_p'=90°-\delta_p'\\ \delta-\omega=\epsilon; & \delta_p'-\omega'=\epsilon'\end{array}\right\}. \quad (43')$$

We note that δ, δ_p' remain constant while ω, ϵ and ω', ϵ' vary.

Generally the centered optical system has k surfaces, separating $k+1$ optical media or optical-spaces. The first medium (initial object-space) is denoted by 1, the last medium (final image-space) by $k+1$. The medium included between the active surfaces i, $i+1$, is denoted by the number $i+1$, and it is the space $i+1$.

Formula (42) may be written more precisely thus:

$$\underset{1,\,k+1}{\Delta}=0,^* \quad (44)$$

and it is clear that we must take the difference between the values of the quantities under the symbol Δ in the spaces $k+1$ and one, respectively.

Supposing, if this is possible, that an optical system, already isoplanatic between the surrounding spaces 1, $k+1$, is also isoplanatic between the spaces 1, $i+1$, there must then exist together with formula (44) also expression:

$$\underset{1,\,i+1}{\Delta}=0$$

and subtracting from (44) itself, we obtain:

$$\underset{i+1,\,k+1}{\Delta}=0. \quad (45)$$

This is the equation of tangential isoplanatism under the assumption that in the object-space too (in fact the space $i+1$ is the object for the following spaces) aberrations exist but isoplanatism is preserved and bundles of rays come, as always, practically, from the transformation of spherical wave surfaces.

8.

There is no difficulty in verifying whether a system satisfies the condition of the general tangential isoplanatism for a given angle of field. For this purpose the equations, from (35) to (42), have immediate application. It is sufficient to solve the equations for the ratio dl_p'/dl, which represents the linear, *tangential and paraxial* magnification (of course around the axis of the bundle) and to verify whether it remains constant for variable ω. The quantities which are in the expression for the magnification are all calculable. In Section II.10, we shall find the expression of the constant (dl_p'/dl).

If the condition of isoplanatism is fulfilled for a certain angle of field, since the optical system has been so far supposed to be centered, we have isoplanatism for the whole conical zone which we obtain rotating the element dl around the optical axis. When $\gamma=0$, such a zone is reduced to a plane ring, centered on the optical axis.

The condition for isoplanatism has particular importance for those systems functioning with wide angles of field, such as the photographic objectives in general and some photogrammetric objectives in particular.

We must emphasize that, in all the reasonings which have been developed, the only limitation on the structure of the optical system is that it shall have a plane of symmetry, in which the element dl and the principal ray, p, lie. It is not necessary that the system be centered, since it is not necessary that the section of the system with the plane of symmetry should have an axis of symmetry: such a section can be constituted by any lines, on condition that they have continuous tangents at all their points. So the results we have obtained are valid in more general conditions than in those of the centered systems. Besides, it is not demanded, as is the case for normal centered systems, that the index between two consecutive optical surfaces be constant: it is sufficient that the indices in the surrounding media are constant.

Formula (42) shows upon which quantities isoplanatism is dependent. From the very beginning we must decide on the element dl which we want to transform, and the axes p and $\bar{p}$ which we make superimposable. We proceed as follows.

Given dl, let us choose the axis p of the bundle through the object point S determining the angle δ. We now need only to choose the axis $\bar{p}$, relative to

* Note: Isoplanatism is not a transitive quality. Only if the centers of symmetry for both systems coincide can it be concluded that isoplanatism of the combined system and of a part presuppose isoplanatism of the remainder. (Editor)

the other point $\bar{S}$. In formula (42) this choice is determined by T_p. When dl and δ (and therefore p) are determined, to each $\bar{p}$ there corresponds a T_p (and therefore a P). We must emphasize that formula (42) *does not depend upon* P (center of the entrance pupil) *being on the optical axis*: P can be anywhere in the meridional plane. This derives from the above mentioned circumstance that formula (42) is valid, in general, for a system having only one plane of symmetry.

If the object-bundle is stigmatic, $t_\omega - t_p = 0$. In such a case, formula (42) does not depend upon the choice of T_p. Then the dependence of formula (42) upon $\bar{p}$ appears through T_p'.

9.

It seemed opportune to deduce from formula (42) in this Section and in the following ones some interesting conclusions.

Let us ask the question: how does the condition of tangential isoplanatism depend upon the structure of the optical system and upon the position of the linear element dl with respect to the optical system itself?

In formula (42) the quantities dl_p, δ_p, ϵ, ω, $(t_\omega - t_p)$, and $(t_p - T_p)$ are intrinsic to the bundles, and therefore do not depend formally either upon the above mentioned structure or position. In regard to their values, we can say that however an optical system may be rotated around an axis normal to the meridian plane or translated in the direction normal to this axis, these values remain unaltered in the object-space while they change in the image-space. The analysis of these changes enables us to conclude that *the condition of tangential isoplanatism does not depend formally either upon the structure of the system or upon the position of the isoplanatic bundles in respect to it* in the following cases:

1° when to a given δ_p there corresponds necessarily a certain δ_p', as in the case considered in Section 14, in which $\delta_p = 0$;

2° when to a given δ_p corresponds a fixed δ_p' (Sections II.15, 16, and 17).

10.

Let us study formula (42) when $\omega \to 0$. Since the tangential paraxial pencil of S is stigmatic, $t_\omega - t_p \to 0$. On the other hand because of the third equation in formulas (43′):

$$\cos\epsilon = \cos\delta_p \cos\omega + \sin\delta_p \sin\omega$$

which for infinitesimal ω becomes:

$$\cos\epsilon = \cos\delta_p + \sin\delta_p d\omega.$$

Then formula (42) gives:

$$\Delta n \sin\delta_p d\omega dl_p = 0. \tag{46}$$

Hence we obtain for the expression of the tangential paraxial magnification introduced in Section II.8;

$$\frac{dl_p'}{dl} = \frac{n}{n'} \frac{\sin\delta}{\sin\delta_p'} \frac{d\omega}{d\omega'}, \tag{47}$$

and on account of the two first equations in (43′):

$$\frac{dl_p'}{dl} = \frac{n}{n'} \frac{\cos(\Omega - \gamma)}{\cos(\Omega' - \gamma_p')} \frac{d\omega}{d\omega'}. \tag{48}$$

For the relations (43′) formula (46) may be written thus:

$$\Delta n \cos(\Omega - \gamma_p) d\omega dl_p = 0. \tag{49}$$

The expressions in formulas (46) and (49) are invariant and they may be called the *paraxial tangential invariants*.

We can therefore conclude that the paraxial tangential pencils of S and $\bar{S}$ are *always* homologous to each other, *viz.* they are always isoplanatic *even if the finite aperture bundles are not.* This is derived necessarily from the circumstance that a' and $\bar{a}'$ (Fig. 2) can be considered as parallel if $\omega \to 0$. The formulas (46) and (49) express a general law for two object points S, $\bar{S}$, one an infinitesimal distance dl from the other, both in the meridian plane. Such a law necessarily is valid for the optical image formation, determined by *each optical surface.* We can say, therefore that formulas (46) and (49) are optical invariants; which means that the expressions

$$n \sin\delta_p d\omega dl_p; \quad n \cos(\Omega - \gamma_p) d\omega dl_p$$

remain unaltered through the surfaces, whether they are dioptrics or mirrors.

This is valid not only for the centered systems; but for those more general systems already mentioned in Section II.8.

Formulas (46) and (49) represent the fundamental law of the optical imagery of a linear element in the paraxial (around the axes of the bright bundles), tangential field.

We remark that the product $\sin\delta_p dl_p$ represents simply the *projection* of the element dl_p *on the normal* to the principal ray p, lying in the meridian plane (Fig. 1). Formula (46) expresses, therefore, the well-known law that: *the product of the index, the projection of the linear element on the normal to the axis of the bundle, and the infinitesimal aperture is invariant for the optical transformation.*[4]

11.

It is remarkable how formula (46) can be directly obtained, as a particular case of the cosine condition. This is logically possible because the paraxial

[4] M. Herzberger, Zeits. f. Physik **53**, 237 (1929).

tangential and stigmatic transformation of S and $\bar{S}$ is a limit-case of the general stigmatic transformation of these object points.

If S and $\bar{S}$ are stigmatically imaged (let us restrict our considerations to the tangential plane) for a general ray a, the cosine condition applies, i.e.,

$$n \cos\varepsilon dl - n' \cos\varepsilon' dl' = \text{constant}.$$

This law may be applied to the axis p of the bundle, by using the angles δ and ω:

$$n \cos(\delta-\omega) dl - n' \cos(\delta'-\omega') dl' = \text{constant}.$$

The value of the constant can be obtained by calculating the left side for a particular value of ω; we choose $\omega = 0$

$$\text{constant} = n \cos\delta dl - n' \cos\delta' dl'.$$

Substituting in the preceding formula we have:

$$n[\cos(\delta-\omega) - \cos\delta] dl = n'[\cos(\delta'-\omega') - \cos\delta'] dl'.$$

Now generally S and $\bar{S}$ *do not transform* stigmatically, but *in any case* the stigmatic transformation exists in the tangential plane when ω is infinitesimal. Therefore, the preceding relation must *always* exist under these conditions. We remark that in these conditions there is also the value $\omega = 0$ we have chosen for the calculation of the constant. The quantities δ, dl, δ', and dl' become δ_p, dl_p, δ_p', and dl_p'.

Formula (46) is thus immediately demonstrated.

This demonstration is important because it deduces the law of the transformation of a linear element in the tangential paraxial field from that of the general stigmatic transformation, and exactly from the general condition binding two infinitely near waves.[5]

12.

Let us study by means of expressions (42) the special case in which the principal rays p and $\bar{p}$ coincide. The bundles are coaxial, and the points S and $\bar{S}$ are separated on the axis. We have the condition of *isoplanatism either longitudinal or on the axis* of the bundle.

The imposed data demand that $\delta = 0$ or $\delta = 180°$. Necessarily then p' and $\bar{p}'$ coincide, and therefore also δ_p' is zero or 180°.

The rigid movement to superimpose the two isoplanatic bundles is reduced to a translation of one bundle with regard to the other along the common axis.

Formula (42), with respect to the above mentioned values of δ and δ_p' (including the mixed cases which *a priori* can be considered possible, in which one δ is zero and the other has the value of 180°) considering the third and fourth expressions of formulas (43′), becomes:

$$n(1-\cos\omega) dl = \pm n'(1-\cos\omega') dl_p'.$$

In this expression dl and dl_p', as length of vectors, are always positive, the indices are positive by definition, and the trigonometrical expressions in brackets are necessarily positive too. Then, of the two signs, we must reject the $-$ sign. Therefore the mixed cases considered *a priori* are impossible. This means that the vectors dl and dl_p' are both directed in the same sense with which radiation travels along the principal rays p and p', or both in opposite sense. This property is true both in refraction and reflection. The final equation becomes thus:

$$\Delta n(1-\cos\omega) dl_p = 0. \qquad (50)$$

Besides if we make dl and dl_p' algebraic, assuming them as positive, if, proceeding from S towards $\bar{S}$ and from S_p' towards $\bar{S}_p'$, we run the principal rays in the sense of the radiation, and as negative in the opposite sense, we can always return to the case $\delta = \delta_p' = 0$.

Formula (50) does not depend upon the position of the isoplanatic rays with respect to the optical system.

This independence had been foreseen, from a general point of view, in Section II.9 and it is due to the fact that, since $\delta = 0$, the value of δ_p' is necessarily zero, in any position of the isoplanatic waves with respect to the optical system. In particular formula (50) *does not depend upon the angle of field*. Besides the explicit datum of the total aperture aberration, which is given in formula (42), by $t_\omega - t_p$, has disappeared. This means that formula (50) keeps the same aspect also in the longitudinal isoplanatism of two stigmatic waves, i.e. in *longitudinal aplanatism*.

If the system is centered and the angle of field is zero, such an aplanatism defines the so called HERSCHELL condition. *Formula (50) must still be valid* and this is possible just because this equation coincides with HERSCHELL'S condition. The latter was previously known as applied to longitudinal aplanatism on the optical axis. We have lately demonstrated its validity also in isoplanatism,[6] and now finally we see the demonstration of its general validity, although limited to the meridional bundles, for an angle of field however finite. HERSCHELL'S well-known condition has then an unexpected validity.

The fact that the algebraical values of dl and dl_p' must always have the same sign means that the longitudinal magnification, in isoplanatism and aplanatism at least, *is always positive*. This circumstance must be valid also in the centered system

[5] M. Di Iorio, Ottica 1, 3 (1947).

[6] M. Di Iorio. Ottica 1, 52 (1947).

when field angle is zero. And it is just so, as a Gaussian formula states; a formula which is valid in any case in the Gaussian field, even in the absence of aplanatism and isoplanatism [formula (56) of Section II.17]. As we shall see in Section 19, this extension may be made also for oblique bundles.

Formula (50) proves the great significance that the axis of the bundle has in these problems; this axis is a much more characteristic element than the optical axis of a centered system.

These considerations, together with those found in Section II.9 with respect to formula (42), enable us to analyze the structure of an optical system, an analysis which by future researches will be more and more extended.

13.

In Section II.1 we stated that from formula (10) we can derive some interesting facts about isoplanatism without knowing the general expression for the quantity:

$$(BL/dl_p')\cos\beta'$$

which appears in it.

Here we wish to show how easily from formula (10) or (11) we can derive the important conditions (49) of Section II.10 and (50) of Section II.12.

Here is the new derivation of formula (49).

As $\omega\to 0$, BL coincides with dl_p' (Fig. 2). Therefore when we have given an angle $d\omega'$, we can immediately calculate the angle β':

$$\beta'+d\omega'=\gamma_p'+(90^\circ-\Omega')$$

and also

$$\cos\beta'=\sin[(\Omega'-\gamma_p')+d\omega'] \\ =\sin(\Omega'-\gamma_p')+\cos(\Omega'-\gamma_p')d\omega'.$$

From formula (11) we derive then (stating $\cos\omega=1$, $\sin\omega=d\omega$);

$$n\cos(\Omega-\gamma)d\omega dl=n'\cos(\Omega'-\gamma_p')d\omega' dl_p'$$

which is formula (49).

Here is the new derivation of formula (50).

If p and $\bar{p}$ are, for hypothesis, supposed to coincide, p' and $\bar{p}'$ must coincide as well. The rigid movement by which the isoplanatic bundles can be superimposed, is reduced to a translation along p', of amplitude dl_p'. Then, for any value of ω', BL is the same as dl_p'. From Figs. 1 and 2 in this case we obtain $\Omega-\gamma=\pm 90^\circ$, $\Omega'-\gamma_p'=\pm 90^\circ$, in which the $+$ sign holds if the vectors dl and dl_p' are oriented with the principal rays and the $-$ sign in the opposite case. Then $\beta'=-\omega'$ if $\Omega'-\gamma_p'=+90^\circ$; $\beta'=180^\circ-\omega'$ if $\Omega'-\gamma_p'=-90^\circ$. By means of these data formula (11) becomes:

$$n(1-\cos\omega)dl=\pm n'(1-\cos\omega')dl_p'$$

which is formula (50), eliminating the double sign by the same considerations as before.

14.

The circumstance now noted in Section II.13, that in longitudinal isoplanatism $BL=dl_p'$ for any value of ω', allows us to make formula (50) clearer. Especially we can easily see why this condition does not contain the aberration $t_\omega'-t_p'$, whatever its amplitude is, and is thus valid, in the same form, for the longitudinal aplanatism.

In the longitudinal isoplanatism BL represents the distance between the intersections of the rays a' and $\bar{a}'$ (Fig. 2) with the principal ray $p'\equiv\bar{p}'$. Since $BL=dl_p'$, such a distance is constant for any value of ω', *and it has the same value which it would have if there were aplanatism.*

The h' appearing in formula (8), which is the fundamental equation, is

$$h'=BH-\bar{B}L.$$

In isoplanatism in general, and therefore also in aplanatism, $(\bar{B}L)$ does not depend upon the aberration, because it has the value of the difference of the optical paraxial lengths between $\bar{S}$, $\bar{S}_p'$, and S, S_p', as we have seen in Section II.1.

On the other hand, BH, being the projection of BL on the ray a' of general aperture ω, in longitudinal isoplanatism has the value of the projection on a' of a segment of $p'\equiv\bar{p}'$ of constant length dl_p', and coincides therefore in value and sign, for the same value of ω', with the BH of longitudinal aplanatism.

We can therefore conclude that the function $h'(\omega')$ is the same, both in longitudinal isoplanatism and aplanatism. This condition is a consequence of the fact that our isoplanatism depends only upon a *translation.*

The coincidence of the function $h'(\omega')$ reaches the same condition in the two cases, according to a condition already stated from a general point of view.[7]

15.

In Section II.9 we saw that the condition of tangential isoplanatism is independent of the structure of the optical system, and of its position with respect to dl, particularly of the angle of field, when the system transforms a given δ into a specified δ_p'. We want now to show some cases illustrating this property.

Let us study, for instance, the condition of *isoplanatism either tangential transversal or normal to the axis of the bundle* characterized by $\delta=\pm 90^\circ$. Formula (42) considering the third of formulas

[7] M. Di Jorio, Ottica 1, 3 (1947).

(43′), gives the condition:

$$\mp n\left(1+\frac{t_\omega-t_p}{t_p-T_p}\right)\sin\omega dl = n'\left(\cos\delta_p'-\cos\epsilon' - \frac{t_\omega'-t_p'}{t_p'-T_p'}\sin\delta_p'\sin\omega'\right)dl_p' \quad (51)$$

the double sign of which corresponds to the double sign of δ.

In this equation δ_p' can be *a priori* general, and its value depends on the characteristics of the optical system and on its position with respect to the element dl. But if when $|\delta|=90°$, we want also to have $\delta_p'=\pm 90°$, we obtain an equation not depending upon the above mentioned data of the optical system, this of course only for the systems which have these values of δ_p'.

Formula (51), making $\delta_p'=\pm 90°$, becomes:

$$n\left(1+\frac{t_\omega-t_p}{t_p-T_p}\right)\sin\omega dl = \pm n'\left(1+\frac{t_\omega'-t_p'}{t_p'-T_p'}\right)\sin\omega' dl_p',$$

where the + sign applies when δ and δ_p' have the same sign, the − sign in the opposite case. To eliminate the double sign, it is enough to make dl and dl_p' algebraic. This can be done by two coordinate axes normal, respectively, to p' and $\bar{p}'$ and lying in the meridional plane so that each coordinate system, made by the principal ray, the above mentioned normal axis, and the axis z (normal to the meridional plane) are, when taken in this order, a left-handed coordinate system.

By these rules the preceding formula may be written thus:

$$\Delta n\frac{t_\omega-T_p}{t_p-T_p}\sin\omega dl_p=0. \quad (52)$$

If the object-space is corrected, we have

$$n\sin\omega dl = n'\frac{t_\omega'-T_p'}{t_p'-T_p'}\sin\omega' dl_p'. \quad (53)$$

This expression is therefore the condition of transversal isoplanatism (for any given field angle) in the case where $|\delta_p'|=90°$.

The form of this condition, as we had in general foreseen in Section II.9, is valid for any optical system and for any angle of field. Particularly for centered systems, supposing the field to be zero ($\Omega=0$), we have transversal isoplanatism on the optical axis. Formula (53) remains unaltered in form, and, introducing in it the symbols peculiar to these conditions, it becomes:

$$n\sin\omega dy = n'\frac{x_\omega'-X_p'}{x_p'-X_p'}\sin\omega' dy_p'$$

which is a well-known formula of LIHOTZKY and STAEBLE.[8]

In the case of the zero field ($\Omega=0$) for a centered system, we can omit the condition that $|\delta_p'|=90°$, because it is automatically fulfilled.

16.

Another case illustrating the condition stated in Section II.9, can be derived from the paraxial tangential invariant (46). If in it we make $\delta=\pm 90°$, we obtain:

$$\pm nd\omega dl_p = n'\sin\delta_p' d\omega' dl_p', \quad (54)$$

where the double sign corresponds to the double sign of δ.

If we state that $\delta_p'=\pm 90°$, make dl_p and dl_p' algebraic, and introduce the left handed coordinate axes already mentioned in Section II.15, formula (54) becomes

$$\Delta nd\omega dl_p=0,$$

which formally has the same aspect of LAGRANGE-HELMHOLTZ's invariant valid on the optical axis of the centered systems.

17.

We can still develop another important case, looking for the paraxial tangential invariant when $\delta=0$ (or $\delta=180°$).

Formula (46) does not give any characteristic relation, because it becomes identically equal to zero. This is a consequence of the fact that this formula (46) is relative to the first order of ω. Let us begin then from formula (50) already containing the condition $\delta=0$, but depending upon the aperture ω in complete form. We still see that in the first order of ω formula (50) becomes identically equal to zero. But if we develop $\cos\omega$ to the second order we obtain

$$\Delta n\omega^2 dl_p=0, \quad (55)$$

where dl can be considered algebraically in the way defined in Section II.12 referring to formula (50).

This invariant, in the same form, must apply also to the optical axis of a centered system, with the single change of writing dx in place of dl. Solving for the longitudinal magnification I_z, formula (55) in this case gives

$$I_z=(dx_p'/dx)=n/n'(\omega/\omega')^2, \quad (56)$$

an expression which coincides with a well-known formula of gaussian optics which connects LAGRANGE-HELMHOLTZ's invariant with the Gaussian relation $I_zI_\omega=I_y$.

Now too we see that a Gaussian invariant is valid in very general cases.

[8] M. Di Jorio, Ottica 1, 13 (1947).

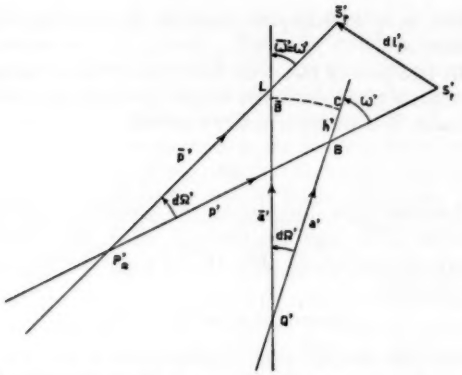

FIG. 5. The condition of tangential isoplanatism by assuming as point of departure the two superposed isoplanatic congruences. The differential general law, for two independent waves, deducted in this special case. In the figure there is the representation of the image-space.

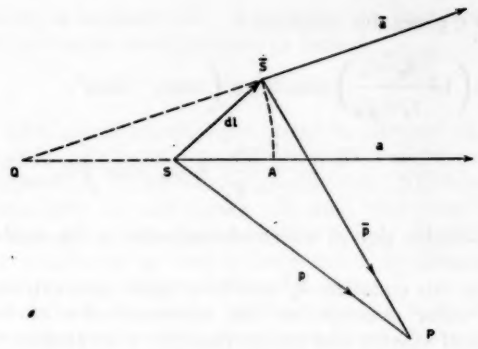

FIG. 6. The condition of tangential isoplanatism by assuming as point of departure the two superposed isoplanatic congruences. The differential general law for two independent waves, deducted in this special case. In the figure there is the representation of the object-space.

Formula (55), being valid for both refraction and reflection, shows that the longitudinal tangential and paraxial magnification (around the axis of the bundle) is always positive. This is true also of the optical axis of centered systems, as formula (56) indicates directly.

The condition expressed in general by formula (55) is easily proved for the spherical refracting surface by the formulas of the tangential astigmatism. The latter, choosing for coordinate origin on both the incident and refracted axes of the astigmatic pencil the point in which these axes meet the spherical refracting surface, is expressed by the formula:[9]

$$(T/t)+(T'/t')=1,$$

where

$$T=\frac{nr\cos^2\varphi}{n\cos\varphi-n'\cos\varphi'};\quad T'=\frac{-n'r\cos^2\varphi'}{n\cos\varphi-n'\cos\varphi'}.$$

The quantity r is the radius of the spherical refracting surface, and φ and φ' are respectively the angles of incidence and refraction on the axis of the pencil.

From these formulas we obtain:

Longitudinal magnification

$$=(dt'/dt)=-[TT'/(t-T)^2]>0$$

because the above expressions show that the product TT' is always negative. We note that formula (55) can be also obtained by the procedure followed in Section II.11, developing the functions of ω to the second order, and we note also that this is naturally possible because the stigmatic transformation must apply to the second order.

The developments of Sections II.15, 16 and 17 demonstrate once again that, according to what was said in Section II.12, the axis of the bundle is an element much more characteristic than the optical axis of the centered systems.

[9] G. Giotti, *Lezioni di Ottica Geometrica* (Zanichelli, Bologna, 1931), p. 381.

APPENDIX

1.

It is perhaps desirable, in order to make clearer the above explained theory and its bases, to make some remarks on the application of Section II.1 of the general differential law for two independent waves in the investigation of the condition of isoplanatism.

In the arguments which are at the basis of the theory the important condition is that the chosen pair of rays, belonging to different congruences infinitely near to each other, can be considered as constituting a pair of a normal congruence. If in the object-space we choose initially two parallel rays, the reason is to be found in the fact that these rays belong, of course, to a normal congruence. Therefore the solution of several problems is reduced to an automatic application of a method. But such a choice is not obligatory at all.

When sometimes we say or we let the reader understand that the conjugates in the image-space of the rays chosen parallel in the object-space are still nearly parallel to each other, we want in short to express the idea that also the conjugates belong to a normal congruence.

Let us suppose that the two isoplanatic bundles are congruent to each other. We have thus one bundle only, in which every ray is double, one of them emanating from S, the other from $\bar{S}$ (in consequence of the optical transformation of the bundle emanating from $\bar{S}$, and of the rigid movement defined by isoplanatism). An one-dimensional manifold of rays of this bundle is plane and lies in the meridional plane.

On each ray of this meridional manifold there is a double point representing the two paraxial images of the given points relative to the same ray taken as axis.

Let us now go the opposite way to Section II.1, separating the two homologous congruences, which can be done in infinite ways.

Let us choose any double ray of the meridional manifold, and let us consider it as principal ray in the two bundles, *viz.*, as axis of the bundle, and denote it by $p'\equiv\bar{p}'$. The double point existing on it, which we mentioned, will be denoted by $S_p'\equiv\bar{S}_p'$. As we see, the choice of the principal ray, which is the fundamental element for isoplanatism, is completely arbitrary.

Let us choose a point P_Ω' on $p' \equiv \bar{p}'$, representing the tangential image of the center P of the entrance-pupil, relative to the axis p'. This center P may thereby be determined when the optical system is assumed, because we obtain it by an inverse optical transformation, an inverse tangential image of p_Ω' along p'. In general therefore, P will not fall on the optical axis of the system, even *if the optical axis exists.* This agrees with the fact that the developed theory asks only (Section II.8) that the optical system possess a plane of symmetry (called meridional or tangential plane). Also the meridian section of the system need *not have an axis of symmetry.* The only restriction, which we have already mentioned in Section II.8, is that such a section is constituted by lines having continuous tangents in all their points.

Let us consider also an arbitrary double ray $a' \equiv \bar{a}'$ intersecting the principal ray $p' \equiv \bar{p}'$ at the double point $B \equiv L$ and making with the principal ray the angle $\omega' = \bar{\omega}'$. The wave passing through B and normal to a' coincides with the one passing through L and normal to $\bar{a}'$.

We accomplish now, in the following way, the doubling of the two bundles, one deriving from $\bar{S}$, the other deriving from S. Let us make a rigid infinitesimal translation along $p' \equiv \bar{p}'$, so as to separate infinitesimally $\bar{S}_{p'}$ from $S_{p'}$. The ray $a' \equiv \bar{a}'$ divides in two parallel rays, and also the points B and L separate so that the former has the same distance from the latter as $S_{p'}$ from $\bar{S}_{p'}$. Now let us make an infinitesimal rotation $d\Omega'$ around an axis normal to the meridional plane and passing through P_Ω'.

In this way we arrive at the definite state of the bundle coming from $\bar{S}$. In particular, $\bar{p}'$ and $\bar{S}_{p'}$ will find themselves in certain positions.

The optical system will be naturally such as to satisfy these conditions imposed *a priori* in the image-space.

The ray $\bar{a}'$ makes with a' the same angle $d\Omega'$ which we have mentioned, and ω' is still the same as $\bar{\omega}'$ (Fig. 5). For construction, L is as far from $\bar{S}_{p'}$ as B from $S_{p'}$. Let Q' be the intersection point of $\bar{a}'$ with a'. Let us denote in the object space the conjugates of the principal rays and of the rays a; *viz.*, the elements: p, $\bar{p}$; a, $\bar{a}$ (Fig. 6). The rays a and $\bar{a}$ *will not generally be parallel;* but they will make an infinitesimal angle and will meet each other at a point Q, conjugate to Q' according to the couple a', $\bar{a}'$. The only substantial difference between these considerations and those explained in Section II.1 lies in this absence of parallelism between a and $\bar{a}$. On the other hand, in Section II.1 we had considered a and $\bar{a}$ parallel to each other, but a' and $\bar{a}'$ did not *strictly* make the same angle of aperture with their own principal rays. Now, on the contrary, the equality between ω' and $\bar{\omega}'$ is a condition stated at the very beginning, because we have begun the study of the image-space, and so we have imposed the exact condition for isoplanatism.

These little differences in the foundation-data of the problem have no value in the treatment, and the considerations which we are developing are used just to exhibit this fundamental circumstance.

On the other hand, the method according to Section II.1 appears to be the most practical, as it has the advantage of the automatic application of a general condition, useful to the study of several problems, which originate therefore from only one principle, the one expressed by the general differential law for two independent waves. Between the waves passing through $S_{p'}$ and $\bar{S}_{p'}$, and normal, respectively, to p' and $\bar{p}'$, there is the difference of optical length already calculated in Section I.2. This same difference exists between the waves passing through B and L and normal, respectively, to a' and $\bar{a}'$, since before the separation they were coincident. Then we can find by the same criterion used in Section II.1 a point $\bar{B}$ on $\bar{a}'$ such as the wave passing through $\bar{B}$ normal to $\bar{a}'$ corresponds (with respect to $\bar{S}$) to the same value of the optical length of the wave passing through B normal to a' (referred to S):

$$(\bar{S}\bar{B})_{\bar{a}} = (SB)_a. \tag{57}$$

The rays a' and $\bar{a}'$, meeting each other at the point Q', can be considered as belonging to the same normal congruence, and the same must consequently be true of the couple a, $\bar{a}$.

We can then consider the elements of wave surfaces $\bar{S}A$ (circular arc with center Q—Fig. 6), $\bar{B}C$ (arc with center Q' Fig. 5), and write:

$$(\bar{S}\bar{B})_a = (AC)_a,$$

or

$$(\bar{S}\bar{B})_{\bar{a}} = (SB)_a - (SA)_a + (BC)_{a'}.$$

Substituting in formula (57) we have:

$$(SA)_a = (h').$$

This is just formula (8), which is thereby shown to coincide with the expression of the general differential law for two independent wave surfaces.

ACKNOWLEDGMENT

It is for me a pleasure and a duty to thank Dr. M. Herzberger for the kind interest he took in this publication. He gave me some valuable references concerning the literature on the subject and offered to help me with my difficulties in English.

Resolving Power Limitations of Grating and Prism Spectrometers

JOHN STRONG
Johns Hopkins University, Baltimore, Maryland
(Received January 10, 1949)

The fact that gratings give better resolving power than prisms in spectrometry in instances where available source energy or available detector sensitivity, and not diffraction blurring of spectrum details, sets the limitation, is shown to be because of the greater dispersion of gratings. The available energy for a given band pass, $\Delta\nu_0$, for either prisms or gratings, is shown to be proportional to the product of efficiency and dispersion. This product is estimated for gratings and prisms. The best grating spacing is indicated to be of the order of one wave-length which, for the visible spectrum, would mean a grating of some 37,400 lines per inch. The importance of obtaining true echelette facets is emphasized and a means of obtaining them is suggested.

INTRODUCTION

THIS paper is concerned with limitations on spectral resolving powers obtainable with gratings and prisms, especially in instances where available source energy or available detector sensitivity, and not diffraction blurring of spectrum details, sets the limitations on attainable resolving power. Slits must be set much wider than the diffraction pattern when the spectral source is weak or when the detector is insensitive.

The distribution of energy in the various spectral orders of a Michelson echelon and an echelette grating has been treated by Michelson and others.* Following these authors, it is here simply shown that substantially all of the incident spectral energy should fall in the center of the blaze of an ideal echelette grating of small echelette angle. The discrepancy between this prediction and experience in the visible spectrum is attributed to the lack of flatness of grating groove facets. The shading of the effective facet by the ineffective facet is here ignored. The energy distribution is assumed, with Conn, to be enveloped by the diffraction pattern of a single isolated one of the effective facets.

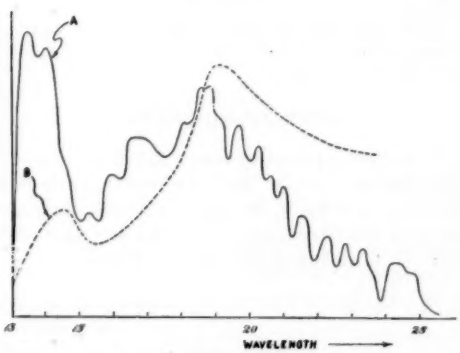

FIG. 1. Curve A: galvanometer deflection *vs.* wave-length. The shape of this curve is determined primarily by the thermopile blackener characteristics, the absorption of a 7-meter laboratory air path, 5 reflections from freshly cleaved β—MgO, the Globar emission, the dispersion of the grating, and its efficiency—the efficiency function, T. Curve B: this curve is A with the CO_2 and H_2O absorption removed, with the Planck emission removed, and with the dispersion of the grating removed. It represents T only approximately, but serves to show the usefulness of an echelette at wave-lengths greater than $d(d=19.26\mu)$.

It is not unreasonable to expect that gratings approach the ideal echelette form in the infra-red more closely than they do for the visible or ultra-violet when one considers the flatness of the grating groove shapes in similitude to the waves they diffract. It is, further, not unreasonable to expect that a second light reruling of a grating face might give more nearly ideal groove shapes for the visible spectrum—the second light ruling serving to correct the imperfections of form left by the first heavy ruling.

We plan to study the distribution of energy by diffraction gratings and carry out experiments on means to improve it. For the present some definite conclusions can be drawn from an old spectrum of my own (see Fig. 1) and from the experiences of others, all cited in Table I. These citations show that gratings perform very well in the infra-red when grating grooves are just one wave-length wide, or even less, rather than three or five wave-lengths wide as is sometimes expected. Figure 1 shows the old spectrum (solid) and the curve of efficiency of the grating (dotted). The latter has five reflections of freshly cleaved MgO, the detector blackness and the globar emissivity remaining in it. The Planck function, the absorption of CO_2 and H_2O, and the dispersion of the grating were removed from curve A to give curve B. The deficiency from 15 to 19μ is presumably due to the MgO reflections; the interpretation of the dotted curve as an efficiency curve is subject to doubt; it does show a sustained efficiency where the wave-length is greater than the groove spacing.

* G. K. T. Conn, Proc. Camb. Phil. Soc. **43**, 240 (1947); A. A. Michelson, Astrophys. J. **8**, 37 (1898); W. E. Williams, Proc. Phys. Soc. London **45**, 699 (1933); K. W. Meissner, J. Opt. Soc. Am. **32**, 200–204 (1942); Robert F. Stamm, and John J. Whalen, J. Opt. Soc. Am. **36**, 1 (1946). This last paper presents calculations following Rowland's formula for intensities which appears in pp. 525–544 of his collected works.

GENERAL CONSIDERATIONS

In order, later, to make comparisons of grating spectrometers with prism spectrometers, let us consider a complete infra-red spectrometric equipment which includes a source, a spectrometer, and a radiation detector with noise limitation of w_0 watts of flux.

For the present no discrimination will be made as to the dispersing means—it may be a grating or prism characterized by a dispersion of $d\theta/d\lambda$ and by a transmission or efficiency of T. We will neglect all sources of radiant energy waste except that incurred through T. Let the entrance slit and exit slit of the spectrometer have the same width and length; also, let the focal length, F, and the area of aperture, A, of collimator and telescope, be equal.

For simplicity, let the source emit according to the Rayleigh-Jeans distribution law,

$$B_\lambda = B_0\Theta/\lambda^4 (\text{watt/cm}^2 \text{ steradian cm}).$$

Here Θ is the absolute temperature of the source.

The energy through the exit slit will be

$$w = TB_\lambda sl(A/F^2)\Delta\lambda \text{ watt},$$

where s and l are the exit and entrance slit height and length, and $\Delta\lambda$ is the wave-length range embraced by it.

$$\Delta\lambda = [s/F(d\theta/d\lambda)].$$

When studying a molecular spectrum it is significant to measure the resolving power by the wave number range embraced by the slits, $\Delta\nu$. To keep this constant, say at the value $\Delta\nu_0$, the slits must embrace a greater wave-length range at longer wave-lengths. In fact, from $\lambda\nu = 1$, we get

$$\Delta\lambda = \lambda^2\Delta\nu_0.$$

Substitution gives

$$w_0 = (B_0\Theta\Delta\nu_0^2 lA/F)T(d\theta/d\lambda) \qquad (1)$$

or

$$\Delta\nu_0 = (Fw_0/B_0\Theta AlT(d\theta/d\lambda))^{\frac{1}{2}}. \qquad (2)$$

There are several things significant about this expression:

First, to reduce the $\Delta\nu_0$ to half its former value it is necessary to increase the detector sensitivity, or the available energy, or the dispersion by a factor of four. The substantial improvement in resolving power in the infra-red which was achieved by Sleator at Michigan by the use of gratings, instead of prisms, was due to the superiority of the dispersion of the gratings used.

Second, the wave number resolving power in the far infra-red, on the basis of equal dispersion, and for a Rayleigh-Jeans source, is independent of wave-length. There is no reason, therefore, to decry the fourth-power fall-off since, where it obtains, the wave number resolving power will surpass that obtainable at the blackbody maximum by $(28)^{\frac{1}{2}}$ [for the Rayleigh-Jeans law gives 28 times the flux that Planck's law gives at the maximum $(hc/\lambda_m k\Theta = 4.965)$].

It will be shown later that $d\theta/d\lambda$ for a grating is proportional to $1/d$ and, since d and λ are approximately equal, proportional to $1/\lambda$. The value of $\Delta\nu_0$ will therefore increase as we go into the infra-red unless A is increased proportionally with λ. This, if nothing else, alerts one to the future need, in the infra-red, for large gratings.

A simple criterion for evaluating the relative merits of gratings and prisms is obtained in the quantity $-T(d\theta/d\lambda)$.

TABLE I.

Author	Grating spacing	Wave-length limits	Remarks
R. W. Wood, Phil. Mag. 20, 770 (1910).	12.3μ and 50μ	4.3μ region	First resolution of an infra-red band was obtained with these first echelette gratings.
W. W. Sleator, Astrophys. J. 68, 125 (1918).	1.69μ 3.38μ 10.6 μ	to 2.86μ to 2.87μ to 6.83μ	Sleator's Fig. 5 shows resolution approximately proportional to $1/d$.
H. M. Randall, J. App. Phys. 10, 768 (1939).	21 μ	15μ to 25μ	At longer wave-length the same relation of wave-length to grating spacing obtains.
John Strong, J. Frank. Inst. 232, 7 (1941).	19.5 μ	25μ	See Fig. 1. Echelette angle was 21°. Angle between telescope and collimator was (22½°).

TABLE II. NaCl prism calculations at 9 and 14μ.

At λ = 9μ:								
Prism Angle	45°	50°	60°	65°	70°	75°	80°	
T	.92	.92	.90	.88	.85	.77	.61	
$(d\theta/d\lambda)$	55	65	90	106	131	173	278	
$T(d\theta/d\lambda)$	51	60	81	93	111	133	151	
At λ = 14μ:								
Prism Angle			60°	65°	70°	75°	80°	85°
T			.90	.88	.87	.84	.71	.37
$(d\theta/d\lambda)$			114	173	210	268	380	840
$T(d\theta/d\lambda)$			102	152	183	225	270	310

THE PRISM

Dependence on Prism Angle

The values of $(d\theta/d\lambda)$ for a prism are computable from the index and prism angle. This $(d\theta/d\lambda)$ increases rapidly with increasing prism angle. The values of T for a prism are also computable from the index and prism angle and absorption of the prism. Computations have been made for a rock salt prism at 9μ and 14μ, neglecting body absorption. The results are given in Table II. From as long ago as when I was a graduate student I have sensed the gain to be obtained with prism angles larger than 60° and I have used larger angles in my work. In fact, it was due to my firm opinion then that prisms were promising, that I had the enthusi-

asm to grow and make large synthetic alkali halide prisms.**

Without, for the present, making the laborious computations for all prisms at all wave-lengths, it is evident from Table II that $d\theta/d\lambda$ for a 60° prism lies within a factor of 2 or so of the value one would get, in practice, at larger prism angles. Even allowing this factor and taking $T_{\text{prism}}=1.0$ and neglecting body absorption, we will see shortly that the grating is superior to the prism.

THE ECHELETTE GRATING

Littrow Case (in the blaze)

When an ideal shallow echelette grating, such as the one depicted in Fig. 2, is used in the Littrow arrangement, as indicated, so that the used wave-lengths are returned on themselves in the center of the blaze the order n_0, then the adjacent orders (n_0+1) and (n_0-1), which fall on either side of the order n_0, will lie at the angles which give just one wave-length more or less path difference. This circumstance puts them almost exactly on the first minima of the single slit diffraction pattern of the echelette facets. Accordingly, little or no energy can go into these competing orders to deplete the energy in the used order n_0. The quantity β in the pattern expression, $[\sin\beta/\beta]^2$, is π.

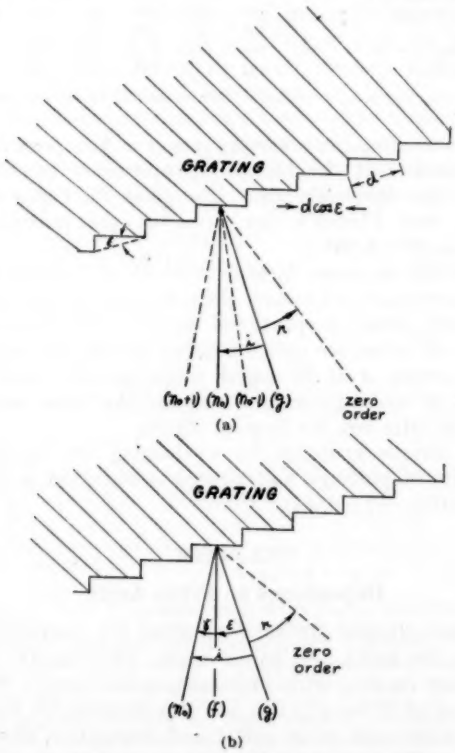

FIG. 2a. Echelette grating used in the Littrow arrangement in the center of the blaze. (n_0) is the direction of incidence and of diffraction of the used wave-length. It is also the facet normal. (g) is the grating normal. $(n_0\pm1)$ are adjacent unused orders of diffraction. FIG. 2b. Echelette grating used in the Littrow arrangement near the center of the blaze. (f) is the facet normal. (g) is the grating normal. (n_0) is the direction of incidence and of diffraction of the used wave-length.

** John Strong, Phys. Rev. **36**, 1663 (1930).

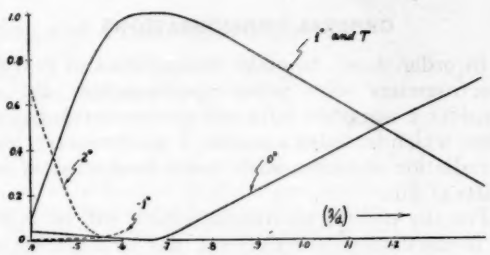

FIG. 3. This figure shows $(\sin\beta/\beta)^2$ for the significant orders of an echelette grating of $\epsilon=20°$ as function of λ/d. Since the sum of all ordinates is nearly unity at all (λ/d)-values, the curve for $n_0=1°$ is also T, the predicted efficiency of the grating.

Now at higher orders $(n_0\pm2)$, $(n_0\pm3)$, etc., β will have values of 2π, and higher; $\sin^2\beta$ is equal to unity, or less than unity. Also, $1/\beta^2\leqq1/40$. Thus $[\sin\beta/\beta]^2$ is of the order of a few percent and little or no energy can go into other orders, including the zero *th* order, to deplete the energy in order n_0. The implication, from consideration of the single slit diffraction pattern, then, is that the efficiency, T, is very nearly unity.

A simple analysis will yield the same result. All the quantities in the equations are shown in Fig. 2a.

$$\beta=(\pi d\cos\epsilon/\lambda_0)\sin(\epsilon+r),$$
$$n_0\lambda_0=2d\sin\epsilon,$$
$$(n_0\pm k)\lambda_0=2d\sin\epsilon\pm k\lambda_0=d(\sin\epsilon-\sin r),$$

where k is an integer order increment. From the above grating equation for the order $(n_0\pm k)$ we have

$$\lambda_0=d/\mp k(\sin\epsilon+\sin r).$$

This gives

$$\beta=\mp k\pi\cos\epsilon(\sin(\epsilon+r)/(\sin\epsilon+\sin r)).$$

Now if a grating is shallow, as we postulated, then

$$\cos\epsilon\sim1.$$

When the orders $(n_0\pm1)$ lie near $r=-\epsilon$, then

$$\cos r\sim1.$$

This gives, for $k\sim1$,

$$\beta=+k\pi \quad\text{and}\quad (\sin\beta/\beta)^2=0.$$

For longer wave-lengths, when $n_0=1$, the validity of this analysis is impaired.

Littrow Case (near the blaze)

Since it would be impossible to use a separate grating for each λ_0, it is necessary to examine the efficiency, T, when the grating is used out of its blaze. T will deteriorate at wave-lengths adjacent to λ_0 because the grating facet will have been rotated so that the blaze lies to one side or the other of the used diffracted light. The following expression is used to estimate T.

$$T=\frac{[\sin\beta/\beta]^2_{n_0}}{\left(\sum_{-\infty}^{\infty}{}_k[\sin\beta/\beta]^2_{n_0+k}\right)}. \qquad (3)$$

The quantities of Fig. 2a have their same meaning. In Fig. 2b γ represents the angular distance at which one is working away from the effective facet normal in the Littrow spectrometer. Before each term of the denominator of the expression for T is computed, it is necessary to find the value of r which corresponds to k. Combining the first two of the following cogent grating equations gives the third equation which defines r.

$$(n_0+k)(\lambda/d)=\sin(\epsilon+\gamma)-\sin r,$$
$$(n_0\lambda/d)=2\sin(\epsilon+\gamma),$$
$$-\sin r=[(n_0+2k)/n_0]\sin(\epsilon+\gamma).$$

With r, obtained from the above equation, β can be computed as follows:

$$\beta=(\pi d\cos\epsilon/\lambda)(\sin\gamma-\sin(\epsilon+r)).$$

Figure 3 shows my computations for a grating of $\epsilon=20°$. At the center of the blaze the grating spacing is 1.47 times the wave-length. The zero and $+2$ orders get some energy and deplete the first-order intensity, as shown in the graph. The effects of the $+3$ and -1 orders are negligible. The efficiency, T, is greater than $\frac{1}{2}$ over an octave of frequency. Abscissa in Fig. 3 are λ/d. The sum of the terms in the denominator of Eq. (3) is approximately unity, as one might expect it to be from the conservation of energy.

PRISM AND GRATING COMPARED

To cover the infra-red from 2μ to 32μ requires five gratings at the rate of one grating per octave. On the other hand, it requires four or five prisms. (Quartz, LiF, NaCl, KBr, and KRS5).

For comparison we will take prism angles as being 60° (except KRS5, for which we take the prism angle 30°. Mr. Robert J. Meltzer has full computations for this prism and he supplied me with the KRS5 figures). Furthermore, without loss of significance, we may consider the efficiencies of prisms and gratings as being equal.

TABLE III. Dispersion of prisms and gratings.

Prisms			Gratings	
Material	λ	$(d\theta/d\lambda)$	λ	$(d\theta/d\lambda)$
LiF 60°	3.3μ	220	4μ	2500
	6μ	420		
NaCl 60°	8μ	81	10μ	1000
	14μ	114		
KBr 60°	14μ	50	20μ	500
	26μ	110		
KRS5 30°	20μ	25	30μ	333
	35μ	50		

Also, without loss of significance, we can take the dispersion of the grating for the first order as:

$$d\theta/d\lambda=[1/d\cos(\epsilon+\gamma)]\sim 1/d\sim 1/\lambda.$$

Table III gives comparisons of $(d\theta/d\lambda)$, for prisms and gratings with the approximations above mentioned.

CONCLUSIONS

Although these considerations of the relative merits of gratings and prisms are approximate, they indicate, unambiguously, the reasons why gratings have proven superior to prisms in the infra-red in the past, and they indicate the direction to move in the future to improve the echelette grating.

Applying the considerations to modern spectrometry, in the visible spectrum, in instances where high resolving power with weak sources is desired, it would seem that the greatest signal will obtain for gratings of the order of 37,400 lines per inch ($1d=.68\mu$), provided the groove form can be controlled as successfully as it is in the infra-red to give all light in one order (as in Fig. 3). Such gratings should be the best for the faintest sources, such as stellar spectra, and should give a gain of at least a factor 2 over gratings of 15,000 lines per inch.

Letters to the Editor

Retina Cones as Dielectric Antennas

G. TORALDO DI FRANCIA
Centro Ricerche Ottiche Ducati, Viale Matteotti 25, Firenze, Italy
December 23, 1948

IN the theoretical researches on retinal sensitivity, too little attention appears to have been paid to the fact that the elementary receptors are of the order of magnitude of a few wave-lengths. In this situation all the laws of conventional ray optics, when applied to the propagation inside the receptors, cease to hold good even as a first approximation, and may happen to be misleading. In particular, the explanation of the Stiles and Crawford effect cannot be based on the simple law of internal total reflection (Wright and Nelson,[1] O'Brien,[2] Platt[3]); and when setting up an experimental model of cone on a macroscopical scale, as made by O'Brien, one ought to multiply by the same factor the wave-length of the radiation used. Thus one would find himself in the region of microwaves. We are then confronted by a rather involved electromagnetic problem, but fortunately in dealing with it we can utilize the considerable amount of theoretical and experimental work which has been accomplished during the last years in microwave technique.

I have recently pointed out[4] the striking analogy between light and retinal receptors on one side, and microwaves and dielectric wave guides on the other. In this connection it is most probable that the tapered part of a cone may have the task of matching the impedances of the outer and the inner segment, in much the same way as a horn-like part in a wave guide may be used to match the impedances of two hollow pipes of different diameter. This is, in substance, the correct formulation of O'Brien's idea.

But what I want to emphasize here is the role of the cones as receptors rather than as transmission lines. From this point of view they must be thought of as tiny antennas, and we are concerned mainly with the difference of impedance between them and the outer medium. In other words, it is important to know their radiation pattern which, on account of the reciprocity theorem,[5] is identical in emission as in reception.

Dielectric antennas in the form of dielectric rods radiating from one of their ends have recently been studied by Zinke and Mallach,[6] who have found that they present some advantage with respect to conventional metallic antennas. Their radiation pattern is almost entirely constituted by a principal lobe, centered on the axis of the antenna and whose aperture varies from 25 to 50°, according to the dimensions and dielectric constant of the rod. One immediately sees that in this range there is comprised the angular aperture of the pupil, as seen from the fovea. In the language of modern physics, we may then say that the retinal receptors present the largest possible cross section for impinging light coming from the pupil, while they have nearly zero cross section for light coming from other directions. This is in striking agreement with our ideas on natural economy.

The principal lobe in the radiation pattern presents in every case an axial maximum and gradually falls off with increasing angle. This is none other than Stiles and Crawford effect. A quantitative comparison would require the knowledge of the ratio ϵ of the dielectric constant of the cones to that of the surrounding medium. We do not know this datum, but it is interesting to set up an inverse argument, as follows: Zinke and Mallach have shown that the ratio D/λ of the diameter of the antenna to the wave-length, in order to obtain the most favorable radiation pattern, must be comprised between 0.36 and 0.58 times $(\epsilon-1)^{-\frac{1}{2}}$. If we make the hypothesis that the cones satisfy this condition and assume for the center of the fovea $D=1\mu$ (see the discussion of Polyak's data by Jones and Higgins)[7] and $\lambda=0.4\mu$ for the wave-length in the vitreum body, we find ϵ comprised between 1.02 and 1.05. These appear to be very reasonable figures.

We finally add that, as regards selectivity of dielectric antennas, Zinke and Mallach have found that an interval of an octave in the frequency is allowable without seriously impairing efficiency. This means that the upper limit for the wave-length may be twice the lower one. And this is exactly the situation for visible light.

[1] W. D. Wright and J. H. Nelson, Proc. Phys. Soc. **48**, 401 (1936).
[2] B. O'Brien, J. Opt. Soc. Am. **36**, 506 (1946); **37**, 275 (1947).
[3] J. R. Platt, J. Opt. Soc. Am. **37**, 669 (1947).
[4] G. Toraldo di Francia, Nuovo Cimento **5**, 110 (1948).
[5] J. C. Slater, *Microwave Transmission* (McGraw-Hill Book Company, Inc., New York, 1942), p. 251.
[6] L'onde électronics **26**, 387 (1946).
[7] L. A. Jones and G. C. Higgins, J. Opt. Soc. Am. **37**, 223 (1947).

Comment on the Note Entitled "Retinal Cones as Dielectric Antennas"

BRIAN O'BRIEN
Institute of Optics, University of Rochester, Rochester, New York
February 17, 1949

IT is evident, as pointed out by G. Toraldo di Francia, that conventional ray optics can be only an approximation when applied to propagation in optical media with boundaries separated by a few wave-lengths. Before preparing the retinal cone model which I described two years ago (see reference 2 of preceding letter), the literature on dielectric antennas was examined. It was concluded that a macroscopic model would provide a reasonable approximation to conditions prevailing in the foveal cones, although it would fail to reproduce the diffraction effects occurring when light enters a foveal cone from the overlying medium.

The similarity of the results for such a model which I have reported, and those calculated for a dielectric antenna model, is evidence that the approximation achieved by the optical model is quite good. In fact, the agreement between the optical model and the observed Stiles and Crawford effect is better than the agreement between the dielectric antenna model and the Stiles and Crawford results.

However, the optical model has served its purpose, and it seems probable that future progress, particularly as regards quantitative theory, can be made best by the dielectric antenna approach. The fact that the calculated results for a dielectric antenna do not agree very closely with the Stiles and Crawford observation is not serious, since more must be known of the numerical constants involved, particularly the refractive index of the various portions of the foveal cone, before very good quantitative agreement can be expected.

In spite of the minor differences cited above, I am in agreement with G. Toraldo di Francia's point of view as expressed in his note and in his earlier paper (see reference 4 of preceding letter), and hope that he will extend this work to detailed calculations based on the geometrical configuration of the foveal cones as disclosed by the most recent histological studies of Polyak and others. When this is done it will be possible to decide just how satisfactory an approximation the optical model provides.

IN MEMORIAM

A. Herman Pfund

A. Herman Pfund, Professor Emeritus in Physics at The Johns Hopkins University and past president of the Optical Society, died January 4, 1949. His passing is a severe blow to his family, his colleagues, and his many friends throughout the country. His scientific achievements were many: the Pfund arc, the Pfund hydrogen series, the on-axis anastigmatic perforated mirror system, infra-red powder filters, the selenium polarizer, the resonance radiometer, and the infra-red gas analyzer, to name a few. He brought added fame and prestige to his university in the field of physical optics, a realm previously enriched by the famed researches of Henry Rowland and R. W. Wood. Professor Pfund had received many honors in recognition of his contributions to experimental physics. He had on occasion expressed particular pleasure for the honors he had received from the Optical Society itself, notably, the office of president in 1943, the Frederick Ives medal in 1939, and the special issue of the Journal dedicated to him in October 1947, as a tribute on his retirement from active faculty status.

A. Herman Pfund

Professor Pfund was a thoroughly delightful, stimulating, and human person who has left his stamp on those who were fortunate enough to have been associated with him. His many ingenious experiments were carried out with an elegance of technique and impressive simplicity of apparatus. He was an excellent teacher, and a steady stream of enthusiastic students went forth from his laboratory into the scientific world. He possessed the knack of stimulating his students by pungent comment and by frequent intimate demonstrations in his laboratory of his own current researches. His attitutde toward his students was one of kind and human understanding, and as a result, he was universally regarded by them with sincere and lasting affection. He was modest, never boastful, generous to the utmost degree, gifted with a lively and pithy sense of humor, and absolutely devoid of pretense. The successes of his career exemplified the virtues of a democratic attitude which, together with his sense of fair play and open dealing, was an integral part of his character.

He will be sorely missed at meetings of the Optical Society where so many of his papers were presented at the formal sessions, and where so many of his stories were presented at the informal corridor sessions! He will be equally mourned by his university colleagues of this and earlier generations and by his countless friends in all walks of life.

Shirleigh Silverman
John Strong

Frank Benford

Frank Benford, member of the Board of Directors of the Optical Society of America, died suddenly at his home in Schenectady, New York, on December 4, 1948. He had only recently retired from the Research Laboratory of the General Electric Company, and was engaged in several writing projects, one being the preparation of a book on Radiometry.

Mr. Benford was born in Johnstown, Pennsylvania, July 10, 1883, and as a child of 6 he went through the Johnstown flood, an experience of which he could tell most vividly.

Frank Benford

Choosing a technical career, he entered the University of Michigan and was graduated in 1910 with the degree of Bachelor of Science in Electrical Engineering. He immediately entered the General Electric Company's Test Course and became a physicist in the Illuminating Engineering Laboratory. During World War I he worked on the theory and design of searchlights, the results of which he published in a series of 22 papers in the early 20's. In 1928 he joined the General Electric Research Laboratory where he remained until his retirement in July, 1948. His work was chiefly on problems connected with radiation, particularly in optics. He also taught courses in optics at Union College and at Rensselaer Polytechnic Institute.

He was granted 20 patents on optical devices and was the author of 109 published papers on optics and mathematics. One important series deals with the distribution of sunshine on buildings and gives charts which enable architects to orient

their buildings to give desired conditions of lighting. He also developed a new method of plotting the distribution of light from an illuminating fixture. This involves the use of lines of equal candlepower, called "isocandles," and it is now widely used. At the time of his death he had a considerable amount of material which he planned to publish in further papers, and it is hoped that this will not be lost, but can be given to the world, perhaps with the aid of his former associates.

Not least among his contributions to science and engineering are his four sons, all of whom have entered technical careers. One is, like his father, an expert in optics; another is a mechanical engineer, another a metallurgist, and the fourth a naval architect.

In addition to contributing the large number of papers which he wrote in the field of optics, Mr. Benford for many years took an active part in the affairs of the Optical Society of America. He frequently served on its committees, and was for a long period one of the associate editors of the Journal.

JAMES STOKLEY
FRANK STUDER

Optical Society of America, Incorporated

Notice of Election of Officers

In accordance with Article III, Section 6 of the By-Laws of the Optical Society of America, the following officers and directors are to be elected at or before the Annual Meeting in October, 1949:

President
Vice President
Secretary for Local Sections
} for a term of two years

Secretary
Treasurer
2 Members-at-Large of the Board of Directors
} for a term of four years.

The present officers are:

	Term expires at annual meeting in
President—RUDOLF KINGSLAKE	1949
Vice President—WILLIAM F. MEGGERS	1949
Secretary—ARTHUR C. HARDY	1949
Treasurer—W. W. GRAEPER	1949
Past President—GEORGE R. HARRISON	1949
Editor—GEORGE R. HARRISON (elected by Directors)	1952
Directors-at-Large:	
STANLEY S. BALLARD	1949
F. M. BISHOP	1949
WALLACE R. BRODE	1949
A. H. BENNETT	1951
E. H. LAND	1951

In accordance with the By-Laws, Article III, Section 4:

> "No member-at-large of the board of directors shall be eligible for re-election."

Stanley S. Ballard, F. M. Bishop, and Wallace R. Brode are not eligible for re-election.

The following Committee on Nominations has been appointed and confirmed in accordance with Article III, Section 6 of the By-Laws:

GEORGE R. HARRISON, *Chairman*
Massachusetts Institute of Technology,
Cambridge 39, Massachusetts.

WALLACE R. BRODE,
National Bureau of Standards,
Washington 25, D. C.

PAUL E. KLOPSTEG,
N. W. Technological Institute,
Evanston, Illinois.

R. C. GIBBS
National Research Council,
Washington, D. C.

E. D. TILLYER,
American Optical Company,
Southbridge, Massachusetts.

It will be the duty of this committee to make nominations for the above-mentioned election. The committee report is to be made not later than July 15, 1949.

Although, after the committee has made its report, an opportunity will be given for additional nominations by petition, members are urged, as soon as possible, to suggest names which should be considered by the committee. Suggestions may be sent to the Chairman or to any other member of the committee.

Only regular, honorary, and regular-emeritus members are eligible to election. A list of members was published in the January, 1948 issue of the Journal of the Optical Society of America. (Later transfers to regular membership will appear in the Secretary's Reports for 1947 [J. Opt. Soc. Am. **38**, 652–654 (1948)] and 1948, which is scheduled for publication in the July, 1949 issue of the Journal.)

ARTHUR C. HARDY, *Secretary*